

## NSAIDS AND BONE ADAPTATION TO MECHANICAL LOADING

TEMPORAL INFLUENCE OF NSAIDS ON MECHANICALLY INDUCED BONE  
FORMATION AND FLUID FLOW STIMULATED CELLULAR PGE<sub>2</sub> PRODUCTION

By CHERYL DRUCHOK, H.B.Sc.Kin., M.A.Sc.

A Thesis Submitted to the School of Graduate Studies in Partial Fulfillment of the  
Requirements for the Degree Doctor of Philosophy

McMaster University

© Copyright by Cheryl Druchok, August 2016

DOCTOR OF PHILOSOPHY (2016)  
(School of Biomedical Engineering)

McMaster University  
Hamilton, Ontario

TITLE: Temporal influence of NSAIDs on mechanically induced bone formation and  
fluid flow stimulated cellular PGE<sub>2</sub> production

AUTHOR: Cheryl Druchok, H.B.Sc.Kin., M.A.Sc. (McMaster University)

SUPERVISOR: Gregory R. Wohl, Ph.D., P.Eng.

NUMBER OF PAGES: xxv, 208

## **LAY ABSTRACT**

Bone is a dynamic tissue that can adapt to mechanical loading. Prostaglandins (PGs) are important signalling factors produced by osteocytes, the bone mechanosensing cells, that help to activate various cells and cell processes leading to changes in bone structure. Blocking PG signalling with non-steroidal anti-inflammatory drugs (NSAIDs) has been shown to influence bone formation induced by mechanical stimulation in animals and humans. The purpose of this study was to examine the timing effects of NSAID administration on: 1) bone formation induced by multiple mechanical loading events in rats and 2) the PG production of osteocyte like cells in response to fluid flow stimulation. The results of this study suggest that NSAIDs, administered either before or after loading, do not affect bone responses to multiple mechanical loading events. Further investigation is needed to determine the translatability of these findings to NSAID use around the time of exercise in humans.

## ABSTRACT

Prostaglandins (PGs) are important signalling factors for bone mechanotransduction. The inhibition of cyclooxygenase, responsible for the synthesis of PGs, with non-steroidal anti-inflammatory drugs (NSAIDs) has been shown to influence bone formation induced by mechanical stimulation. The purpose of this study was to examine the timing effects of NSAID administration on: 1) bone formation induced by multiple mechanical loading events in a rat model and 2) the PGE<sub>2</sub> response of MLO-Y4 osteocyte like cells stimulated by fluid shear stress. The rat forelimb compression model was used to induce bone formation in male and female rats using a 1-month loading protocol (12 loading sessions). The right forelimbs were loaded and the left forelimbs served as non-loaded controls. NSAIDs were administered orally either before or after loading. Fluorochrome labels were administered to the rats to determine mineral apposition rate (MAR). The NSAIDs examined (indomethacin, NS-398 and ibuprofen) did not significantly affect periosteal MAR, administered either before or after loading, suggesting NSAIDs do not affect bone adaptation to multiple mechanical loading events. To examine *in vitro* effects of NSAIDs on PGE<sub>2</sub> production, an orbital shaker was used to apply fluid shear stress to MLO-Y4 cells seeded in 6-well culture plates. Indomethacin was added to the culture media either before or after loading and media PGE<sub>2</sub> concentrations were determined at various time points by enzyme immunoassay. Fluid shear stress increased PGE<sub>2</sub> production of MLO-Y4 cells and indomethacin administration inhibited that response when administered both before and after fluid flow. However, PGE<sub>2</sub> production was influenced by the media changes that occurred in the *in vitro* experiments, making it difficult to differentiate between indomethacin effects and media change effects. The *in vitro* experiments revealed the difficulties of modeling the timing effects of NSAID administration on MLO-Y4 PGE<sub>2</sub> production in response to fluid flow.

## **ACKNOWLEDGEMENTS**

It is with great appreciation that I acknowledge the continuous support and guidance of my supervisor, Dr. Greg Wohl, throughout my research. He provided me with immense knowledge and insight. He encouraged me throughout the ups and many downs and was always there to help me through the numerous frustrations. I thank him for having the confidence in me to succeed and for making this research possible.

I would also like to thank my committee members Dr. Rick Adachi, Dr. Karen Beattie and Dr. Cheryl Quenneville for all of their support throughout this process.

A massive thanks to my family and friends (you know who you are) for all of their support throughout what some of them consider to be my never-ending academic career. It really would be never-ending if it weren't for them.

## TABLE OF CONTENTS

DESCRIPTIVE NOTE	ii
LAY ABSTRACT	iii
ABSTRACT	iv
ACKNOWLEDGEMENTS	v
TABLE OF CONTENTS	vi
LIST OF FIGURES	xv
LIST OF TABLES	xviii
LIST OF ABBREVIATIONS AND SYMBOLS	xix
DECLARARTION OF ACADEMIC ACHEIVEMENT	xxv
CHAPTER ONE	
INTRODUCTION	
1.1 Introduction	1
CHAPTER TWO	
BACKGROUND	
2.1 Bone Structure and Composition	7
2.2 Bone Adaptation	9
2.3 Mechanotransduction and Osteocytes	12
2.4 Bone Mechanical Stimulation	14

2.4.1	<i>In vivo</i> Mechanical Loading	15
2.4.1.1	Lamellar and Woven Bone Formation	19
2.4.2	<i>In vitro</i> Mechanical Loading	21
2.5	Prostaglandins and Bone	24
2.5.1	Prostaglandins	24
2.5.2	Mechanotransduction and Prostaglandins	26
2.5.3	Timing of COX-2 Induction in Response to Mechanical Stimulation	29
2.5.4	PGE <sub>2</sub> Release and Actions	32
2.5.5	PGE <sub>2</sub> Receptors	34
2.5.6	Effects of Prostaglandins on Bone	35
2.5.6.1	Prostaglandins and Bone Formation	36
2.5.6.2	Prostaglandins and Bone Resorption	37
2.6	NSAIDs and Bone	40
2.6.1	NSAIDs	40
2.6.2	Effects of NSAIDs on Bone	43
2.6.2.1	NSAIDs and Bone Cells	44
2.6.2.2	NSAIDs and BMD	46
2.6.2.3	NSAIDs and <i>In vivo</i> Loading	48
2.6.2.4	NSAIDs and <i>In vitro</i> Loading	53
2.6.2.5	Long Term Effects of NSAIDs on Bone	55

## CHAPTER THREE

### MATERIALS AND METHODS: *IN VIVO* MECHANICAL LOADING

3.1	Animals and Housing	57
3.2	Rat Forelimb Compression Model	57
3.3	Experimental Protocols	59
3.3.1	NSAID Pharmacokinetics	60
3.3.2	NSAID Administration	62
3.3.3	NSAID Dosing	63
3.4	Development of Loading Protocol	64
3.4.1	Loading Protocol Parameters	65
3.4.2	1-Month Loading Protocol in Male Rats (INDO and NS-398)	65
3.4.3	2-Week Loading Protocol in Male Rats (IBU and CBX)	65
3.4.4	2-Week Loading Protocol in Female Rats (IBU and CBX)	67
3.4.5	Rat Forelimb Strain Gauging	68
3.4.6	1-Month Loading Protocol in Female Rats (IBU)	70
3.5	Bone Histomorphometry	71
3.5.1	Fluorochrome Labeling	71
3.5.1.1	1-Month Loading Protocol	72
3.5.1.2	2-Week Loading Protocol	72

3.5.2	Sacrificing and Dissection	72
3.5.3	Bone Sample Preparation	73
3.5.4	Image Capture	74
3.5.5	Grid Template Development	74
3.5.6	MAR Determination	76
3.6	Statistics	77

## CHAPTER FOUR

### RESULTS: *IN VIVO* MECHANICAL LOADING

4.1	1-Month Loading Protocol in Male Rats: Indomethacin	79
4.2	1-Month Loading Protocol in Male Rats: NS-398	83
4.3	2-Week Loading Protocol in Female Rats: Ibuprofen and Celebrex	85
4.4	1-Month Loading Protocol in Female Rats: Ibuprofen	87

## CHAPTER FIVE

### DISCUSSION: *IN VIVO* MECHANICAL LOADING

5.1	Discussion	89
5.2	NSAID Administration Before and After Loading	91
5.3	Potential Factors Influencing NSAID Effects on Bone Adaptation	95
5.3.1	NSAID Pharmacokinetics	96

5.3.1.1	Type of NSAID	96
5.3.1.2	Timing of NSAID Administration	99
5.3.1.3	NSAID Dosing	101
5.3.2	Sex of Subjects	104
5.4	Differential Effects of NSAIDS on BFR, MAR and MS/BS	105
5.5	Lamellar and Woven Bone Formation	107
5.6	Exogenous Bone Mechanical Loading vs. Exercise	109
5.7	Limitations	111
5.7.1	Sample Size	111
5.7.2	Standard Deviations	117

## CHAPTER SIX

### MATERIALS AND METHODS: *IN VITRO* MECHANICAL LOADING

6.1	MLO-Y4 Cell Line	121
6.2	MLO-Y4 Cell Culturing and Seeding	122
6.3	Indomethacin Administration	123
6.4	Development of Fluid Flow Protocol	125
6.4.1	Parallel Plate Flow Chamber Model	125
6.4.2	Parallel Plate Flow Chamber System	127
6.4.3	Parallel Plate Flow Chamber Limitations	127
6.4.4	Orbital Shaker Model	129
6.4.5	Orbital Shaker System	130

6.5 <i>In vitro</i> Mechanical Loading Experimental Timelines	131
6.5.1 Three Media Changes at 30mins, 3.5hrs and 6.5hrs	132
6.5.2 Two Media Changes at 30mins and 3.5hrs	133
6.5.3 One Media Change at 30mins	133
6.5.4 No Media Changes	133
6.6 Cell Count Determination	135
6.7 Media PGE <sub>2</sub> Concentration Determination	135
6.8 Statistics	136

## CHAPTER SEVEN

### RESULTS: *IN VITRO* MECHANICAL LOADING

7.1 Parallel Plate Flow Chamber Experiments	137
7.1.1 CON and PRE Groups	137
7.1.2 CON and POST Groups	138
7.2 Orbital Shaker Experiments	139
7.2.1 Three Media Changes at 30mins, 3.5hrs and 6.5hrs	139
7.2.2 Two Media Changes at 30mins and 3.5hrs	141
7.2.3 One Media Change at 30mins	143
7.2.4 No Media Changes	145
7.2.5 Media Changes in the CON Group	147

## CHAPTER EIGHT

### DISCUSSION: *IN VITRO* MECHANICAL LOADING

8.1 Parallel Plate Flow Chambers	148
8.2 Orbital Shaker	149
8.3 Effect of Media Changes on the Control (CON) Group	152
8.4 Effect of Media Changes on the PRE and POST Groups	158
8.5 Limitations	162
8.5.1 <i>In vivo</i> vs. <i>In vitro</i>	162
8.5.2 Orbital Shaker	165

## CHAPTER NINE

### CONCLUSION

9.1 Conclusion	170
----------------	-----

REFERENCES	175
------------	-----

APPENDIX I: MAR ( $\mu\text{m}/\text{day}$ ) of the male ulnas that underwent the 2-week loading protocol in the IBU/CBX experiment.	194
---	-----

APPENDIX II: MAR ( $\mu\text{m}/\text{day}$ ) of the male ulnas that underwent the 2-week loading protocol in the IBU/CBX experiment.	195
--	-----

APPENDIX III: The <i>p</i> -values determined by post-hoc analyses for each Section of the male IBU/CBX experiment.	196
APPENDIX IV: Dehydrating, infiltration and embedding procedure and schedule.	197
APPENDIX V: MAR ( $\mu\text{m}/\text{day}$ ) of the male ulnas that underwent the 1-month loading protocol in the indomethacin experiment.	198
APPENDIX VI: MAR ( $\mu\text{m}/\text{day}$ ) of the male ulnas that underwent the 1-month loading protocol in the NS-398 experiment.	199
APPENDIX VII: MAR ( $\mu\text{m}/\text{day}$ ) of the male ulnas that underwent the 1-month loading protocol in the NS-398 experiment.	200
APPENDIX VIII: The <i>p</i> -values determined by post-hoc analyses for each Section of the male NS-398 experiment.	201
APPENDIX IX: MAR ( $\mu\text{m}/\text{day}$ ) of the female ulnas that underwent the 2-week loading protocol in the IBU/CBX experiment.	202

APPENDIX X: MAR ( $\mu\text{m}/\text{day}$ ) of the female ulnas that underwent the 2-week loading protocol in the IBU/CBX experiment.	203
APPENDIX XI: The $p$ -values determined by post-hoc analyses for each Section of the female IBU/CBX experiment.	204
APPENDIX XII: MAR of ( $\mu\text{m}/\text{day}$ ) of the female ulnas that underwent the 1-month loading protocol in the ibuprofen timing experiment.	205
APPENDIX XIII: MAR of ( $\mu\text{m}/\text{day}$ ) of the female ulnas that underwent the 1-month loading protocol in the ibuprofen timing experiment.	206
APPENDIX XIV: The $p$ -values determined by post-hoc analyses for each Section of the female IBU timing experiment.	207
APPENDIX XV: Body masses of the rats used in the <i>in vivo</i> mechanical loading experiments.	208

## LIST OF FIGURES

2.1	Schematic of the osteocyte lacuna-canalicular network.	9
2.2	Schematic diagram of the rat forelimb compression model.	16
2.3	Fluorescent light microscope images of rat ulna cross-sections A) An example of lamellar bone formation. B) An example of woven bone formation.	19
2.4	Synthesis of prostaglandins.	25
2.5	Schematic diagram of potential PG signal transduction pathways involved in the mechanical stimulation of osteocytes.	29
3.1	Material testing system setup.	58
3.2	Schematic of the rat forelimb compression model.	59
3.3	MAR of Sections 1-7 of the male ulnas that underwent the 2-week loading protocol in the IBU/CBX experiment.	67
3.4	Cross-sectional image of a female rat ulna that underwent forelimb loading in the 2-week loading protocol.	68
3.5	Load/strain relationship of male (left) and female (right) ulnas during forelimb loading.	70
3.6	Cross-sectional image of a loaded ulna with the 20-segment, 7-section grid overlaid.	75
3.7	Cross-sectional image of a non-loaded ulna with the 20-segment, 7-section grid overlaid.	76

3.8	Colour coded 7-section grid of an ulna cross-section.	77
4.1	MAR ( $\mu\text{m}/\text{day}$ ) of Sections 1-7 of the male ulnas that underwent the 1-month loading protocol in the indomethacin experiment.	81
4.2	The $p$ -values determined by post-hoc analyses for each Section of the indomethacin experiment.	82
4.3	MAR ( $\mu\text{m}/\text{day}$ ) of Sections 2, 3, 5 and 6 of the male ulnas that underwent the 1-month loading protocol in the NS-398 experiment.	84
4.4	MAR ( $\mu\text{m}/\text{day}$ ) of Sections 2, 3, 5 and 6 of the female ulnas that underwent the 2-week loading protocol in the IBU/CBX experiment.	86
4.5	MAR ( $\mu\text{m}/\text{day}$ ) of Sections 2, 3, 5 and 6 of the female ulnas that underwent the 1-month loading protocol in the ibuprofen timing experiment.	88
6.1	Parallel plate flow chamber system.	126
6.2	Media PGE <sub>2</sub> concentration 30mins after fluid flow in the parallel plate flow chambers.	129
6.3	A) Orbital shaker used to generate fluid shear stress with a 6-well culture plate in position. B) Schematic of the orbital shaker setup in the incubator.	131
6.4	<i>In vitro</i> mechanical loading experimental timelines.	134

7.1	Media PGE <sub>2</sub> concentrations in the CON and PRE groups at 30mins in the parallel plate flow chamber experiments.	137
7.2	Media PGE <sub>2</sub> concentrations in the CON and POST groups at 30mins and 3.5hrs in the parallel plate flow chamber experiments.	138
7.3	A) Experimental timeline for the three media change experiment. B) Media PGE <sub>2</sub> concentrations at 30mins and 24hrs in the three media change flow experiment.	140
7.4	A) Experimental timeline for the two media change experiment. B) Media PGE <sub>2</sub> concentrations at 30mins and 12hrs in the two media change flow experiment.	142
7.5	A) Experimental timeline for the one media change experiment. B) Media PGE <sub>2</sub> concentrations at 30mins and 24hrs in the one media change flow experiment.	144
7.6	Experimental timeline for the no media change experiment at A) 24hrs and B) 12hrs. C) Media PGE <sub>2</sub> concentrations at 12hrs and 24hrs in the no media change flow experiment.	146
7.7	Media PGE <sub>2</sub> concentrations at 24hrs in the CON group in the experiments with no, one and three media changes.	147

## LIST OF TABLES

2.1	COX-1/COX-2 ratios of NSAIDs used in this study.	43
2.2	Summary of studies examining the effects of NSAIDs on mechanically induced bone formation <i>in vivo</i> .	53
3.1	<i>In vivo</i> mechanical loading experimental groups.	60
3.2	Pharmacokinetics of the NSAIDs used in the <i>in vivo</i> experiments.	62
5.1	Typical human NSAID doses and corresponding doses in rats using the milligram/kilogram <sup>0.75</sup> scaling calculation.	103
5.2	E values calculated using the resource equation for each of the <i>in vivo</i> loading experiments.	117
6.1	<i>In vitro</i> mechanical loading experimental groups.	124

## LIST OF ABBREVIATIONS AND SYMBOLS

%	per cent
°C	degrees Celsius
$\alpha$	alpha
$\beta$	beta
$\tau$	shear stress
$\eta$	fluid viscosity
$\rho$	density of culture media
$\geq$	greater than or equal
=	equal
<	greater than
>	less than
↓	impairs bone formation
↑	enhances bone formation
↔	no effect on bone formation
$\pi$	pi
$\mu\epsilon$	microstrain ( $10^{-6}$ mm/mm)
$\mu\text{g}$	microgram
$\mu\text{l}$	microlitre
$\mu\text{m}$	micrometre
$a$	orbital radius of rotation of shaker

AA	arachidonic acid
AkT	protein kinase B
ALP	alkaline phosphatase
ANOVA	analysis of variance
<i>b</i>	width of chamber
BFR	bone formation rate
BMD	bone mineral density
BMU	basic multicellular unit
BW	body weight
CAF	central animal facility
CaMOS	Canadian Multi-Centre Osteoporosis Study
cAMP	cyclic adenosine monophosphate
CBX	Celebrex
cm	centimetre
CO <sub>2</sub>	carbon dioxide
CON	control, no NSAID administration
COX	cyclooxygenase
CREB	cAMP response element-binding protein
CS	calf serum
Cx43	connexin 43
DAG	diacylglycerol
DKK1	dickkopf Wnt signalling pathway inhibitor 1

dL.Ar	double-label area
dL.Pm	double-label perimeter
E	number of degrees of freedom of analysis of variance
ECM	extracellular matrix
ED50	dose required to inhibit 50% of the activity
EP1	prostaglandin E1 receptor
EP2	prostaglandin E2 receptor
EP3	prostaglandin E3 receptor
EP4	prostaglandin E4 receptor
ERK	extracellular signal-regulated kinase
F	flow
<i>f</i>	frequency of rotation
FBS	fetal bovine serum
FosB	FBJ murineosteosarcoma viral oncogene homolog B
Fz	frizzled
g	gram
GPCR	G-protein couple receptor
GSK-3 $\beta$	glycogen synthase kinase 3 $\beta$
<i>h</i>	distance between plates
hr(s) or HR	hour(s)
Hz	Hertz
IBU	ibuprofen

IgG	immunoglobulin G
INDO	indomethacin
IP3	inositol triphosphate
Ir.L.t	interlabel time
Ir.L.Th	interlabel thickness
kg	kilogram
KO	knockout
L	litre
LEFT	left forelimb
LRP5	low-density lipoprotein receptor-related protein 5
M	molar
MAR	mineral apposition rate
MEM	modified Eagle's medium
mg	milligram
microCT	micro-computed topography
min	minute
mL	milliliter
MLO-Y4	murine long bone osteocyte Y4
mm	millimetre
mRNA	messenger ribonucleic acid
MrOS	Osteoporotic Fractures in Men Study
MS/BS	mineralizing surface

n	number of units in a subgroup of a sample
N	Newton
nm	nanometre
NSAID	non-steroidal anti-inflammatory drug
OFF	oscillatory fluid flow
OPG	osteoprotegerin
<i>p</i>	p-value
Pa	pascal
PFF	pulsatile fluid flow
pg	picogram
PG(s)	prostaglandin(s)
PGE <sub>2</sub>	prostaglandin E <sub>2</sub>
PGG <sub>2</sub>	prostaglandin G <sub>2</sub>
PGH <sub>2</sub>	prostaglandin H <sub>2</sub>
PI3k	phosphoinositide 3-kiase
PKA	protein kinase A
PKC	protein kinase C
PLA <sub>2</sub>	phospholipase A <sub>2</sub>
PLC	phospholipase C
POST	NSAID administration before loading
PRE	NSAID administration after loading
<i>Q</i>	flow rate

r	Pearson's product-moment correlation coefficient
RANK	receptor activator of nuclear factor kappa-B
RANKL	receptor activator of nuclear factor kappa-B ligand
rpm	rotations per minute
S	static
SF	steady flow
Sost	sclerostin
s.q.	subcutaneous
STD	standard deviation
$t_{1/2}$	half-life
TRAP	tartrate-resistant acid phosphatase
Wnt	wingless-related integration site

## **DECLARARTION OF ACADEMIC ACHEIVEMENT**

I, Cheryl Druchok, completed all experimentation in this thesis with the exception of the mechanical loading and bone sample preparation of the indomethacin 1-month loading experiment, which was completed by Kyle Eastwood. I reassessed the bone sections from the indomethacin experiment using a different technique than was previously published.

## **CHAPTER ONE**

### **INTRODUCTION**

#### **1.1 Introduction**

It is estimated that more than 1.5 million or 10% of Canadians over the age of 40 have osteoporosis [1]. That number increases with age, with osteoporosis affecting one in four women and one in eight men over 50 years of age [2]. Osteoporosis was estimated to cost between \$2.3 billion and \$4.1 billion in 2010 [3], a substantial economic burden to Canadian society. As the age of the Canadian population increases so too will the cost of osteoporosis care and treatment. Developing strategies to combat this disease and more importantly prevent it are essential and start from bone health basics.

Osteoporosis is a bone fragility disease characterized by an imbalance of bone formation and bone resorption, where bone resorption exceeds bone formation. In a non-osteoporotic state, bone formation and resorption are tightly coupled; bone formation and resorption are balanced. These coupled activities constitute bone remodeling. Bone remodeling maintains both bone quantity and quality during young adulthood and adulthood, approximately between the ages of 20 and 50 [4]. After this time the processes become uncoupled and resorption begins to exceed formation. The cause of osteoporosis is not clear but a number of factors may contribute to altered bone remodeling. In general, genetic factors, endocrine factors (age-related hormonal changes), nutritional factors and physical activity determine an individual's susceptibility to osteoporosis [4]. The relative contribution of these factors to osteoporosis is not well established but physical activity

does play a major role. Despite hormonal and nutritional interventions, an absence of weight-bearing activity will lead to bone loss [4]. Studies suggest that regular physical activity throughout life can help to mitigate age-related bone loss and can prevent osteoporosis [5,6]. Peak bone mineral density or bone mass is directly related to physical activity prior to achieving peak bone mass in young adulthood, and the higher an individual's peak bone mass, the lower their risk of osteoporosis later in life [7]. The contributions of initial bone mass and subsequent bone loss contribute approximately equally to the determination of bone mass in elderly individuals [8]. Continuing physical activity beyond the age of peak bone mass accrual delays the onset of bone loss and reduces the rate of bone loss with age [5,6]. Physical activity at any age can benefit bone health.

Mechanical loading of bone is an important regulator of bone turnover. Bone is a dynamic tissue that can adapt to mechanical loading with changes in structure to achieve a better balance between stress and load. Mechanical loading stresses the bone, initiating an osteogenic response through the process of mechanotransduction. A mechanical signal is transduced into a chemical signal, which in turn activates various cells and cell processes. The details of the mechanotransductive process are not complete but many pathways and intermediaries have been identified.

Prostaglandins (PGs), specifically prostaglandin E-2 (PGE<sub>2</sub>), are one key signalling factor in the mechanotransductive process of bone formation. PGE<sub>2</sub> is synthesized via the cyclooxygenase (COX) enzyme by bone cells in response to mechanical stimulation. It is associated with bone remodeling and formation and has been

shown to trigger the upregulation of bone osteogenic signals in response to mechanical stimuli. Inhibition of the COX enzyme by non-steroidal anti-inflammatory drugs (NSAIDs) has been shown to affect bone responses to mechanical loading [9–15]. This effect is of a temporal nature; NSAID effects on bone formation are dependent upon the timing of administration. In addition, it appears that a number of factors influence how NSAIDs will affect bone adaptation to mechanical loading, including the NSAID taken, the age and sex of subjects examined, the mechanical stimuli involved and the overall state of the bone environment [12–15].

NSAIDs are a common treatment for musculoskeletal conditions and are an effective analgesic for many chronic pain conditions. As such, a large portion of the population commonly uses NSAIDs and they are one of the most commonly used drugs in the world [16,17]. In 2010, more than 29 million adults in the U.S. were estimated to be regular users of NSAIDs, 41% more than in 2005 [18]. With such a large portion of the population taking NSAIDs it is important to determine how they may affect bone health. The prevalence of NSAID use is even greater in older adults, with over 20% of adults over the age of 65 using prescription NSAIDs and an even larger percentage using nonprescription NSAIDs [19]. The number of Canadians 65 years of age or older is expected to double in the next 20 years to reach 10.4 million seniors by 2036, and by 2051 an estimated 1 in 4 Canadians will be 65 or older [20]. Along with the increase in the elderly population there too will come an increase in the use of NSAIDs. This stresses the importance of understanding how NSAIDs may affect bone adaptation to mechanical

loading both before osteoporosis arises, to lessen the prevalence, as well as after it is present in the elderly population, to mitigate the disease burden.

The overall goal of this study was to better understand the mechanisms responsible for bone formation induced by multiple mechanical loading events, specifically the role that prostaglandins play in bone mechanotransduction and the influence of NSAIDs on that process. This was accomplished through the examination of the temporal effects of NSAID administration on adaptations in bone structure and cellular and molecular signalling. Understanding the mechanisms that orchestrate bone formation in response to mechanical stimulation can provide a basis for future development of strategies to enhance bone mass following anabolic loading. We need to take advantage of the intrinsic ability of bone to adapt to mechanical loading. If we better understand the pathways that orchestrate bone adaptation to loading, then we can take advantage of them and target them with specific loading regimes or therapeutics to further enhance the benefits of physical activity. Understanding how NSAIDs affect the response of bone to physical stimuli is important given the crucial role of physical activity in maintaining bone health, the aging population and the extensive and growing use of NSAIDs [18].

To investigate the temporal effects of NSAID administration on bone adaptation responses to multiple mechanical loading events, two main objectives were addressed:

1. To determine the timing effects of inhibiting mechanotransductive signals, specifically PGE<sub>2</sub> production, with NSAID administration, on lamellar bone formation induced by multiple mechanical loading events in a rat model.

The hypothesis was that NSAID administration before mechanical loading would impair bone formation, whereas administration following loading would enhance bone formation, compared to no NSAID administration.

2. To gain a better understanding of the *in vivo* experiments by examining the timing effects of NSAID administration on osteocyte signalling, specifically PGE<sub>2</sub> production, in response to fluid-flow induced shear stress.

The hypothesis was that NSAID administration would differentially affect PGE<sub>2</sub> production depending on the timing of delivery, either before or after loading. NSAID administration before loading would impair the immediate increase in PGE<sub>2</sub> production whereas NSAID administration after loading would impair the longer term production of PGE<sub>2</sub>.

Following a review of the pertinent background information, the experimental methods used to examine the effects of NSAIDs on lamellar bone formation induced *in vivo*, using the rat forelimb compression model, are described along with the resultant findings and corresponding discussion. The *in vitro* experimental methods used to

examine NSAID effects on osteocyte PGE<sub>2</sub> production in response to fluid shear stress follow. The results of the *in vitro* experimentation and a discussion of the findings are then presented. Finally, a summary of the *in vivo* and *in vitro* findings and the next steps in this research are discussed.

## **CHAPTER TWO**

### **BACKGROUND**

#### **2.1 Bone Structure and Composition**

Bones are the primary structural elements of the body. They serve multiple purposes: protecting vital organs, providing a rigid framework for movement, participating in mineral homeostasis and acting as the primary site of hematopoiesis. All of these functions are vital, emphasizing the importance of maintaining bone health.

Bone tissue consists of two components: cells and extracellular matrix (ECM). The ECM is composed of four components: hydroxyapatite mineral, collagen, water and small amounts of proteoglycans and noncollagenous proteins. Bone cells carry out the formation and maintenance of the ECM. There are four types of bone cells. Osteoclasts are the cells responsible for bone resorption. They are large multinucleated cells derived from mononuclear hematopoietic cells. Osteoblasts are mononuclear cuboidal cells differentiated from mesenchymal cells. They produce osteoid, the organic portion of the bone matrix, and are found on bone surfaces. Osteocytes are former osteoblasts that have become embedded in the newly formed bone; they are found throughout the bone. Osteocytes sit in cavities called lacunae and communicate with each other and with osteoblasts via processes passing through tunnels known as canaliculi. Processes from adjoining cells are connected by gap junctions. Bone lining cells are like osteocytes, quiescent osteoblasts. They are osteoblasts that did not become buried in the newly formed bone and remained on the bone surface. Lining cells cover more than 90% of the

surfaces of adult bone [21] and maintain communication with osteocytes and osteoblasts through gap junctions. The exact role of bone lining cells is not understood, but it has been suggested that they may be involved in bone remodeling [21].

The human body is composed of two types of bone: cortical and trabecular. Cortical bone is the dense bone primarily found in the shaft of long bones, whereas trabecular bone is found in the ends of long bones surrounded by a cortical bone shell. Cortical and trabecular bone contain two major types of bone tissue: lamellar bone, a slow forming organized bone, and woven bone, a fast forming but weaker bone. Cortical bone has a porosity of 5-10%, whereas trabecular bone has a porosity of 50-90% [22]. Cortical bone contains three porosities: 1) the vascular porosity, 2) the lacunar-canalicular porosity and 3) the collagen-apatite porosity [23]. The vascular porosity consists of primary and secondary Haversian canals and Volkmann canals which contain blood vessels, nerves and interstitial fluid. The lacunar-canalicular porosity contains osteocytes and interstitial fluid. The collagen-apatite porosity surrounds the collagen and crystallites of the hydroxyapatite mineral.

Cortical bone is composed of several circular layers or lamellae in repeating structural units known as osteons (Figure 2.1). A Haversian canal is at the centre of the osteon and is approximately aligned with the long axis of the bone. It contains blood vessels and nerves. Volkmann canals are short transverse canals connecting Haversian canals to each other and to the outer surface of the bone. These canals also contain blood vessels and nerves. Cortical bone can be characterized as primary or secondary bone. Primary bone is tissue laid down *de novo* on an existing bone surface during growth,

commonly referred to as modeling. Secondary bone results from remodeling, the resorption of existing bone and the replacement by new lamellar bone. In adult humans, most cortical bone is composed entirely of secondary bone. Rats do not typically undergo true cortical bone remodeling [24] and as such the cortical bone exhibits only a few secondary osteons [25].

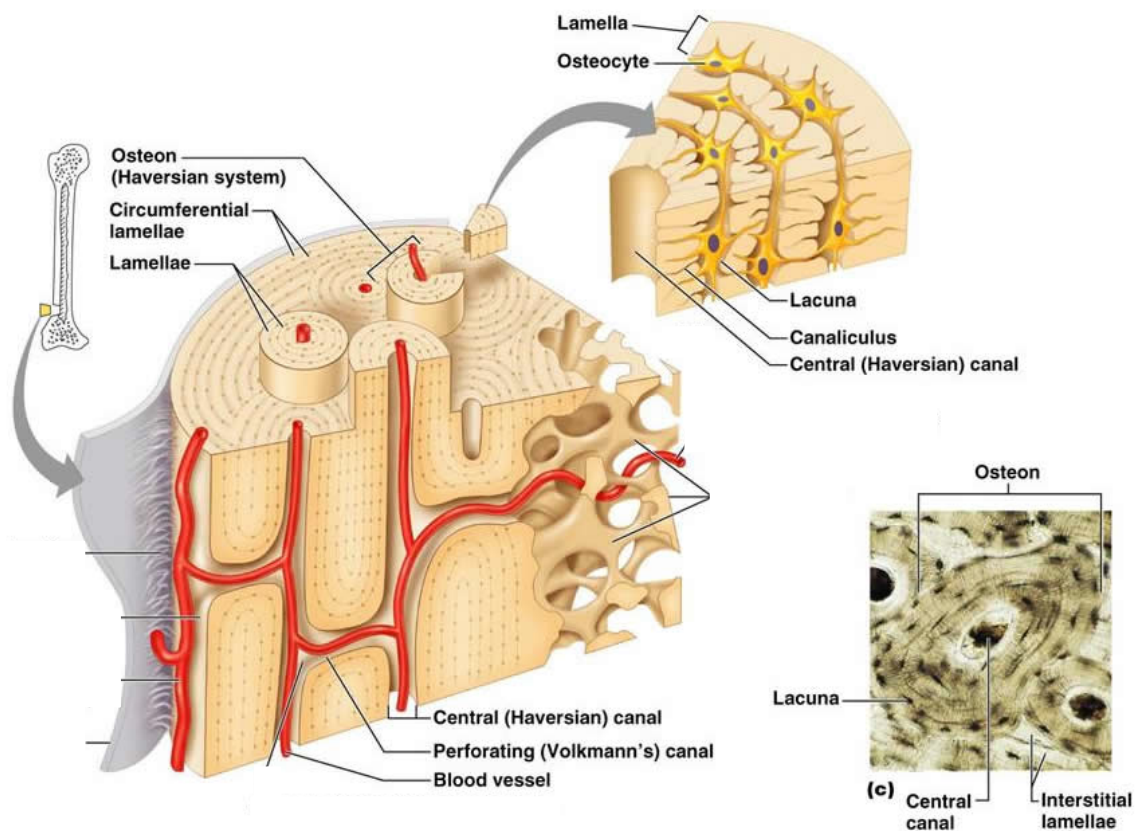


**Figure 2.1** Schematic of the osteocyte lacuna-canalicular network [26].

## 2.2 Bone Adaptation

Bone is a dynamic tissue that adapts its shape and structure to mechanical stimulation from daily physical activity. Julius Wolff was the first to propose that

mechanical strain is responsible for determining the architecture of bone [22]. Bone tissue is able to adapt its mass and three-dimensional structure to mechanical usage to obtain a higher efficiency of load bearing [22]. Non-mechanical factors, such as hormones and disease, can influence bone adaptation but they cannot replace or substitute for mechanical factors, as is demonstrated by the extensive bone loss that occurs in immobilized states [4].

Bone is optimized for daily loading activities but if loading patterns change then so too will the bone to maintain structural stability. Bone achieves this via a self-regulating biologic mechanism first described by Frost [27] as the mechanostat theory. Frost [27] suggested that bone has a homeostatic regulatory mechanism that can sense changes in mechanical demands and alter bone structure to meet these new demands. Below a certain threshold of use bone will be resorbed because it is not functionally needed, and above a certain threshold, where mechanical demands are higher than typical, bone formation will occur to meet these new mechanical demands. That is, bone regulates itself according to the loading environment. The bone homeostatic control system or the mechanostat has a stimulus – strain or strain-related characteristics, a sensory mechanism – osteocytes, and an effector mechanism that can bring the system back to homeostasis – modeling and remodelling [27].

Bone modelling and remodelling are the mechanisms that bone uses to adapt to mechanical loading. Bone remodelling is the process in which bone is constantly maintained and renewed by the coupled action of osteoblasts and osteoclasts. It involves the resorption of existing bone by osteoclasts and subsequent new bone formation by

osteoblasts in the same location with no major net change in bone structure. Together, osteoclasts and osteoblasts form the basic multicellular unit (BMU) that reconstructs the internal bone structure. Bone remodelling is responsible for maintaining or altering mineral balance, adapting bone structure to meet changing mechanical loading demands and repairing microdamage caused by excessive loading or fatigue. Uncoupling of the osteoblast and osteoclast activity, when bone resorption begins to exceed bone formation, leads to bone loss and subsequently osteoporosis.

Bone modelling is the process by which bone is formed by osteoblasts without prior bone resorption and occurs on the surfaces of bone. This process is largely observed during growth and in strength training athletes [28]. It produces large net increases in bone size, density and mechanical properties. Bone modelling works to maximize the functional capacity of bone. In mature bone, a substantial and somewhat novel change in the loading environment can trigger bone modelling. In animals, bone modelling can be induced experimentally through *in vivo* external mechanical loading of a bone, such as the forelimb compression model [29]. This loading method can induce different types of bone formation depending upon the nature of the loading protocol.

Bone mechanotransduction is responsible for bone adaptation to mechanical stimuli; it maintains the dynamic balance between bone formation and resorption. Mechanotransduction is the process by which mechanical stimuli are converted into biochemical signals and subsequently cellular responses. Bone mechanotransduction is an essential process for maintaining the integrity and health of bone tissue. Understanding

bone mechanotransduction is important for understanding how bone adapts to mechanical stimuli and how best to harness the bone formation potential.

### **2.3 Mechanotransduction and Osteocytes**

The currently favoured model of bone mechanotransduction involves osteocytes and the lacunar-canalicular system. Mechanical loading strains the bone causing changes within this system that can stimulate osteocytes, the receptor cells residing within the system. The osteocytes then produce secondary signals that activate osteoblasts and osteoclasts, the effector cells, to produce an appropriate tissue-level response [30]. The mechanisms of mechanotransduction, mechanosensitivity, and response signalling in bone are not fully understood.

Osteocytes are widely believed to be the main mechanosensing structures of bone, responsible for coordinating the regulation of bone adaptation. Osteocytes are the largest bone cell population, spaced regularly throughout the mineralized matrix supporting the belief that they are bone mechanosensors. Mature osteocytes reside within the lacunar-canalicular system of bone. Their cell bodies sit in the lacunae with their long slender processes radiating out in all directions through the bone matrix via narrow canals, the canaliculi (Figure 2.1). They are connected to one another via their processes and have the ability to communicate with each other and other bone cells through this extensive network of processes connected by gap junctions. The structure of the lacunar-canalicular system allows communication with various cells throughout the entire bone and ensures access to oxygen and nutrients. Osteocyte viability may play a crucial role in the

maintenance of bone homeostasis and integrity. Osteocyte apoptosis can occur due to a number of factors including: microdamage, estrogen deprivation, elevated cytokines, osteoporosis, and aging [31]. Osteocytes are recognized as the bone mechanosensors but how they sense mechanical loads and coordinate the subsequent events leading to alterations in bone adaptation is not completely understood.

Mechanical stresses produced by different stimuli, including substrate deformation, fluid flow shear stress and hydrostatic pressure, all act upon osteocytes to a degree. But, the exact mechanism responsible for transducing bone mechanical loading into a useable cellular signal is not well understood. Mechanical loading of bone causes deformations of the cortical bone matrix. The loading creates volume changes in the fluid filled cavities of the lacunar-canalicular system, which causes temporary pressure gradients to develop and moves interstitial fluid throughout the system. This load induced fluid flow is thought to play a role in transducing mechanical signals imposed upon the bone into functional signals at the cellular level. There are a number of potential biophysical stimuli induced by loading within the bone cell environment including: hydrostatic pressure, strain, shear stress and electric potentials [32–34]. In addition, each of these factors has properties such as magnitude and frequency, which vary with loading conditions and can affect cellular responses. Mechanical loading of bone likely generates all of these signals at the same time, likely at varying degrees/levels, depending upon the nature of the loading. Distinguishing each of their roles is difficult.

Strong evidence exists to support fluid shear stresses, caused by the flow of canalicular interstitial fluid, as a predominant mechanism of cell stimulation [35,36].

Fluid shear stress has been widely studied as it can generate osteogenic responses in osteocytes, including the production of prostaglandins (PGs) [37,38]. The flow of canalicular interstitial fluid is believed to mechanically stimulate osteocytes through the generation of fluid shear stresses acting upon both cell bodies and processes. The mechanisms responsible for transducing that mechanical signal into cellular biochemical signalling is poorly understood. The potential mechanisms likely involve a change in the conformation of a protein due to applied mechanical forces [39]. Some likely candidates include the integrin-cytoskeleton complex, membrane channels, G-protein dependent pathways, mechanosomes and primary cilia [40]. Fluid flow may also have an electrokinetic effect on osteocytes through strain-generated potentials [31]. Either mechanism, or both in combination, might activate osteocytes, although cell culture experiments suggest that cells are more sensitive to fluid shear stresses than they are to electric potentials [41]. Strain-generated potentials may modulate the movement of ions such as calcium.

## **2.4 Bone Mechanical Stimulation**

The mechanotransductive mechanisms responsible for mechanically induced bone formation, although extensively studied both *in vivo* and *in vitro*, are still not completely understood due to the complexity of the process. Many mechanisms cannot be discerned from *in vivo* models, and *in vitro* models do not fully depict the *in vivo* biomechanical environment of bone cells, making it difficult to fully understand mechanotransduction.

A number of models exist for studying bone mechanical behaviour, each with limitations. *In vivo* experimentation allows the whole bone and cell environment to be studied in its natural state. The major drawback of *in vivo* models is the systemic complexity of using a whole animal. It is difficult to investigate the cellular and molecular mechanisms of bone modeling from such studies. Together with *in vitro* studies, which provide a closer look at cellular processes not afforded by *in vivo* studies, a better understanding of the mechanisms of bone mechanical stimulation can be obtained.

*In vitro* models are the method of choice for examining bone mechanotransduction at the cellular and molecular levels. Cell culture systems provide a local environment that is tightly controlled and can be manipulated depending upon the desired conditions. The major disadvantage of *in vitro* models is the lack of native environment for bone cells. The environment is greatly simplified and as such their behaviour and activity do not completely reflect *in vivo* processes. However, some aspects of bone mechanical stimulation cannot be easily examined *in vivo* and therefore *in vitro* studies are relied upon, while realizing their limitations.

#### **2.4.1 *In vivo* Mechanical Loading**

Mechanical loading effects on bone adaptation can be assessed using animal models. Such methods allow control of the loading environment and assessment and quantification of the resulting bone formation. Various mechanical loading techniques for the purpose of inducing *de novo* bone formation have been utilized. The non-invasive, external axial compressive loading of the murine tibia or ulna has become the method of

choice for studying mechanically induced bone formation in rats and mice. The axial compression is meant to mimic physiological loading through the joints. The forelimb compression model is used to study cortical bone responses in the central diaphysis of the ulna.

The rat forelimb compression model, which has benefits not offered by previous loading methods, has been used extensively by researchers to study cortical bone adaptation to mechanical loading [29] (Figure 2.2). Loading the forelimb in axial compression causes bending of the ulna, with the greatest compressive strain occurring on the medial periosteal surface of the ulna [42]. The forelimb model is non-invasive and the loading contact points are at the wrist and elbow, both of which are away from the midpoint of the ulna, the expected site of the highest strain and therefore the greatest bone formation. This ensures that any bone apposition that occurs in this area is a direct result of the strain produced from the bending of the ulna due to the applied load, and not from contact with the loading points themselves.

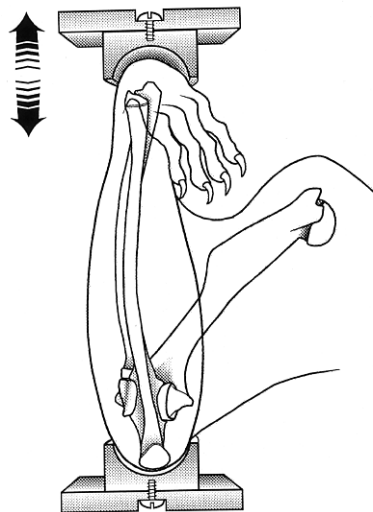


**Figure 2.2** Schematic diagram of the rat forelimb compression model [43].

*In vivo* mechanical loading models have helped to identify factors affecting cortical bone adaptation. Three such factors have been shown to be key: a dynamic stimulus, loading duration and accommodation to loading [44,45]. A dynamic stimulus, the primary stimulus of bone adaptation [46], has been shown to be effective at a minimum frequency of 0.5 Hz, but higher frequencies, up to approximately 10-20 Hz, induce greater bone formation [47]. Experimental results suggest that bone formation increases with either increased load magnitude or frequency [45]. Loading duration refers not only to the length of time the bone is being loaded but also to the lengths and number of rests the bone experiences. It has been shown that bone loses more than 95% of its mechanosensitivity after only 20 loading cycles [45]. It is thought that, if given time to rest, the cells may then be able to respond to the loading again. Resensitization has been shown to occur in seconds or hours depending on the nature of the loading stimulus. Time to rest is needed between loading bouts as well as between cycles [43,48]. Experiments have shown that there is an osteogenic benefit of even short-term (in the order of seconds) recovery periods in restoring sensitivity to loaded bone [49]. Bone adaptation occurs in response to a novel change in the loading environment, a new mechanical stimulus. Bone must be loaded above a certain strain threshold to induce a change in bone formation [27]. This threshold is a product of local loading history and may vary based on factors such as age, sex and loading model. Once accommodation to the new load has occurred, the load will no longer induce a response. The initial loading stimulus is suggested to have the greatest influence on bone formation, not the long-term accumulation of loading [50].

Inserting a rest period and stopping loading can reverse the effects of accommodation and restore mechanosensitivity [51].

These factors can be manipulated in a number of ways in non-invasive loading models, including the forelimb compression model, to induce different types of bone formation, such as lamellar or woven bone. The parameters of loading that are commonly modulated, each of which influences the amount and type of bone formation, are: force/strain magnitude, frequency, number of loading cycles and sessions and number and placement of rest periods (between cycles and loading sessions). The magnitude of the force/strain is controlled as it is tightly correlated to the amount of bone production [52]. The force magnitude is dependent on bone geometry and material properties and therefore differs with animal sex, age and weight/size. The strain magnitudes that stimulate bone formation depend on the animal used as well as the other loading parameters. In general, local peak strains between 1200 and 2000 microstrain ( $\mu\epsilon$ ) [52,53] have been shown to induce a lamellar bone formation response. However, this likely depends upon the model used. A frequency of 2-4 Hz is commonly used, as it coincides with the stride frequency range in rats during locomotion [54]. Various loading protocols have been implemented in the literature to stimulate bone formation, each differing with regards to the above parameters; this can make it difficult to compare study outcomes. Establishing a loading protocol that induces the desired bone response and allows for the examination of treatment effects in the chosen model is most important.

### 2.4.1.1 Lamellar and Woven Bone Formation

Osteogenic signals can arise from various sources including bone cells and vasculature. Signalling from these different pathways may be key to the different responses of cortical bone to non-damaging dynamic strain (lamellar bone) versus damaging dynamic strain (woven bone) (Figure 2.3). Lamellar bone is believed to form in response to molecular signals produced by mechanotransductive pathways within the bone [45]. In comparison, woven bone formation in response to fatigue loading is mediated by signals in response to damage and dynamic strain (mechanotransduction) [45]. Osteogenic signals from sources other than bone cells, such as the vasculature, may play a key role in the formation of woven bone in response to both dynamic strain and damage versus lamellar bone induced by dynamic strain alone.

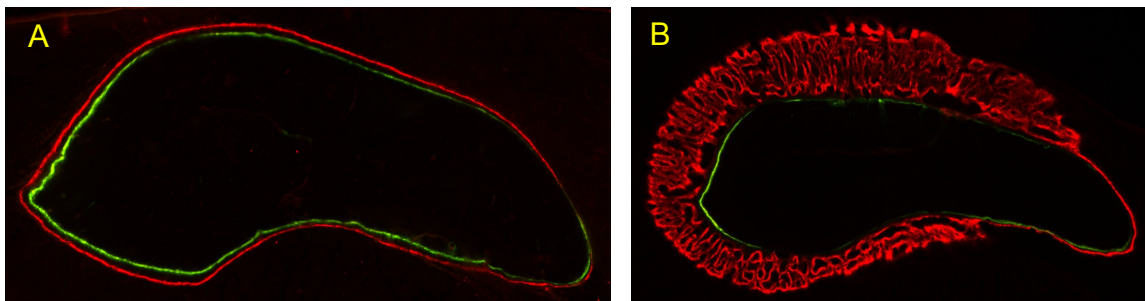


**Figure 2.3** **Fluorescent light microscope images of rat ulna cross-sections.** Calcein green (green) and alizarin complexone (red) fluorochrome labels have been incorporated into the newly formed bone around the perisoteum of the ulna. The original bone cross-section is the dark kidney-shaped space surrounded by the fluorochrome labels. **A) An example of lamellar bone formation.** The separation between the green and red labels demonstrates the new bone formation that has been mechanically induced. The relatively uniform separation between the labels is typical of lamellar bone formation. **B) An example of woven bone formation.** The large amount of red label that extends outward from the periosteal surface is new bone that has been created in response to damaging mechanical loading.

The bone formation response to mechanical stimuli depends not only on the magnitude of the peak forces, but also on the loading frequency and the number of cycles incurred by the bone. Together these will determine the resultant bone type, lamellar or woven. Lamellar bone forms in response to lower levels of strain, anabolic stimuli, and is a slow forming but very strong, dense bone. It is highly organized consisting of parallel layers or lamellae. Lamellar bone has fewer cells compared to woven bone [22]. Woven bone forms in response to high levels of strain or high amounts of loading, which cause fatigue damage of the bone. It is poorly organized and weaker compared to lamellar bone but it forms rapidly, enabling it to provide support to damaged bone quickly. The amount of woven bone formation directly parallels the amount of induced fatigue damage [55]. The collagen fibres and mineral crystals are randomly arranged but it is more mineralized than lamellar bone helping to compensate for its poor organization [22]. Woven bone has a low mineral density and high cellularity [22].

The molecular mechanisms responsible for the osteogenic responses of bone, either lamellar or woven, to mechanical loading are not fully understood. Early *in vivo* loading studies did not differentiate between lamellar and woven bone, or they employed loading protocols that induced both lamellar bone and woven bone, so signals responsible for each individual bone response could not be differentiated. More recent studies have examined the genetic, molecular and cellular responses to lamellar and woven bone formation. There are large differences in the timing and magnitude of gene expression between the vascular and molecular responses of lamellar and woven bone formation [56]. During lamellar bone formation genes related to cell signalling,

movement, proliferation and metabolism show peaks in transcriptional activity 4-8 hours [57–59] after loading and return to basal levels by 24 hours [56,58,59]. There is only a modest increase in osteoblast differentiation and very little cellular proliferation in lamellar bone formation, indicating existing osteoblasts are active [56]. Woven bone formation is associated with a greater number of differentially regulated genes, with earlier and significantly greater upregulation of osteogenic genes being shown [56]. Specifically, cellular proliferation and angiogenesis appear to be important for woven but not lamellar bone formation [56]. Inflammation, cytoskeletal remodelling, cell adhesion and developmental pathways are also affected in woven bone formation [56]. The magnitude of the molecular response dictates the magnitude of subsequent bone formation, thus the reason for much less lamellar bone formation following mechanical loading compared to woven bone [56].

#### **2.4.2 *In vitro* Mechanical Loading**

Mechanical loading of bone results in a number of potential stimuli for bone cells and as such a number of methods have been employed to stimulate bone cells *in vitro* based upon these, including; substrate deformation or stretching, vibration platforms, pressure and fluid shear stress.

Mechanical loading of bone likely generates a number of mechanical signals at the same time, likely at varying degrees, depending upon the nature of the loading. Distinguishing each of their roles is difficult. Unlike *in vivo* loading, *in vitro* experiments generally use just one type of force application to stimulate cells, separating the forces

from one another. Fluid shear stresses are believed to be one of the main mechanical factors stimulating osteocytes when bone is mechanically loaded [23]. Fluid shear stresses are generated by the flow of interstitial fluid within the lacuna-canalicular system, where the osteocytes reside, when the bone is loaded [60]. Mechanical loading in bone occurs on the organ level, with compression and tension occurring on opposite regions, generating a pressure gradient across the bone. This drives fluid from one side to the other, creating fluid shear stresses. Pressure gradients are also created within individual canaliculi [61]. Fluid shear stresses are dependent upon the nature of the mechanical loading and vary throughout the bone environment. Theoretical models have predicted that *in vivo* physiological fluid shear stresses experienced by osteocytes within the lacuna-canalicular system are between 0.8 and 3 Pa [62].

Various flow profiles have been studied and implemented in *in vitro* flow experiments including: steady flow (SF), pulsatile fluid flow (PFF) and oscillatory fluid flow (OFF). It is unknown which flow profile is most physiologically relevant. However, oscillatory fluid flow is considered to be the most representative of *in vivo* conditions because when bone is loaded, matrix deformation occurs causing pressurization of the bone [63]. This pressurization causes fluid to flow in the lacuna-canalicular system along a pressure gradient. When the load is then removed, the pressure gradient reverses and so too does the fluid flow direction [63]. This creates an oscillating fluid flow profile. Fluid flow generally takes place at 1 Hz frequencies in these models, which is typical of locomotion [64]. However, greater frequencies have been recorded during activity [65] and have been studied [66].

Similar to *in vivo* models, flow parameters can be manipulated in *in vitro* models of fluid shear stress. Along with the flow profile, the shear stress amplitude, frequency and duration of flow can all be altered and all have been shown to affect bone cell responses [63,66–70]. In general, studies implement fluid shear stresses between 1 and 2 Pa [70–74], falling within the range of predicted *in vivo* stresses [62]. Flow durations are generally 1 to 2 hours in length [70,73–75]. Oscillating frequencies vary depending upon the study, but generally 1 Hz is the frequency most used [70,73–75]. In general, most cell responses exhibit a dose responsive behaviour, with greater shear stresses, frequencies and durations, increasing the responses to fluid flow. As well, cells appear to respond to the parameters in a synergistic manner [66].

Fluid-flow induced shear stress has been widely studied in bone cells *in vitro* [63,66,76,77]. Several methods exist for generating fluid-flow induced shear stress, including the orbital shaker and the parallel plate, each with their own advantages and limitations. Parallel plate flow chamber systems have been used extensively to study *in vitro* bone mechanotransduction [33,63,76]. They have the ability to apply a well-defined shear stress and can decouple flow rate from flow frequency [63]. However, due to the complexity and expense of these systems only a limited number of samples can be evaluated in a single experiment. In addition, the cells undergo a large amount of manipulation when they are loaded into these systems. Orbital shakers address some of the limitations of parallel plate flow chambers. Most importantly, the cells experience a lot less manipulation during set up with the orbital shaker. Orbital shakers are simple to use and allow a number of experimental groups to be run simultaneously. However, they

too have limitations; the magnitude of shear stress can only be estimated in the system and the fluid flow is not truly oscillatory. It is important to understand the strengths and limitations of each model, in order to choose the one best suited to address the individual aims of each study.

## **2.5 Prostaglandins and Bone**

### **2.5.1 Prostaglandins**

Prostaglandins are eicosanoids, which are signalling molecules derived from oxygenated 20-carbon polyunsaturated fatty acids. They act in an autocrine/paracrine manner via G-protein coupled receptors (GPCRs) [78]. PGs are produced in most tissues and cells, including bone and are well recognized modulators of skeletal homeostasis. They are not stored in cells and are rapidly degraded *in vivo* [78]. The predominant polyunsaturated fatty acid substrate for cyclooxygenase in humans which gives rise to the 2-series of PGs is arachidonic acid (AA). The 2-series PGs are one of the most important of the physiologically active PGs and the PGs most studied in bone because they are highly produced by cells of the osteoblastic lineage, osteoblasts and osteocytes, and can have substantial effects on both bone resorption and formation [78].

The production of PGs involves three steps (Figure 2.4): (1) mobilization of AA; (2) conversion of AA to unstable intermediates, prostaglandin G<sub>2</sub> (PGG<sub>2</sub>) and then prostaglandin H<sub>2</sub> (PGH<sub>2</sub>); and (3) conversion of PGH<sub>2</sub> by synthases to prostaglandin E<sub>2</sub> (PGE<sub>2</sub>) and other PGs [79]. The conversion of AA to PGs is catalyzed by a bifunctional enzyme generally called cyclooxygenase (COX). Nonsteroidal anti-inflammatory drugs

(NSAIDs) inhibit the action of COX and therefore inhibit prostaglandin synthesis. There are two enzymes for COX, COX-1 and COX-2. COX-1 is constitutively expressed at relatively stable levels in most tissues with little regulation, whereas COX-2 is generally expressed at very low basal levels in most tissues but can be induced rapidly to high levels by multiple factors including cytokines, hormones, growth factors and mechanical strain [78]. In bone, the basal level of COX-1 mRNA expression is far greater than that of COX-2 [80].

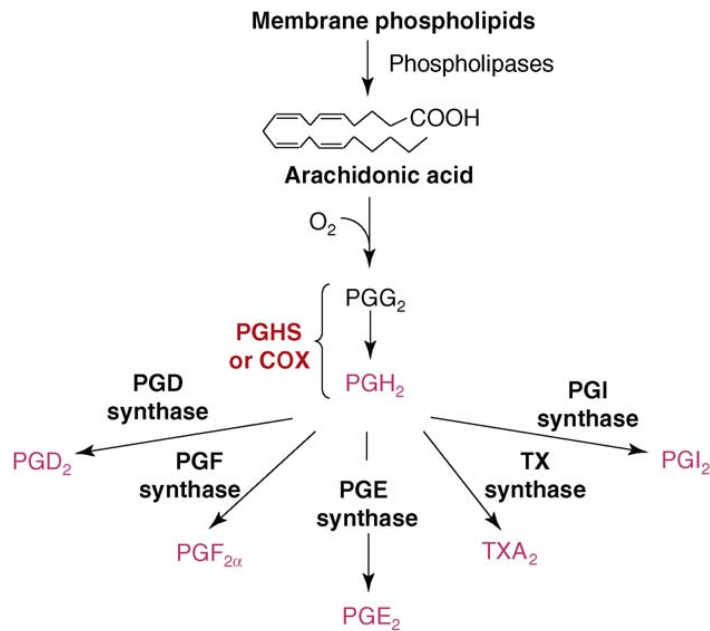


**Figure 2.4** Synthesis of prostaglandins [78].

Despite having similar catalytic mechanisms, COX-1 and COX-2 appear to be independently functioning biosynthetic pathways [78]. This is due in part to the differential regulation of their expression. COX-1 has relatively few identified functional regulatory elements and COX-1 mRNA is constitutively expressed in most tissues [78]. COX-2 has multiple potential transcriptional regulatory elements and COX-2 mRNA is

rapidly and transiently inducible in many tissues [78]. Rat osteoblasts and osteoclasts *in vivo* express detectable levels of COX-2 protein at basal levels [81]. Activation of COX-2 mRNA expression is faster, more pronounced and transient compared to COX-1 [81]. There are clear differences in PG production by COX-1 and COX-2 with COX-2 being more efficient at producing PGs in many circumstances [78]. The role of COX-1 in bone is still not completely clear.

### **2.5.2 Mechanotransduction and Prostaglandins**

Fluid flow within the lacunar-canalicular system appears to be a primary mechanical stimulus for osteocytes. It has the potential to affect a number of different mechanisms to induce cellular biochemical responses. The intracellular signalling pathways activated by the sensing mechanisms and the manner in which osteocytes orchestrate these signals to produce an appropriate tissue level response are not well understood. However, a number of intracellular signalling pathways have been identified. They range from second messengers such as intracellular calcium and cAMP to intermediate protein kinase signalling cascades to late responses such as PGE<sub>2</sub> release and altered gene expression [40].

The release of PGE<sub>2</sub> by bone and bone cells has long been known to be one of the responses to mechanical stimuli [76,82]. PGE<sub>2</sub> is one of the likely intermediaries for cell-to-cell communication between osteocytes and osteoblasts and osteoclasts. Support for the role of prostaglandins in bone mechanotransduction stems from studies

demonstrating that the inhibition of COX and subsequently PG production can affect mechanically induced bone formation [9–12,14].

The events and signalling pathways responsible for the induction of COX-2 and subsequently PGE<sub>2</sub> production remain uncertain but several potential pathways have been identified (Figure 2.5). They include a G protein-linked mechanotransducer and the integrin-cytoskeleton complex [83]. Support for the involvement of G proteins comes from the decreased PG production following mechanical loading when G protein inhibitors are applied to bone cell cultures [84]. The G protein-linked mechanotransducer resides in the cell membrane and a conformational change can occur with mechanical stimulation. Fluid flow can activate phospholipase C (PLC) and initiate inositol triphosphate (IP<sub>3</sub>) signalling through a G-protein-mediated mechanism leading to COX-2 expression and PGE<sub>2</sub> production [40]. This pathway also controls the release of intracellular calcium which can alter COX-2 expression [38].

Intracellular calcium modulates the functions of various enzymes linked to PG production including, phospholipase A<sub>2</sub> (PLA<sub>2</sub>), which releases arachidonic acid from the plasma membrane and protein kinase C (PKC), which has been shown to affect the PGE<sub>2</sub> response to mechanical stimulation in osteocytes [85]. The generation of arachidonic acid is a necessary step in PG production; it is the substrate for PG production by COX. Arachidonic acid can be generated through pathways involving PLA<sub>2</sub> and/or the combined action of PLC and diacylglycerol (DAG) lipase. Intracellular calcium modulates the function of these pathways [85]. Ajubi et al. [85] showed that both PLA<sub>2</sub> and the combination of PLC and DAG lipase are involved in the generation of

arachidonic acid in the acute PGE<sub>2</sub> response of osteocytes to fluid shear stress. However, PGE<sub>2</sub> release in response to fluid flow has been shown to be independent of intracellular calcium signalling [86].

The integrin-cytoskeleton complex has also been identified as another potential pathway responsible for the synthesis of PGs [84]. Integrins are transmembrane proteins that bind the extracellular matrix on the outside of cells to the actin cytoskeleton, acting as mechanotransducers [84]. The cytoskeleton is physically linked to many cellular components, including ion channels, PKC and PLA<sub>2</sub> [85], and some may be involved in fluid flow-induced PG production. COX-2 has been shown to be upregulated by mechanical loading through the formation of focal adhesions and subsequent ERK and PKA signalling pathways in osteoblasts [87]. As well, disruption of the cytoskeleton has been shown to inhibit COX-2 expression and PGE<sub>2</sub> production in response to fluid shear stress [84,88,89].

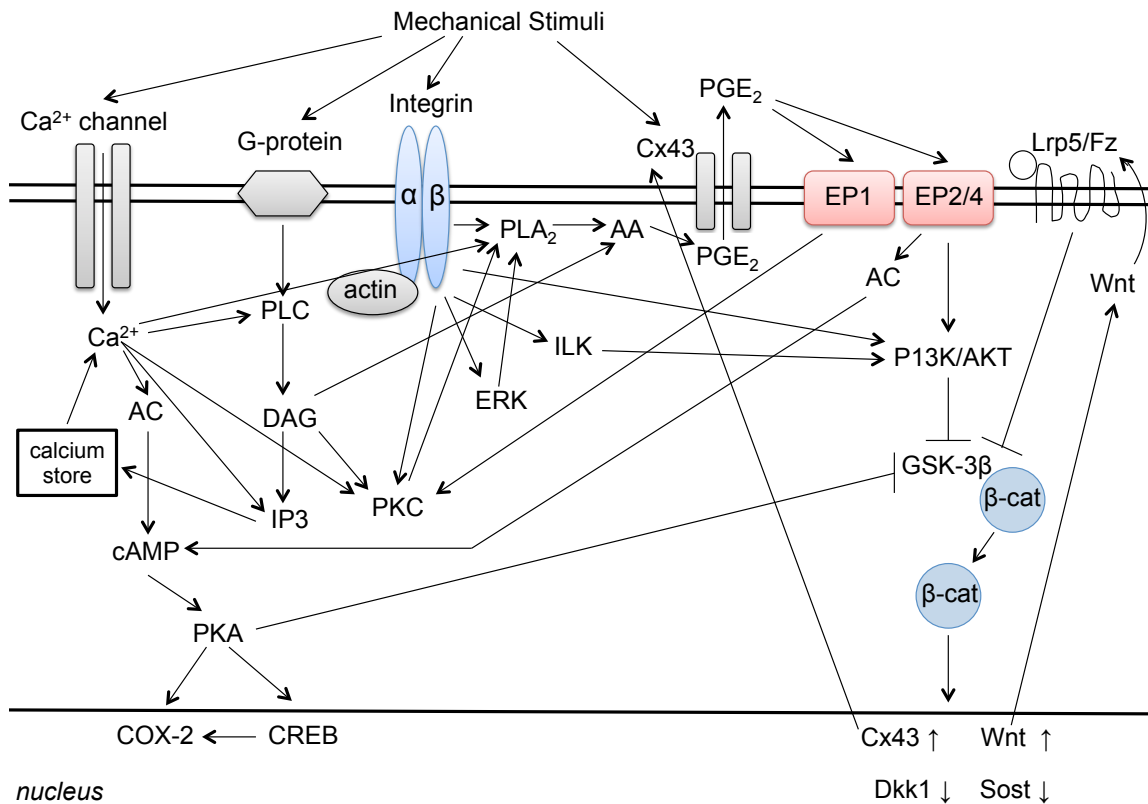


**Figure 2.5 Schematic diagram of potential PG signal transduction pathways involved in the mechanical stimulation of osteocytes.**

### 2.5.3 Timing of COX-2 Induction in Response to Mechanical Stimulation

The mechanisms by which mechanical stimuli induce COX-2 mRNA and protein expression in osteocytes are not well understood. However, it is well known that mechanical stimulation alters COX-2 mRNA and protein expression in a time dependent manner, highlighting the importance of the timing of NSAID delivery around the time of mechanical loading.

COX-2 mRNA induction exhibits a biphasic pattern in response to stimulation. The time between the two peaks of COX-2 expression varies depending upon the tissue or cell type and the stimuli. It has been shown to be as short as 10 hours or as long as

24-48 hours [90,91]. The biphasic pattern is present whether or not the stimuli are present throughout the entire induction period [91] or just after induction [90]. It is believed that the biphasic pattern, specifically the second peak, is likely the result of autoamplification by PGE<sub>2</sub>, as PGE<sub>2</sub> can induce COX-2 [92]. As PGE<sub>2</sub> increases, it stimulates COX-2, enhancing its own production [91]. Support for autoamplification is provided by the observation that in general, COX inhibitors reduce the second induction peak with no effect on the initial induction peak [81]. A similar trend to the mRNA biphasic pattern is seen in the COX-2 protein expression. Protein expression increases to peak levels a few hours after COX-2 mRNA induction and is followed by a plateau and a second peak in levels [93]. It is unknown whether or not COX-2 enzyme activity is closely correlated to the mRNA and protein biphasic pattern [81].

Upon exposure to mechanical loading or strain, bone and bone cells stimulate PG synthesis, especially PGE<sub>2</sub>. This is an early response, occurring within 5-15 minutes *in vitro* [76] and 1 hour *in vivo* [94]. This synthesis can last 10-15 minutes or for 1-24 hours [76]. COX-2 activity is necessary for the early PG synthesis because it has been shown that both nonspecific and specific COX inhibitors block this PG production [95]. In addition, mechanically induced bone formation is reduced following COX-2 inhibition, as a result of a lack of PGs [10–12].

COX-2 is an early response gene induced by mechanical loading and its mRNA is upregulated in bone and bone cells, without any effect on COX-1 expression [76,95]. It is believed that the COX-2, produced by the early upregulation of mRNA, is not responsible for the immediate rise in PG production in response to mechanical loading [81]. The

mechanically induced COX-2 mRNA expression starts 15-60 minutes after loading and peaks 1-3 hours later [76,90]. It was shown that COX-2 mRNA levels in rat tibiae subjected to 4-point bending return to control levels 24 hours post-loading [81]. Induced COX-2 protein synthesis starts 1-3 hours later than mRNA induction and peaks 2-9 hours later in bone tissues [96]. So, COX-2 protein synthesis starts 1-4 hours post loading and peaks at 3-12 hours. Since the mechanically induced COX-2 production is delayed after loading, the early release of PG (within the first hour) seems to be a result of COX-2 already available, and not induced COX-2. Therefore, the PGs responsible for signalling mechanically induced bone formation are a result of constitutive COX-2.

More support for a lack of a role of induced COX-2 in mechanotransduction is provided by studies that administered COX inhibitors after loading and found no effect on bone formation [11,12]. Plasma levels of COX inhibitors do not reach their peak until 2-6 hours after administration [11] and therefore, if they are given after loading they would not be in effect until the period of induced COX-2 protein increased and peaked. So, induced COX-2 activity does not appear to be involved with mechanotransduction.

COX-2 is expressed when a prolonged period of PGs is required, as is the case in inflammation or when mechanical loading triggering bone adaptation and various cell responses, including differentiation and replication, are needed [81]. Induced COX-2 produces large amounts of PGs that can then induce bone formation. Chow and Chambers [11] showed that daily administration of indomethacin (a nonspecific COX inhibitor) for 7 days post-loading inhibited bone formation, indicating that induced COX activity is required for the subsequent bone response to mechanical loading. The induced

COX-2 protein level can remain elevated for 1-3 days which is thought to supply enough PGs for a bone formation response to occur [93].

The differences in the activity of COX-1 and COX-2 throughout mechanotransduction may be dependent on the local AA concentration and the availability of AA [97]. When AA concentration is low, COX-2 is most active, and when AA concentration is high, COX-1 is most active [98]. The immediate phase of PG synthesis involves a high concentration of AA as it is quickly released, stimulating the activity of both COX-1 and COX-2, leading to a production of PGE<sub>2</sub> within minutes [97]. During the delayed response, AA release may be gradual, limiting the availability, so now only COX-2 is active and responsible for the production of PGE<sub>2</sub> after mechanical stimulation [97].

In summary, COX-1 is involved in the immediate PG response, within several minutes of stimulation, associated with phospholipid remodeling [98]. COX-1 expression is restricted to the immediate PG response. COX-2 induced PG synthesis, however, occurs over several hours and is active in both the immediate and delayed PG responses [10,98]. COX-2 is able to induce prolonged PG synthesis and is integral in promoting long-term PG effects.

#### **2.5.4 PGE<sub>2</sub> Release and Actions**

The exact mechanisms by which mechanical stimuli activate PGE<sub>2</sub> synthesis are not well understood. However, it is well established that upon stimulation by fluid shear stress, osteocytes release PGE<sub>2</sub>. That release has been shown to occur through

hemichannels. Hemichannels are formed by connexins, proteins that form gap junctions on unopposed cell membranes. Osteocytes express hemichannels formed by connexin 43 (Cx43). These hemichannels are mechanosensitive and their opening is controlled by mechanical stimulation [99]. Fluid flow induced shear stress can stimulate the opening of hemichannels expressed in osteocytes, creating a channel for the release of intracellular PGE<sub>2</sub> [37]. The upstream events that control PGE<sub>2</sub> release are poorly understood, but mechanical stimulation of osteocytes results in the release of PGE<sub>2</sub>. Once released through Cx43 hemichannels, PGE<sub>2</sub> can act in an autocrine and/or paracrine manner.

The COX-2/PGE<sub>2</sub> system interacts with other pivotal bone regulatory signals including the Wnt/ $\beta$ -catenin pathways [100] (Figure 2.5). The Wnt/ $\beta$ -catenin signalling pathway is an important regulator of bone mass and bone cell function. This pathway is important in osteoblasts for differentiation, proliferation and the synthesis of bone matrix [100]. It is also involved in osteocyte autocrine stimulation. PGE<sub>2</sub> autocrine stimulation via the EP2 receptor activates PI3K/Akt and cAMP-PKA signalling pathways, which leads to the downstream inhibition of GSK-3 $\beta$  and the intracellular accumulation of  $\beta$ -catenin [71,101–103].  $\beta$ -catenin then translocates to the nucleus where it alters the expression of a number of key target genes [101]. Cx43 expression can increase as a result, which in turn increases gap junction activity and promotes gap junction mediated communication in osteocytes [71,104,105]. Another effect is a reduction in sclerostin and DKK1 and increased expression of Wnt, which then leads to the binding of Wnt to LRP5-Fz and amplification of the load signal through further

inhibition of GSK-3 $\beta$  [101]. PGE<sub>2</sub> release occurs both before and independent of LRP5 and Wnt/ $\beta$ -catenin signalling [106]. In osteocytes, the Wnt/ $\beta$ -catenin pathway transmits anabolic signals of mechanical loading to other osteocytes and cells on the bone surface [101].

Released PGE<sub>2</sub> can also bind to one of its G-protein-coupled receptors (GPCRs) and activate adenylate cyclase [87]. Subsequently, PKA phosphorylates the CREB transcription factor, which can bind to the promoter of the COX-2 or the FosB/DeltaFosB gene [107]. PLC is also activated by GPCRs, resulting in the synthesis of IP3 and DAG, the latter may stimulate PKC [87], all of which may be involved in the PGE<sub>2</sub> response of bone to mechanical loading.

### **2.5.5 PGE<sub>2</sub> Receptors**

PGE<sub>2</sub> effects are associated with four classes of GPCRs: EP1, EP2, EP3 and EP4 [78]. EP receptors are expressed in osteoblastic, osteoclastic and osteocytic cells [79]. The effects of PGE<sub>2</sub> on bone have most often been associated with cAMP production and PKA activation [78]. PGE<sub>2</sub> can induce COX-2 [92] and this autoamplification is believed to occur via the activation of the EP1 receptor, which subsequently increases intracellular calcium [108]. EP3 receptor activation inhibits cAMP production [78].

EP2 and EP4 receptors have been extensively studied in bone. EP4 is the most abundant cAMP-related receptor in rat bone tissue and cells [109]. Both EP2 and EP4 receptors can stimulate cAMP formation [78]. The cAMP pathway is able to crosstalk

with several other pathways that regulate cell growth, migration and apoptosis [78]. Both EP4 and EP2 receptors have been implicated in the anabolic effects of PGE<sub>2</sub> *in vitro* [78] and appear to be involved in the regulation of osteoblast function including the ability of osteoblasts to support osteoclast formation [78]. The EP2 receptor, expressed in osteoblast precursor cells, mediates bone formation [110]. EP4 receptor knockout (KO) mice have been shown to have reduced bone mass [79] and bone biomechanical properties were reduced in both EP2 and EP4 KO mice [111,112]. Studies with EP KO mice have implicated EP4 and, to a lesser extent, EP2 in PG mediated bone resorption and have shown that EP4 is essential for a local anabolic response to exogenous PGE<sub>2</sub> [109,112].

Much of the complexity of PGE<sub>2</sub> effects on bone may be attributable to the multiple transmembrane GPCRs for PGE<sub>2</sub> and their ability to activate different signalling pathways.

### **2.5.6 Effects of Prostaglandins on Bone**

Prostaglandins have a complex relationship with bone. They are important for bone mechanotransduction and influence both bone formation and resorption. To better understand the roles that PGs play in bone, studies have examined the effects of exogenous PGE<sub>2</sub> on bone both *in vivo* and *in vitro*. This, however, lacks the ability to demonstrate how endogenous PGE<sub>2</sub> truly affects bone processes *in vivo*. Studies implementing COX knockout animal models or NSAIDs are used to infer the mechanisms of actions of endogenous PGs in bone. However, little is known about

endogenous PG concentrations and how they vary under different conditions, because it is difficult to determine PG concentrations *in vivo*. Determining how PGs will affect bone processes is complicated and not fully understood. However, it is evident that PGs influence various bone activities.

### **2.5.6.1 Prostaglandins and Bone Formation**

Systemic exogenous PGE<sub>2</sub> can increase both bone resorption and formation; however, formation can be greater, resulting in increases in bone mass, both cortical and cancellous [113–118]. But, the effects of PGE<sub>2</sub> on bone have been shown to be dose and timing dependent [100,119–123]. Continuous or high doses of exogenous PGE<sub>2</sub> in rats and mice can lead to bone loss, whereas intermittent or low doses can be anabolic [119–125].

PGE<sub>2</sub> increases *in vivo* bone formation and bone mass mainly by increasing the number of osteoblasts present on bone surfaces and by inducing the production of new bone [118]. PGE<sub>2</sub> has been shown to induce early response genes [126], recruit and stimulate differentiation in mesenchymal stem cells [127] and induce the expression of EP4 *in vivo* and *in vitro* [109], ultimately increasing the number of osteoblasts and osteogenic activity [118,128]. Exogenously administered PGE<sub>2</sub> likely acts on EP4 receptors [109].

Exogenous PGE<sub>2</sub> has also been shown to induce COX-2 expression in MC3T3-E1 osteoblastic cells [92] and *in vivo* [80]. COX-2 activity and the endogenous production of PGE<sub>2</sub>, however, was shown not to be essential for the anabolic action of PGE<sub>2</sub> *in vivo* or

*in vitro* [80]. In addition, it has been shown that even without a COX-2 gene or in the presence of NSAIDs, osteoblast differentiation *in vitro* can be enhanced by the induction of endogenous PGs with freshly added serum and some osteogenic agonists [79]. Inducing COX-2 and PG production by these factors might engage additional osteogenic signalling pathways that stimulate the differentiation of early osteoblastic precursors [79]. Endogenous PGs can enhance or inhibit the osteogenic effects of factors inducing them, depending on the inducing factor.

PGE<sub>2</sub>, however, has been shown to have a dose dependent effect on bone and bone cells [100,119–123]. Dose dependent effects on growth, differentiation, EP receptor expression, OPG/RANKL expression, ALP expression and components of the Wnt signalling pathway in pre-osteoblasts have been shown [100,119]. Lower PGE<sub>2</sub> concentrations appear to enhance osteoblast activity; they increase pre-osteoblast proliferation, OPG, ALP and EP4 receptor expression and Wnt signalling in osteoblast-lineage cells [100,119]. In contrast, higher doses of PGE<sub>2</sub> inhibit cell proliferation and differentiation [100], inhibit collagen synthesis [110], inhibit the expression of OPG, ALP and EP2 receptors and increase the expression of Wnt inhibitors and EP3 receptors in pre-osteoblast cells [100,119]. Therefore, it appears that the net effect of higher doses of PGE<sub>2</sub> is decreased osteoblast activity.

#### **2.5.6.2 Prostaglandins and Bone Resorption**

PGs can influence osteoclast activity as well. PGs can enhance the stimulation of osteoclast differentiation by several resorption agonists, including cytokines, hormones

and growth factors [79]. Multiple agonists can also stimulate PG dependent osteoclast formation in culture [78]. PGE<sub>2</sub> stimulates osteoclast formation and differentiation and bone resorption in culture, largely mediated via the EP4 receptor with minor contributions from EP2 receptors [78,79,129]. The EP2 receptor may also be involved in the effects of PGE<sub>2</sub> on hematopoietic precursors [79]. COX-2 is expressed in cells of the hematopoietic lineage and induction of COX-2 is likely responsible for the PG enhancement of stimulated osteoclastogenesis [78]. Without a COX-2 gene or in the presence of a COX-2 inhibitor, in culture, PGE<sub>2</sub> production is decreased and osteoclast formation is reduced [79,110]. PGs produced by COX-2 are necessary for maximal *in vitro* osteoclastogenesis in response to multiple agents [79]. However, the effects of PGs on the hematopoietic lineage in regards to resorption and osteoclastic development *in vivo*, are not well known. Some studies, however, have found PGE<sub>2</sub> to have inhibitory effects on osteoclast formation from hematopoietic precursors [78]. PGE<sub>2</sub> added to isolated osteoclasts actively resorbing bone *in vitro* transiently inhibited their activity and involved both the EP4 and EP2 receptors [79,130]. EP4 and EP2 receptor expression is down regulated during differentiation in culture and this may be one way osteoclasts escape the inhibitory effects of PGE<sub>2</sub> [78].

Osteoblasts have a role in the regulation of bone resorption. Studies suggest that PGE<sub>2</sub> and COX-2 are involved in the process of osteoclast differentiation through osteoblasts and the RANK/RANKL/OPG pathway [79]. Osteoblasts express receptor activator of nuclear factor kappa-B (RANK) ligand (RANKL), which binds to its receptor, RANK, on the surface of osteoclasts and their precursors, regulating precursor

differentiation and osteoclast activation and survival. Osteoblasts secrete a decoy receptor osteoprotegerin (OPG), which blocks RANK/RANKL interaction by binding to RANKL, preventing osteoclast differentiation and activation. The major effect of PGE<sub>2</sub> on bone resorption is generally considered to occur indirectly via the upregulation of RANKL expression and inhibition of OPG expression in osteoclast supporting cells, osteoblasts and/or their precursors [78,119,129]. The induction of RANKL can be blocked by COX inhibitors demonstrating that PG production is involved in RANKL expression in osteoblasts [91]. Han et al. [131] showed that RANKL can induce COX-2 expression and in turn the production of PGE<sub>2</sub> in osteoclastic cells. Inhibition of COX-2 with celecoxib inhibited osteoclast differentiation, which was reversed by the addition of exogenous PGE<sub>2</sub>, suggesting that COX-2-dependent PGE<sub>2</sub> induction by RANKL is required for osteoclast differentiation [131]. PGE<sub>2</sub> can stimulate bone resorption indirectly via increased expression of RANKL by osteoblasts and via direct effects on osteoclasts and their precursors.

PGE<sub>2</sub> influences both osteoblast and osteoclast activity, which subsequently affects bone formation and resorption. It appears that PGE<sub>2</sub> concentration is important for determining the resultant effect on bone. Further study is therefore needed to determine how exogenous PGE<sub>2</sub> levels relate to endogenous levels and how to best optimize PGE<sub>2</sub> concentrations *in vivo* to promote bone formation, not resorption.

## **2.6 NSAIDs and Bone**

### **2.6.1 NSAIDs**

NSAIDs variably inhibit the activity of both COX-1 and COX-2. COX is the enzyme that catalyses the synthesis of prostaglandins from the substrate arachidonic acid. The COX enzyme has two distinct active sites, the cyclooxygenase active site and the peroxidase active site [132]. The cyclooxygenase site cyclizes arachidonic acid and adds a hydroperoxy group to form PGG<sub>2</sub> [132]. The peroxidase site of the same COX molecule reduces this hydroperoxy group to the hydroxy group to form PGH<sub>2</sub> [132]. NSAIDs inhibit the cyclooxygenase active site of COX, but have no effect on the peroxidase active site [132]. NSAIDs compete with arachidonic acid for the active site of the enzyme; this competition leads to inhibited production of prostaglandins.

The cyclooxygenase active sites or the NSAID binding sites of COX-1 and COX-2 differ by a single amino acid [132]. This produces a side pocket as part of the NSAID binding site of COX-2, which is not present in the NSAID binding site of COX-1 and increases the overall size of the binding site [132]. Because of this, NSAIDs can be non-selective or selective. Non-selective NSAIDs fit the NSAID binding sites of both COX-1 and COX-2 and act as competitive inhibitors of both enzymes. COX-2 selective inhibitors are larger than non-selective NSAIDs. The conformation of COX-2 selective NSAIDs does not allow them to easily fit into the NSAID binding site of COX-1, but allows them to fit into the side pocket of the NSAID binding site of COX-2 [133,134].

The interaction of NSAIDs with COX generally follows a two-step kinetic sequence. The first step involves rapid binding of the inhibitor at the surface near the

membrane-binding region of the enzyme; this is the entrance to the channel leading to the COX active site [135]. This forms a reversible enzyme-inhibitor complex between COX and NSAIDs, leading to competitive inhibition [136]. The second step involves the translocation of the inhibitor along the channel and subsequent association within the COX active site [135]. This step is the time-dependent conversion of the initial enzyme-inhibitor complex to one in which the inhibitor is bound more tightly. Formation of the tightly bound complex occurs in seconds to minutes and is thought to reflect the induction of a subtle protein conformational change [136]. These two steps are common for COX-1 and COX-2 inhibition for the majority of NSAIDs. A third kinetic step has been identified to occur with some COX-2 selective inhibitors, including celecoxib and NS-398 [135]. It is thought to involve a re-arrangement of the inhibitor in the active site, which results in a tightly bound enzyme-inhibitor complex that optimizes the inhibitor and protein conformational changes in the active site and side pocket [135].

NSAIDs can be sub-categorized based on their kinetic mechanism of inhibition: 1) competitive reversible inhibitors; 2) time-dependent reversible inhibitors; and 3) irreversible covalent modifiers [136]. Competitive reversible inhibitors are purely reversible COX inhibitors, competing with arachidonic acid for the COX active site, such as ibuprofen. Time-dependent reversible inhibitors exhibit more complex kinetics than simple, competitive inhibitors. They form an initial reversible enzyme-inhibitor complex but this complex is then converted to a more stable enzyme-inhibitor complex in a time-dependent manner. The dissociation of the inhibitor from the complex occurs very slowly. Indomethacin, NS-398 and Celebrex fall into this category. Indomethacin inhibits

both COX-1 and COX-2 in a time-dependent manner [137]. NS-398 and Celebrex inhibit COX-2 in a time-dependent manner but inhibition of COX-1 is not time dependent, it is reversible [137]. Selective COX-2 inhibitors are competitive inhibitors of both COX-1 and COX-2 but exhibit selectivity for COX-2 in the time dependent step by binding tightly at the active site and causing a conformational change in the isoenzyme structure [136]. The only NSAID that covalently modifies COX-1 and COX-2 is aspirin; it involves initial reversible binding and then an irreversible change of the active site [136].

The COX-2 selectivity of NSAIDs is defined by the COX-1/COX-2 ratio (Table 2.1). A greater COX-2 selectivity is reflected by a larger ratio. The ratio can vary, however, depending on the assay used, *in vitro* or *in vivo*, and the conditions the assay was performed under [138]. These ratios may vary ten fold depending upon assay conditions [138]. The most direct method to determine the ratio is with an *in vitro* assay using IC<sub>50</sub> values, the concentrations required to inhibit 50% of the activities of purified recombinant human COX-1 and COX-2 [139]. It can also be determined *in vitro* using a whole blood assay [139]. However, *in vitro* assays do not completely reflect *in vivo* conditions; *in vivo* assays provide the most relevant COX-1/COX-2 ratios. *In vivo* assays, developed in the rat, determine the dose required to inhibit 50% of the activities (the ED<sub>50</sub> value) of COX-1 (as determined by synthesis of gastric prostaglandins) and of COX-2 (as determined by synthesis of prostaglandins induced in response to carrageenan injected into an air pouch) [140]. However, clinical data provide the most meaningful classification of NSAIDs with respect to COX-2 selectivity [138]. Based on that, COX-2

specific inhibitors only inhibit COX-2 mediated events and not COX-1-mediated events even at high doses; celecoxib is an example of a COX-2 specific inhibitor [138]. COX-2 selective inhibitors inhibit COX-2-mediated events at low doses, but inhibit COX-1 mediated events at higher doses; NS-398 is an example [138]. Non-selective inhibitors inhibit COX-1 mediated events preferentially or inhibit COX-1 and COX-2 mediated events approximately equally; ibuprofen and indomethacin are non-selective NSAIDs [138].

**Table 2.1 COX-1/COX-2 ratios of NSAIDs used in this study.**

<b>Drug</b>	<b>Human recombinant enzymes (COX-1 IC50/COX-2 IC50) [141]</b>	<b>Whole blood assay (COX-1 IC50/COX-2 IC50) [142]</b>	<b><i>In vivo</i> (COX-1 ED50/COX-2 ED50) [143]</b>
<b>celecoxib</b>	375	7.6-9.09	>33
<b>ibuprofen</b>	0.215	0.592	0.1
<b>indomethacin</b>	0.1	0.562	2
<b>NS-398</b>		14.3	

Adapted from [138]. COX-1/COX-2 ratio expressed as the ratio of the 50% inhibitory concentration/dose for COX-1 to the 50% inhibitory concentration/dose for COX-2. Ratios <1 indicate preferential inhibition of COX-1 and ratios >1 indicate preferential inhibition of COX-2.

### **2.6.2 Effects of NSAIDs on Bone**

NSAID effects on bone appear to be very complicated, likely due to their mechanism of action and the complex nature of PG effects on bone. NSAIDs are designed to reduce inflammation through the inhibition of PG synthesis. As such, they may help to reduce inflammation-mediated bone loss. However, they have also been shown to reduce bone formation in response to mechanical loading, by blocking mechanotransductive signals mediated through PGs. Determining the dominant action

may depend upon several factors including the NSAID in use, the dosing and timing of administration, the age and sex of subjects examined, the mechanical stimuli involved, if any, and the overall state of the bone environment. Further investigation is needed to determine how to best manage NSAID administration to limit adverse effects on bone and even possibly encourage positive outcomes.

#### **2.6.2.1 NSAIDs and Bone Cells**

NSAIDs can affect osteoblast activity. They have been shown to adversely affect osteoblasts; they can induce cell death, arrest cell cycle and inhibit proliferation in osteoblasts and bone marrow mesenchymal stem cells [144–147]. Interestingly, non-selective NSAIDs, at therapeutic doses, were shown not to have cytotoxic effects on human osteoblasts [147] or bone marrow mesenchymal stem cells [145] but the selective NSAID celecoxib did [147]. However, non-selective NSAIDs have been found to have cytotoxic effects on rat calvarial osteoblasts [144]. Evans and Butcher [148] found that both a non-selective NSAID, indomethacin, and a COX-2 selective inhibitor had similar effects on most of the osteoblast parameters they examined; both decreased the number of human osteoblasts in culture without affecting DNA synthesis and in both cases the osteoblasts could recover and increase in number after brief exposure to the NSAID. Interestingly, some studies demonstrated that the inhibited proliferation and cell death caused by the presence of NSAIDs, in osteoblasts and bone marrow mesenchymal stem cells, were independent of decreased PG production [144–147]. This suggests NSAIDs may affect osteoblastic cells through mechanisms not associated with PG synthesis.

Both indomethacin and NS-398 have been shown to inhibit osteoblast differentiation from human mesenchymal stem cells while simultaneously increasing the number of adipocytes, suggesting a diversion of stem cell differentiation towards an adipocyte lineage instead of an osteoblast lineage [149]. However, Pountos et al. [150] found no direct effect of NSAIDs on human mesenchymal stem cells osteogenic differentiation. NSAIDs have shown variable effects on ALP activity [146,148,151] and collagen synthesis [146,152] in osteoblasts. Mineral deposition by osteoblasts has also been shown to be diminished in the presence of indomethacin and NS-398 [149].

Interestingly, however, in MC3T3-E1 osteoblast cells COX inhibitors stimulated cell growth [151]. The authors suggested that since indomethacin inhibited PGE<sub>2</sub> synthesis, that endogenous PGE<sub>2</sub> may have been suppressing proliferation of MC3T3-E1 cells and that COX inhibitors may have eliminated the growth suppressive effect of endogenous PGE<sub>2</sub> [151]. They found that exogenous PGE<sub>2</sub> effects on cells differed with concentration; a PGE<sub>2</sub> concentration similar to conditioned media suppressed cell growth, but higher concentrations were stimulatory [151]. The effects of NSAIDs on osteoblastic cells appear to differ depending upon the cell source, the NSAID selectivity and the methodology employed.

NSAIDs can also affect osteoclastic activity. Both indomethacin and NS398 have been shown to inhibit osteoclast differentiation and the resorption activity of mature osteoclasts [149]. *In vitro* studies also suggest that celecoxib influences osteoclast formation through osteoblasts and by acting directly on circulating osteoclast precursors to inhibit osteoclast formation, without cytotoxic effects [153].

NSAID effects on osteoclasts appear to be dependent upon the state of the bone environment. Under certain inflammatory conditions, COX-2 dependent PG synthesis is critical for bone resorption and osteoclastogenesis induced by the pro-inflammatory molecules and celecoxib can inhibit those activities [154,155]. But under normal conditions, non-inflammatory states, this does not occur [155,156]. In ovariectomized mice celecoxib decreased serum levels of C-telopeptide, a marker of bone resorption, but not in sham-operated mice [157]. NSAIDs have been shown to induce different effects on the osteogenic differentiation of mesenchymal stem cells (MSCs) under inflammatory and noninflammatory conditions [158]. Liu et al. [155] found that celecoxib significantly elevated osteoclast surface and decreased bone mass and bone mineral density (BMD) in normal control female rats but did not affect bone formation, consistent with other studies [157]. It appears that NSAIDs may help to inhibit bone resorption in pathological inflammatory conditions, such as rheumatoid arthritis and estrogen deficiency, but under more normal conditions NSAIDs may not.

#### **2.6.2.2 NSAIDs and BMD**

Data regarding the associations between NSAID use and BMD are multifaceted. Higher BMD has been reported in individuals who use NSAIDs compared to non-users [159–163]. However, NSAID use has also been shown to be associated with lower BMD [161] and to have no effect on BMD [161,164]. It has been suggested that the state of the bone environment may play a large role in determining the effects that NSAIDs may have on bone [14,161]. This stems from the results of the Canadian Multi-Centre Osteoporosis

Study (CaMOS), where the daily use of COX-2 inhibitors was associated with higher BMD in postmenopausal women not on hormone therapy, lower BMD in men and no consistent effect on BMD in postmenopausal women using hormone therapy [161]. The COX-2 inhibitory effects of NSAIDs may benefit the pro-inflammatory and high bone turnover state associated with postmenopausal women, not on hormone therapy, by decreasing inflammation and subsequently inhibiting resorptive activities. In contrast, in a low bone turnover and low inflammatory state, as occurs in men, the dominant action of NSAIDs may be inhibition of mechanotransductive signalling and bone formation. This is evidenced in the CaMOS where men taking COX-2 inhibitors exhibited lower BMD [161]. The inconsistent effect of COX-2 inhibitor use on BMD found in postmenopausal women, using hormone therapy, may be a result of a lack of domination. Hormone replacement therapy does not revert women to a premenopausal state completely [165] and therefore somewhat of a pro-inflammatory state may still exist. In these individuals there may not be one dominant action, resulting in a lack of effect on BMD.

The type of NSAID may play a role in determining how it will affect the bone. In the Osteoporotic Fractures in Men Study (MrOS) [166], NSAIDs and COX-2 selective inhibitors were differentiated. NSAIDs were associated with lower femoral neck trabecular BMD but were not associated with cortical BMD [166]. Contrastingly, COX-2 selective inhibitors were positively correlated with femoral neck trabecular BMD [166]. Carbone et al. [160] found that users of NSAIDs with higher COX-2 selectivity had higher BMD values at multiple sites. A lack of differentiation in the type of NSAID used may contribute to the differing relationships between BMD and NSAID use.

NSAID use has been associated with an increased risk of fractures [167]. Despite findings supporting increased BMD in certain NSAID using populations, the bone quality of these individuals may be altered and contributing to increased fracture risk. Vestergaard [168] found an association between NSAID use and an increased risk of any fracture, with no differences existing with regards to fall related fractures and fracture energy. An increased BMD despite no reduction in fracture risk [159], an increased risk of fractures with no excess BMD loss [168] and excess risk of fractures observed in epidemiological studies [164,167], may suggest an effect of NSAIDs on bone biomechanical competence.

### **2.6.2.3 NSAIDs and *In vivo* Mechanical Loading**

Multiple studies have shown that prostaglandins mediate some of the anabolic effects of mechanical loading on bone (Table 2.2). Both *in vivo* [94] and *in vitro* [95,169] studies have shown increased prostaglandin synthesis following mechanical stimulation. The role of prostaglandins in mechanically induced bone formation has been demonstrated through the use of NSAIDs. NSAIDs inhibit the action of COX, the enzyme responsible for the production of prostaglandins and therefore inhibit prostaglandin synthesis [78]. Pead and Lanyon [9] were the first to demonstrate that NSAIDs can inhibit bone formation induced by mechanical loading. Since then, several other studies have demonstrated that NSAIDs impair mechanically induced bone formation [10–12]. Prostaglandins produced in response to loading are thought to be largely the result of

loading induced COX-2 expression; both selective and non-selective NSAIDs have been shown to impair bone formation [9–12].

However, a temporal effect of NSAID administration on mechanically induced bone formation has been shown. Generally, when administered prior to mechanical loading, NSAIDs diminish bone formation responses, but the same does not hold true for administration following loading [11,12]. However, all of the aforementioned *in vivo* studies examining the effects of NSAIDs on bone formation only involved one loading event. More recent studies [13–15,170,171] have examined NSAID effects on bone formation induced by multiple loading events and have shown contrasting results.

*In vivo* animal studies examining the effects of NSAIDs on bone formation vary with regards to the method of mechanical loading, the bone examined, the animals used and the NSAID implemented. Pead and Lanyon [9] were the first to demonstrate that NSAIDs, specifically indomethacin, administered prior to loading can impair the osteogenic response of bone to mechanical loading. Chow and Chambers [11] confirmed this finding in the trabecular bone of the vertebra. In addition, they showed that indomethacin administered daily, starting either before or after the loading, impaired the bone response [11]. However, one dose of indomethacin 6 hours after loading did not affect the bone response to loading [11].

Forwood [10] was the first to demonstrate that a COX-2 selective NSAID, NS-398, administered prior to loading, impaired bone formation. The bone formation rate (BFR) was suppressed by both indomethacin and NS-398 but the mineral apposition rate (MAR) and mineralizing surface (MS/BS) was only suppressed by NS-398. It should

be noted that Forwood [10] examined lamellar bone formation on the endocortical surface of the tibia but woven bone was also formed on the periosteal surface under the loading conditions. Li et al. [12] also showed that tibial endocortical lamellar MS/BS and BFR were suppressed by indomethacin and NS-398. Li et al. [12] did, however, demonstrate that NS-398 and indomethacin impair the lamellar BFR on the periosteal surface of the ulna, independent of woven bone formation. Both NSAIDs only slightly impaired the MAR and MS/BS. They also showed that the timing of NSAID administration affects the subsequent bone response. Tibial endocortical MS/BS and BFR were suppressed by NS-398 when it was injected 3 hours and 30 minutes before the loading, with the 3 hours prior impairing BFR more than 30 minutes. When NS-398 was injected 30 minutes following loading there was no effect on bone formation. With regards to lamellar bone formation independent of woven bone formation, ulnar periosteal BFR was suppressed by NS-398 to the same extent when it was injected 3 hours and 30 minutes before loading. NS-398 only slightly suppressed periosteal MAR and MS/BS at 3 hours and 30 minutes prior to loading. Injection 30 minutes after loading did not affect ulnar periosteal BFR, MS/BS or MAR. So, NS-398 administration before loading impaired periosteal BFR but had little effect on MAR and MS/BS. This in agreement with Forwood [10] and Chow and Chambers [11].

The previously discussed studies employed only one loading session to create the lamellar bone response. A more recent study by Sugiyama et al. [13] more closely resembles the methods employed in this project, examining the effects of NSAIDs on bone formation induced by multiple loading sessions. Sugiyama et al. [13] showed that

daily NS-398 administration and 6 days of loading (over 2 weeks) did not affect the bone response to mechanical loading in either trabecular or cortical bone. However, woven bone was formed in the cortical region of the proximal to middle tibiae and lamellar bone in the cortical region of the middle fibulae as well as in the trabecular region of the proximal tibiae. Therefore, the bone response included both woven bone and lamellar bone formation. Cunningham [170] examined the effects of ibuprofen administration either before or after exercise on bone formation induced by 9 simulated resistance training exercise sessions, occurring every other day over the course of 3 weeks, in rat tibiae. No effect of ibuprofen was found, either before or after loading, on periosteal lamellar BFR, MS/BS or MAR, but woven bone formation was also induced in the tibiae [170].

A few studies have examined the effect of NSAIDs on bone formation induced by multiple exercise sessions in humans. Kohrt et al. [14] examined whether the timing of NSAID use influences BMD adaptations to exercise in premenopausal women, aged 21-40. The women participated in a 9-month weight-bearing exercise training program, with exercise sessions occurring 3 days/week. Kohrt et al. [14] found that taking ibuprofen before exercise did not impair the BMD response to exercise compared to taking a placebo. Interestingly, the women taking ibuprofen after exercise had significantly greater changes in total hip, femoral neck, trochanter and femoral shaft BMD compared to the placebo and ibuprofen before group. This suggests that NSAID treatment following mechanical loading may be able to enhance the effects of mechanical loading on bone formation. The same group also examined how NSAID timing

influenced BMD adaptations to exercise in men and women 60-75 years of age. Using a very similar exercise regime of 9 months, they found that ibuprofen use either before or after exercise did not alter BMD responses to exercise training [15]. The authors did note however, that ibuprofen use either before or after exercise appeared to have a more deleterious effect, although not significant, on BMD in women than in men [15]. Similar to the study in elderly subjects, Duff et al. [171] found ibuprofen administration immediately following resistance exercise 3 times/week, for 9 months, did not benefit BMD in postmenopausal women. The results of these human studies suggest NSAID effects on bone adaptation to exercise are likely influenced by a number of factors including age, sex and the state of the bone environment.

Taken together the various results shown in the *in vivo* studies, with regards to the effect of NSAIDs on bone formation, suggest that prostaglandins do play a role in bone formation and the timing of NSAID administration can influence the outcome. However, the complexity of the mechanism and signalling pathways is evident with the various effects shown.

**Table 2.2 Summary of studies examining the effects of NSAIDs on mechanically induced bone formation *in vivo*.**

Number of Loading Sessions	Subject	NSAID	Timing of NSAID Administration	Effect on Bone Formation	Study
1	rooster (ulna)	indomethacin (i.v.)	1 hr before	↓	[9]
1	rat (vertebrae)	indomethacin (oral)	3 hrs before 6 hrs after before or after and for the next 7 days	↓ ↔ ↓	[11]
1	rat (tibia)	indomethacin NS-398 (oral)	3 hrs before 3 hrs before	↓ ↓	[10]
1	rat (ulna and tibia)	indomethacin NS-398	3 hrs before (oral) 3 hrs before (oral) 30 mins before (i.p.) 30 mins after (i.p.)	↓ ↓ ↓ ↔	[12]
1	rat (tibia)	NS-398 (i.p.)	3 hrs before 20 mins before 20 mins after	↓ ↓ ↔	[172]
6	mouse (tibia)	NS-398 (sub.q.)	3 hrs before	↔	[13]
9	rat (tibia)	ibuprofen (oral)	2 hrs before	↔	[170]
9 months	premenopausal women	ibuprofen (oral)	1-2 hrs before immediately after	↔ ↑	[14]
9 months	elderly men postmenopausal women	ibuprofen (oral)	1-2 hrs before immediately after	↔ ↔	[15]
9 months	postmenopausal women	ibuprofen (oral)	immediately after	↔	[171]

↓ - impairs bone formation; ↑ - enhances bone formation; ↔ - no effect on bone formation

#### 2.6.2.4 NSAIDs and *In vitro* Mechanical Loading

Studies examining the effects of NSAIDs on mechanically stimulated bone cells are limited. Methodologies vary greatly, including the cell type used, the loading mechanism, the type of NSAID used and the timing of NSAID administration.

Indomethacin, a non-selective NSAID, has been shown to reduce the PGE<sub>2</sub> response of

stretched rat calvarial cells [173,174]. Jiang et al. [175] showed that indomethacin decreases the release of PGE<sub>2</sub> from MLO-Y4 osteocyte like cells stimulated by fluid flow. In addition, indomethacin reduced the fluid flow stimulation of Cx43 expression and intercellular coupling mediated by gap junctions in MLO-Y4 cells [175], suggesting PGE<sub>2</sub> is an important factor in gap junction mediated communication.

NS-398 has also been shown to inhibit PGE<sub>2</sub> production in mechanically stimulated bone cells. Bakker et al. [169] subjected primary mouse long bone cells to pulsatile fluid flow for 1 hour with NS-398 present 30 minutes prior to loading, during the one hour of fluid flow and 24 hours after. NS-398 inhibited the stimulating effect of fluid flow on PGE<sub>2</sub> production immediately after loading and 24 hours later. In the static, no flow group, NS-398 slightly reduced PGE<sub>2</sub> production at 1 hour but after 24 hours of incubation PGE<sub>2</sub> concentrations were significantly lower than in the no flow group without NS-398. Bakker et al. [169] also demonstrated a similar effect in human bone cells from trabecular bone biopsies. In addition, the static human bone cells exposed to NS-398 showed significantly lower PGE<sub>2</sub> concentrations at 1 hour compared to the static group without NS-398. Westbroek et al. [95] subjected chicken calvarial osteocytes to one hour of pulsatile fluid flow and then incubated them for two hours in the presence of NS-398; it significantly decreased the production of PGE<sub>2</sub>.

Overall, studies examining mechanical stimulation of bone cells demonstrate that NSAIDs inhibit the PGE<sub>2</sub> production of cells, but how that subsequently affects other bone cells or activities is not known.

### **2.6.2.5 Long Term Effects of NSAIDs on Bone**

Research is limited regarding long-term NSAID use ( $\geq 1$  month) and bone metabolism. The available research has shown variable effects in animals. Long-term use of NSAIDs has been studied mostly in the context of determining the effectiveness of NSAIDs in preventing bone loss in ovariectomized models. Since PGE<sub>2</sub> can stimulate bone formation and resorption, blocking it with NSAIDs may inhibit both bone formation and resorption, with the resulting effects likely depending upon the balance of bone activities or the state of the bone environment at the time of treatment.

The effects of NSAIDs on ovariectomy-related decreases in bone volume and BMD have been variable. NSAIDs have shown effectiveness in studies 6 weeks [176] and 10 weeks [177] in length and partial effectiveness in longer term studies (3 to 9 months) [178,179]. However, NSAIDs have also been shown to be ineffective at preventing bone loss induced by ovariectomy in as little as 1 month [157] and after 4 months of treatment [180]. In addition, NSAIDs were shown to cause greater decrements in trabecular bone indices in ovariectomized rats compared to vehicle treated animals [181]. Ibuprofen was shown to enhance bone loss in ovariectomized rats and even induce cancellous bone loss in intact rats in just 3 weeks [182]. However, a lack of effect of NSAIDs on bone indices including BMD and biomechanical properties has also been shown in intact animals [157,179,180]. Selective COX-2 inhibitor use for only 1 month suppressed bone formation and increased bone resorption, without significant loss of bone in male gonad-intact middle-aged rats [183]. Boiskin et al. [184], however, found no

effect of indomethacin administration for either 1 or 2 months on bone formation or resorption in male rats.

The variable effects of NSAIDs on bone metabolism highlight their complex relationship with bone. The age and sex of the animals, the state of the bone environment, as well as the NSAID type, non-selective vs. COX-2 selective, and dose and duration of treatment all likely influence the relationship.

## CHAPTER THREE

### MATERIALS AND METHODS: *IN VIVO*

#### 3.1 Animals and Housing

All experimental procedures and protocols were approved by McMaster's Animal Research Ethics Board. Animals were housed within McMaster University's central animal facility (CAF) where they were maintained on a 12:12 light-dark cycle at approximately 22°C. The rats were housed one per cage and given food and water *ad libitum*. Male and female Sprague Dawley rats were purchased from Charles River at 11-12 weeks old. They were aged in the CAF until approximately 18 weeks of age before loading protocols began because by that time bone growth has slowed down substantially in the rat [185].

#### 3.2 Rat Forelimb Compression Model

The rat forelimb compression model is a noninvasive *in vivo* loading model that can induce lamellar bone formation. The major benefit of this model is that the points of contact for loading are at the wrist and elbow, away from the region of interest, the mid-diaphysis. The mid-diaphysis experiences the highest strains and therefore the greatest bone formation [42]. Using contact points away from the region of interest avoids confounding effects of periosteal compression and subsequent bone formation.

All forelimb loading was performed using a material testing system (eXpert 5601, ADMET, MA, USA) (Figure 3.1). Custom cups were designed and manufactured to hold

the carpus (wrist) and olecranon (elbow) during loading, similar to Figure 3.2. The loading actuator is attached to the upper cup housing the wrist and applies a downward displacement. The wrist and elbow were able to rotate freely in their cups. The rat was placed on a custom designed table while the loading was performed. The height of the bottom cup (holding the elbow) was adjusted such that the elbow was not being pulled up or down but rather sat naturally as it would when the rat was laying on its back.

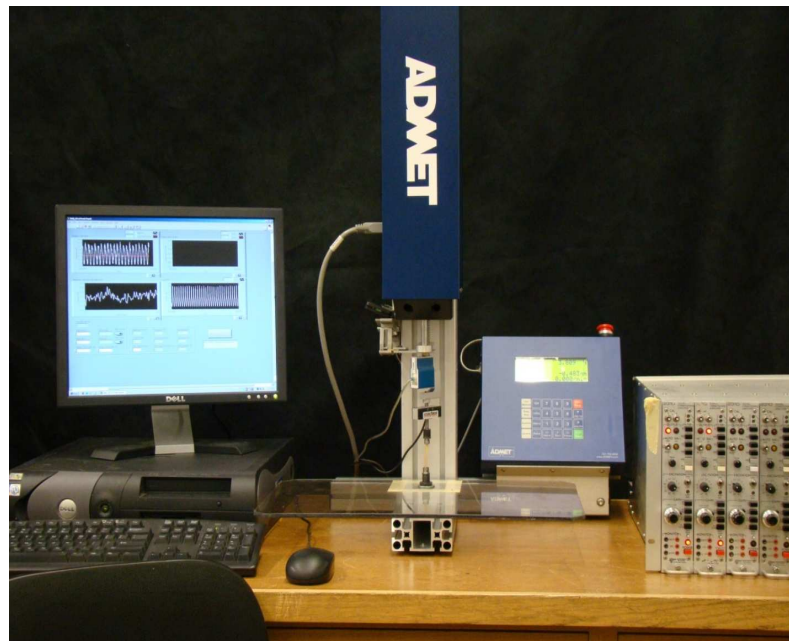


**Figure 3.1** Material testing system setup.

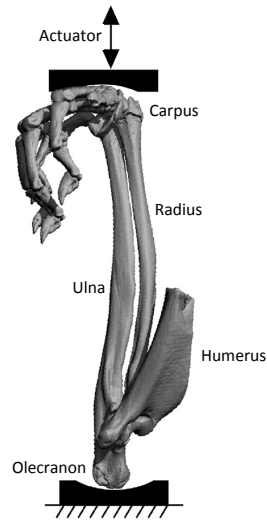


**Figure 3.2 Schematic of the rat forelimb compression model [186].**

### **3.3 Experimental Protocols**

For all loading protocols right forelimbs were loaded and left forelimbs were internal non-loaded controls. All rats were anaesthetized with isofluorene (5% at 1 L/min) and injected with buprenorphine (0.01 mg/kg). The rats were then maintained on isofluorene (2% at 1 L/min) and the required loading protocol was applied. NSAIDs were administered orally using a flavoured gelatin vehicle and dose time was dependent upon the experiment performed. The NSAID dose and timing for each experiment are shown in Table 3.1.

**Table 3.1** *In vivo* mechanical loading experimental groups.

Experiment	NSAID and Dose	Experimental Groups
Male 1-Month Loading n=4/group	indomethacin (INDO) low dose - 0.2 mg/kg high dose - 2 mg/kg	Control (CON) - no NSAID Low PRE (L-PRE) - 2 hrs prior to loading Low POST (L-POST) - immediately after loading High PRE (H-PRE) - 2 hrs prior to loading High POST (H-POST) - immediately after loading
Male 1-Month Loading n=10/group	NS-398 dose - 2 mg/kg	CON - no NSAID PRE - 2 hrs prior to loading POST - immediately after loading
Male 2-Week Loading n=5/group	ibuprofen (IBU) dose - 30 mg/kg  Celebrex (CBX) dose - 10 mg/kg	CON - no NSAID IBU-PRE - 1 hr prior to loading IBU-POST - immediately after loading CBX-PRE - 1 hr prior to loading CBX-POST - immediately after loading
Female 2-Week Loading n=5/group	ibuprofen (IBU) dose - 30 mg/kg  Celebrex (CBX) dose - 10 mg/kg	CON - no NSAID IBU-PRE - 2 hrs prior to loading IBU-POST - immediately after loading CBX-PRE - 2 hrs prior to loading CBX-POST - immediately after loading
Female 1-Month Loading n=5/group	ibuprofen dose - 30 mg/kg	CON - no NSAID PRE-1HR - 1 hr prior to loading PRE-2HRS - 2 hrs prior to loading PRE-3HRS - 3 hrs prior to loading

### 3.3.1 NSAID Pharmacokinetics

NSAID pharmacokinetics depend on a number of factors including: the type of NSAID, the route of administration, the dose, the subject studied as well as the age and sex of the subjects [187] (Table 3.2). NSAID pharmacokinetics differ in rats and humans and rat sex has been shown to influence NSAID metabolism. For example, male rats have

been shown to metabolize celecoxib and piroxicam much faster than female rats [188,189]. In male rats the elimination half-life of celecoxib was 3.7 hours and in female rats it was 14 hours [188], much closer to the 11 hours in humans [190]. The sex difference means that female rats would achieve a higher exposure to celecoxib than males when administered the same dose. Sex differences in the rat are not unusual and have been partly attributed to sex-specific expression of different genes [191].

NSAID effects on bone formation were examined in both male and female rats in this study to address the potential effects of sex on NSAID pharmacokinetics. The timing of NSAID administration before loading was chosen so that peak plasma concentrations would occur at the time of loading. NSAID dose timing in the male rats in this study was based on the literature (Table 3.2). The timing of NSAID administration in the female rats was based on the male pharmacokinetics while taking into the account that females may metabolize the NSAIDs more slowly. As a result, the dosing times before loading in the female 2-week protocol were adjusted so that they occurred one hour earlier than the males. The female ibuprofen timing experiment was designed to identify the optimal administration time before loading that would impair bone formation, as this was the hypothesis, NSAID administration before loading impairs bone formation. There does not appear be any literature describing ibuprofen pharmacokinetics in female rats so three dosing times were examined.

**Table 3.2 Pharmacokinetics of the NSAIDs used in the experiments.**

NSAID	Subject	Route of administration	Peak plasma concentration	Half-life	Study
celecoxib	human	oral	2-4hrs	11.2-15.6hrs	[190]
celecoxib	rat	intravenous		3.7hrs males 14hrs females	[188]
	rat (male)	oral	1hr		
ibuprofen	rat (male)	intravenous		2hrs	[187]
		oral		1hr	[192]
		oral	1hr	2hrs	[193]
ibuprofen	human	oral	1-3hrs	2hrs	[194–196]
indomethacin	rat (male)	oral	2-6hrs	6.5hrs	[197,198]
indomethacin	rat	oral, intravenous	0.5hrs	4hrs	[199]
	human	oral	1hr	2hrs	
indomethacin	human	oral	1-2hrs	2.6-11.2hrs	[200–202]
NS-398	rat (male)	intraperitoneal injection	30-40mins	1hr	[203]
NS-398	rat	oral		4hrs	[204]
NS-398	rat		2-6hrs		[81]

### 3.3.2 NSAID Administration

NSAIDs were administered orally using a flavoured gelatin vehicle. Stock solutions of indomethacin (Indomethacin – CAS 53-86-1, Cayman Chemical Company, MI, USA) and NS-398 (NS-398 – CAS 123653-11-2, Cayman Chemical Company, MI, USA) were created by dissolving the crystalline solids in dimethyl sulfoxide (DMSO) at concentrations of 17 mg/ml and 25 mg/ml, respectively. Celebrex capsules of 200 mg (Celebrex, Pfizer, Quebec, CAN) were opened and the contents were dissolved in DMSO to create a stock solution of 100mg/ml. Ibuprofen liquid capsules of 200mg (Ibuprofen Liquid Capsules, Life Brand, Toronto, CAN) were dissolved in water to create a stock solution of 20 mg/ml. The NSAID stock solutions were then diluted with the flavoured gelatin vehicle to produce the appropriate doses in 2.5 ml of gelatin per animal.

### **3.3.3 NSAID Dosing**

The indomethacin and NS-398 doses used in the male 1-month loading protocols were based on previous studies that showed a dose of 2 mg/kg impaired bone formation induced by a single loading event [10,12]. Forwood [10] examined the effects of three doses of indomethacin and NS-398, 0.02 mg/kg, 0.2 mg/kg and 2 mg/kg. All three doses of NS-398 impaired endocortical lamellar BFR and MS/BS but only 2 mg/kg impaired MAR. An indomethacin dose of 2 mg/kg impaired BFR, the only dose that showed an effect on any of the bone formation indices. Indomethacin doses in humans are in the range of 25-150 mg [201], equivalent to 0.4-2.1 mg/kg for a 70 kg person.

Previous mechanical loading studies in rats have not examined the effects of Celebrex on bone formation. Therefore the Celebrex dose, 10 mg/kg, was based on an effective daily dose of between 5 mg/kg and 30 mg/kg in rats [205]. The dose has been implemented in studies examining fracture and ligament healing and ectopic bone formation [205–207] and was shown to decrease PGE<sub>2</sub> concentrations in muscle tissue [207]. Typical doses in humans range between 100 and 800 mg, depending on the ailment [208], which is equivalent to 1.4 mg/kg to 11.4 mg/kg, based on a 70 kg person. The dose implemented in this study would be on the high end of the human dose on a per kilogram basis. However, celecoxib pharmacokinetics have been shown to differ between humans and rats.

The ibuprofen dose chosen in this study, 30 mg/kg, has been implemented previously in the literature for various studies in rats. The effect of ibuprofen administration both before and after multiple simulated resistance training exercise

sessions on bone formation in rats used the same dose [170]. The dose was also implemented in a number of fracture healing studies [206,209–211]. The dose used in human exercise studies examining the effects of ibuprofen on BMD was 400 mg/day [14,15]. Based on a 70 kg person, that dose is approximately 5.7 mg/kg. Ibuprofen pharmacokinetics in humans appear to be similar to the pharmacokinetics in male rats (Table 3.2), but how they compare to the pharmacokinetics in female rats is not known. However, the dose implemented in this study would be equivalent to 2100 mg/day for a 70 kg person, based on a milligram/kilogram conversion. That dosing is more typical of taking multiple doses (400 mg), throughout the day (3-4 times/day), not a single dose, once per day [195].

### **3.4 Development of Loading Protocol**

The loading protocols implemented in this study were designed to induce lamellar bone formation in the ulna, stimulated as a result of mechanotransductive signalling. A 1-month and a 2-week loading protocol were implemented in male rats to examine the timing effects of NSAIDs on mechanically induced lamellar bone formation. Male rats were used initially to avoid the possibility of any hormonal influences. However, upon discovering that male and female rats may metabolize NSAIDs at different rates [188,189], the loading protocol was implemented in female rats. Examining the effects of NSAIDs on lamellar bone formation in female rats may more closely relate to humans because it appears that NSAID metabolism may be more similar in humans and female rats [188,190].

### **3.4.1 Loading Protocol Parameters**

The loading protocol parameters for all of the experiments remained unchanged except for the target load, which changed depending upon the sex of the rats. Cyclic loading was applied in a triangular waveform at a frequency of approximately 2 Hz for 300 cycles with 20 second pauses after every 20 cycles (15 sets of 20 cycles). The target load was approximate because the control system for the ADMET material testing system had significant overshoot. For example, the target loads were 20 N for males. To achieve this load at a frequency of 2 Hz, an input load of approximately 9.5 N was used. The forelimb was unloaded to a load of approximately 2 N. The loading rate was 235 N/sec. Although the input parameters remained constant throughout the loading, the response of the system did show some variability. Notably, changes in the stiffness of the forelimb throughout a given loading bout resulted in slight variations of frequency and peak load.

### **3.4.2 1-Month Loading Protocol in Male Rats (INDO and NS-398)**

The timing effects of the NSAIDs indomethacin and NS-398 on lamellar bone formation were first examined in male rats in a 1-month loading protocol. Male rats were loaded 3 days/week (Monday, Wednesday and Friday) for 4 weeks for a total of 12 days of loading.

### **3.4.3 2-Week Loading Protocol in Male Rats (IBU and CBX)**

The timing effects of ibuprofen and Celebrex on lamellar bone formation were examined in male rats in a 2-week protocol. A 2-week loading protocol was implemented

in male rats to determine if a protocol shorter in length than the 1-month protocol could induce a consistent and measurable amount of lamellar bone. The 2-week protocol involved loading 3 days/week (Monday, Wednesday and Friday) for a total of 6 days of loading. The protocol, however, did not induce lamellar bone formation in the male rats (Figure 3.3), as evidenced by a lack of difference in mineral apposition rate (MAR) in the CON (loaded with no NSAID dosing) ulnas compared to the LEFT (non-loaded controls). The only difference between the 2-week and 1-month loading protocols was the number of loading sessions, 6 vs. 12, respectively. This suggests that if the length of the protocol is changed (*ie.* the number of loading sessions) then the other loading parameters need to be adjusted to compensate. In this protocol, an increase in the load magnitude or the number of cycles may have helped to compensate for the decreased number of loading sessions. However, care must be taken when changing the other parameters, so as to not damage the bone with increased loading.

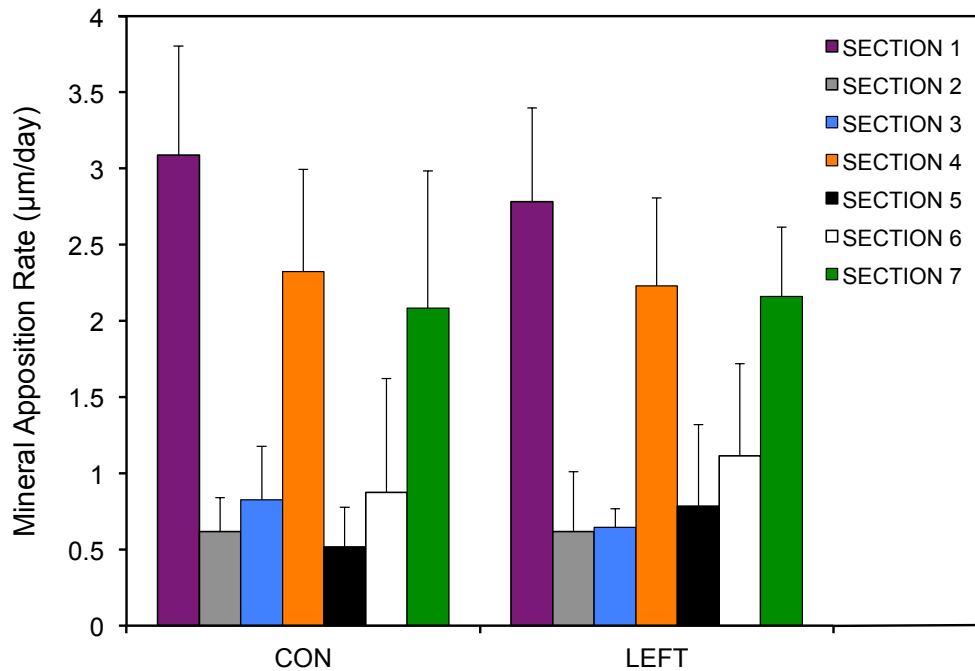


**Figure 3.3** MAR of Sections 1-7 of the male ulnas that underwent the 2-week loading protocol in the IBU/CBX experiment. Values are mean  $\pm$  standard deviation (STD). No differences ( $p>0.05$ ) were detected between the LEFT group and the CON group in any of the Sections. See 3.5.5 *Grid Template Development* for an explanation of the 7 Sections. See Appendix I for graphs depicting all groups examined in the male 2-week loading protocol. n=5/CON; n=6/LEFT.

### 3.4.4 2-Week Loading Protocol in Female Rats (IBU and CBX)

A similar 2-week protocol was also implemented in female rats to examine the effects of ibuprofen and Celebrex on lamellar bone formation. The only difference between the male and female protocols was the target load; it was adjusted to 15-16 N for females in the 2-week protocol. This load was chosen because in a pilot 3-week loading protocol with five female rats, a load of 14 N induced lamellar bone formation. The load was increased in the 2-week loading protocol in order to achieve lamellar bone formation in two weeks, as opposed to three. To achieve this load an input load of approximately

8 N was used. In this experiment 11 of the 26 ulnas exhibited woven bone formation (Figure 3.4), a bone response to damage, suggesting that the load magnitude was too high. To better characterize the load-strain relationship, ulnas were strain gauged to determine the load required to produce strains capable of inducing a lamellar bone formation response in female rats during a 1-month loading protocol. The 1-month protocol was chosen because it produced a consistent lamellar bone formation response in previous experiments with male rats whereas the 2-week protocol in male rats did not induce lamellar bone formation.

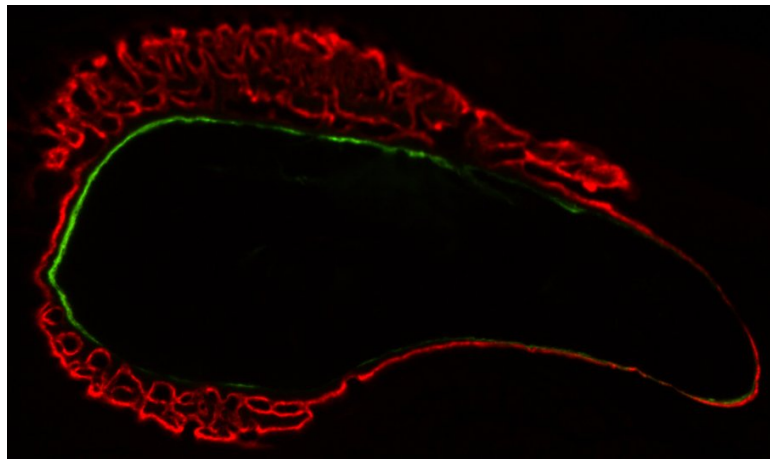


**Figure 3.4** Cross-sectional image of a female rat ulna that underwent forelimb loading in the 2-week loading protocol. An example of woven bone formation due to excessive loading.

### 3.4.5 Rat Forelimb Strain Gauging

To understand the load/strain relationship of the ulna during forelimb loading, left forelimbs of male and female rats from previous experiments (n=6/sex) were strain gauged. Post-mortem, the front limbs were detached at the shoulder. The medial aspect of the ulna was carefully exposed and a single-gauge strain gauge (FLK-1-11-015LE, TML

Tokyo Sokki Kenkyujo Co. Ltd., Tokyo, Japan) was attached approximately 1 mm distal to the midpoint. The forelimbs were placed in the loading apparatus as they were during the *in vivo* loading. They were loaded for 20 cycles at 4 N as a warm-up. Ten cycles of loads of 4-8 N were applied to the female forelimbs and loads of 4-13 N to the males, to determine the load strain relationships.

A scatter plot of the load/strain relationship was constructed with the 6 ulnas for each sex (Figure 3.5). A linear line of best fit was determined for each sex.

Based on the load-strain relationship in Figure 3.5, the load of 15-16 N used for the female rats in the 2-week protocol corresponded with strains of 3800-4000  $\mu$ strain. Strains of this magnitude are generally damaging to the bone [212] and the woven bone formation seen in 11 of 30 female rats in the 2-week protocol (which were loaded to 15-16N) is consistent with these strains being damaging. The threshold strain for osteogenesis in similar female rats has been shown to be approximately 2300  $\mu$ strain at the ulnar midshaft and 3000  $\mu$ strain distal to the midpoint [9]. Based on the load/strain relationship for the female forelimbs and the results of the 2-week protocol, a load of 13-14 N, corresponding to strains of 3100-3500  $\mu$ strain, was chosen as the target load for the female rats in the 1-month protocol.

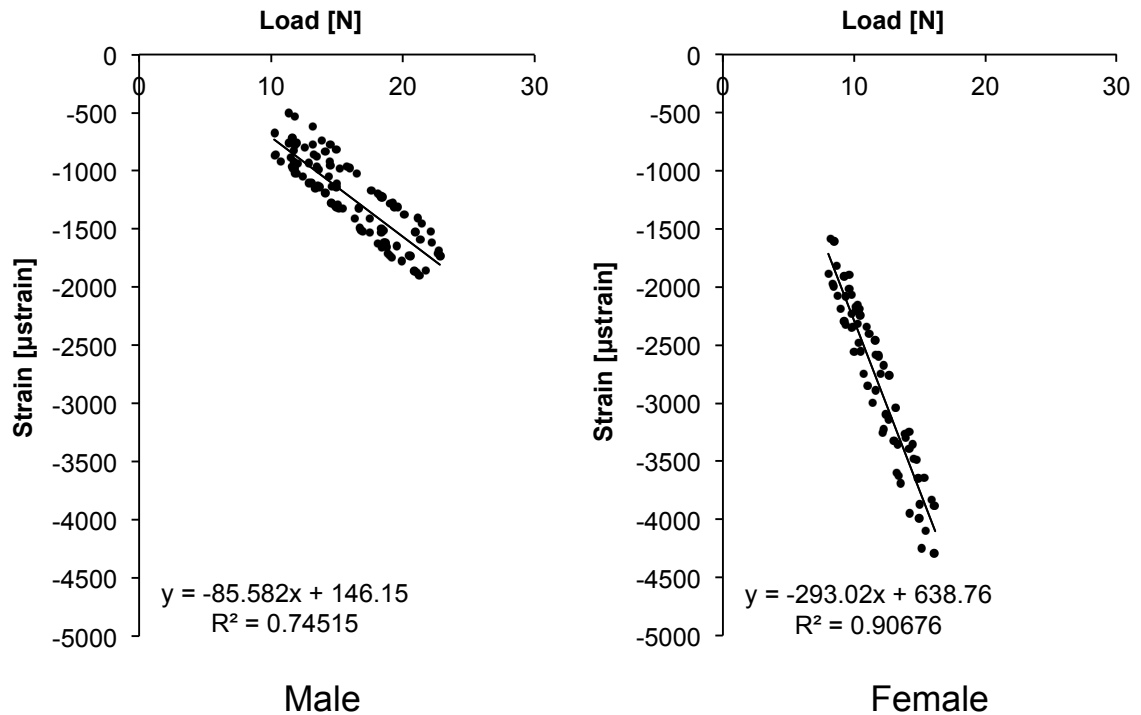


**Figure 3.5** Load/strain relationship of male (left) and female (right) ulnas during forelimb loading.

### 3.4.6 1-Month Loading Protocol in Female Rats (IBU)

The 1-month loading protocol was implemented in female rats to examine the timing effects of ibuprofen dosing before mechanical loading on lamellar bone formation. The 1-month protocol used with the female rats was the same as that used with the male rats except the target load was 13-14 N, based on the load/strain relationship determined with the forelimb strain gauging. To achieve this load an input load of approximately 8 N was set in the ADMET controller.

### **3.5 Bone Histomorphometry**

#### **3.5.1 Fluorochrome Labeling**

To measure bone formation the rats were injected with fluorochrome labels.

Fluorochrome labeling is a widely used standard technique in skeletal research, which is simple and efficient for the investigation of the dynamics of bone formation [213]. In animal research this technique can be used for the measurement of various bone indices. The fluorochrome labels have a high affinity for calcium and bind readily to it. The labels bind to calcium inside living cells that are forming new bone [213]. When they are bound to calcium ions, they become incorporated at sites of mineralization in the form of hydroxyapatite crystals. In the first 24-36 hours after administration, the label will bind with calcium and the unincorporated label will be excreted [213]. The two labels used during these studies were alizarin complexone and calcein green. Alizarin and calcein have different excitation and emission wavelengths. Alizarin fluoresces red and calcein fluoresces green. The timing of administration was dependent upon the loading protocol used as described in the following sections.

Calcein (Alfa Aesar, Lancaster, UK) salt was diluted into Millipore water at a concentration of 5 mg/mL. Alizarin complexone (Alfa Aesar, Lancaster, UK) salt was diluted into Millipore water at a concentration of 10 mg/mL. One molar hydrochloric acid and sodium hydroxide solutions were used for pH balancing (pH between 7.2-7.4). The solutions were administered through subcutaneous injections in the abdomen. Calcein doses were 20 mg/kg (4 mL/kg) and alizarin doses were 30 mg/kg (3 mL/kg).

### **3.5.1.1 1-Month Protocol**

To measure bone formation in the indomethacin experiment, male rats were injected with calcein (20 mg/kg, s.q.) on Day 6 and alizarin (30 mg/kg, s.q.) on Day 24. To measure bone formation in the NS-398 experiment, male rats were injected with calcein (20 mg/kg, s.q.) on Day 6 and 20 and alizarin (30 mg/kg, s.q.) on Day 13 and 27. Female rats were injected with calcein on Day 6 and alizarin on Day 24. Rats were euthanized by CO<sub>2</sub> on Day 30 for the males and Day 27 for the females (three days after the last loading cycle) and both forelimbs were dissected, dehydrated and embedded to prepare them for histological analysis (see 3.5.3 *Bone Sample Preparation*).

### **3.5.1.2 2-week Protocol**

To measure bone formation in the 2-week protocol, rats were injected with calcein (20 mg/kg, s.q.) on Day 3 and alizarin (30 mg/kg, s.q.) on Day 10. Rats were euthanized by CO<sub>2</sub> on Day 15 and both forelimbs were dissected, dehydrated and embedded to prepare them for histological analyses (see 3.5.3 *Bone Sample Preparation*).

### **3.5.2 Sacrificing and Dissection**

Rats were sacrificed three days after the last loading session through CO<sub>2</sub> asphyxiation. Rats were first anesthetized using 4-5% isofluorene at 1 L/min and then placed in a charged CO<sub>2</sub> housing for at least five minutes. Rat forelimbs were then harvested for histology. Minimal amounts of soft tissue were removed from the ulnas,

leaving the muscle on the bone as not to disrupt the periosteum. After removal, bones were stored in a 70% ethanol solution at 4°C until the start of the dehydrating process.

### **3.5.3 Bone Sample Preparation**

For histological evaluation, the forelimbs were embedded in a plastic resin to ensure integrity when cutting them into thin sections (~100 µm) for examination and analysis. Briefly, after harvesting, forelimbs were placed in 15 mL Falcon tubes and dehydrated in increasingly concentrated ethanol solutions (70%, 95%, and 100%) stored at 4°C (Appendix IV). The forelimbs were then placed in glass vials with xylenes to remove fat, which were also stored at 4°C. In the same vials, the forelimbs then underwent infiltration with a solution of methyl methacrylate, dibutyl phthalate and benzoyl peroxide. The vials were also stored at 4°C to prevent the resin from hardening. The final embedding required the forelimbs to be placed in 4 mL glass vials and for the solution to be warmed to 37°C to achieve a hard resin that could be sectioned properly. After three days of curing, the resin was hard and the embedded forelimbs were sectioned. The embedded forelimbs were cut perpendicular to the long axis at the area of interest, where the most bone formation was expected to occur, approximately 1 mm distal to the midpoint [214]. An Isomet low speed diamond wafer saw (Buehler, Lake Bluff, IL) was used to cut a section approximately 100 µm thick. The sections were fixed to a microscope slide using Permout (Fisher Scientific, Toronto, CAN) and the cross-section was examined under a fluorescent microscope.

### **3.5.4 Image Capture**

A Nikon DS-Fi microscope (Nikon, Tokyo, Japan) was used to image the slides and images were captured using a RETIGA 2000R camera (QImaging, Vancouver, CAN) and accompanying NIS-Elements AR software package. Single channel images of the calcein and alizarin labels were captured with different optical filters and then merged together by the software to create one image containing both of the labels.

### **3.5.5 Grid Template Development**

A 20-segment, 7-section grid template was developed to analyze the mineral apposition rate (MAR) of the ulna cross-sectional images (Figure 3.6). The grid was designed to differentiate sections of the bone where bone formation occurred as a result of mechanical loading compared to normal ongoing periosteal growth. The grid divided each bone into repeatable representative sections. To determine which areas of the bone exhibited bone formation resulting from mechanical loading, non-loaded (left) ulna cross-sectional images were first opened in ImageJ (<http://rsbweb.nih.gov/ij/>) and then rotated so that lateral prominences were horizontal. The images were then visually examined to identify similar regions across ulnas that did and did not contain bone formation. Based on that initial examination, 10 segments of equal width were created to divide the ulna in the cranial-caudal (anterior-posterior) direction in order to segment them into key areas of bone formation (Figure 3.7). The 10 segments were then further divided into medial (Segments 1-10) and lateral (Segments 11-20) segments. The medial and lateral sections were created by extending a horizontal line from the posterior

(Segments 1 and 20) and anterior (Segments 10 and 11) tips of the ulna. With the 20-segment grid overlaid on the non-loaded ulna cross-sectional images, the segments were then grouped to create 7 sections. The sections were formed by identifying segments in a region that contained bone formation or did not. For example, in most non-loaded ulnas, Segment 1 and 2 contained bone formation whereas Segments 3-5 did not. So Segment 1 and 2 were grouped to form Section 1 and Segments 3-5 were grouped to form Section 2. The sections allow for the identification of the ulnar regions where bone formation occurs primarily (or even exclusively) as a result of mechanical loading. The grid was created in Powerpoint (Microsoft Office 2013). Each image was loaded into Powerpoint and overlaid with the grid. The grid template was scaled to each bone individually, maintaining segment proportionality, such that the anterior and posterior tips of the bone aligned with the edges of the grid. The proportional size of each ulna cross-sectional image was maintained throughout the process.

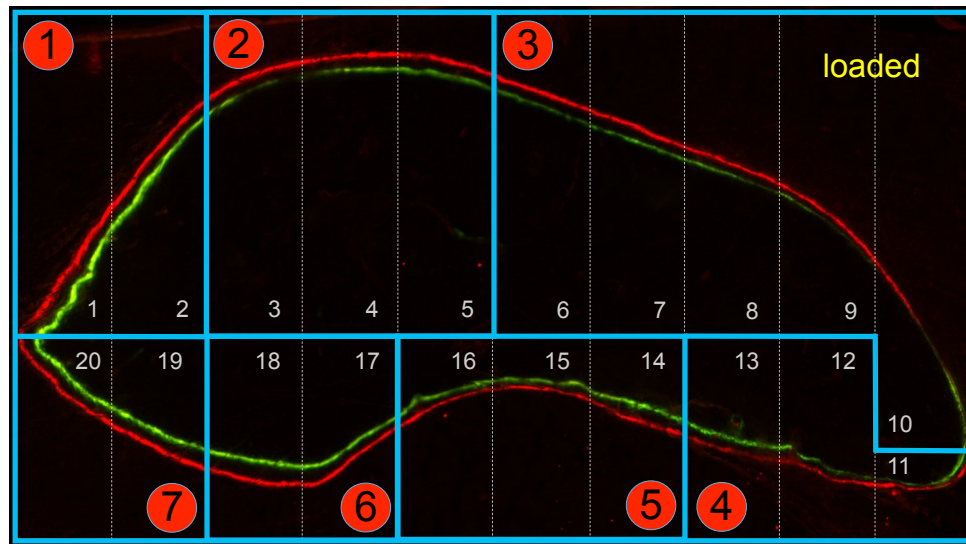


**Figure 3.6** Cross-sectional image of a loaded ulna with the 20-segment, 7-section grid overlaid.

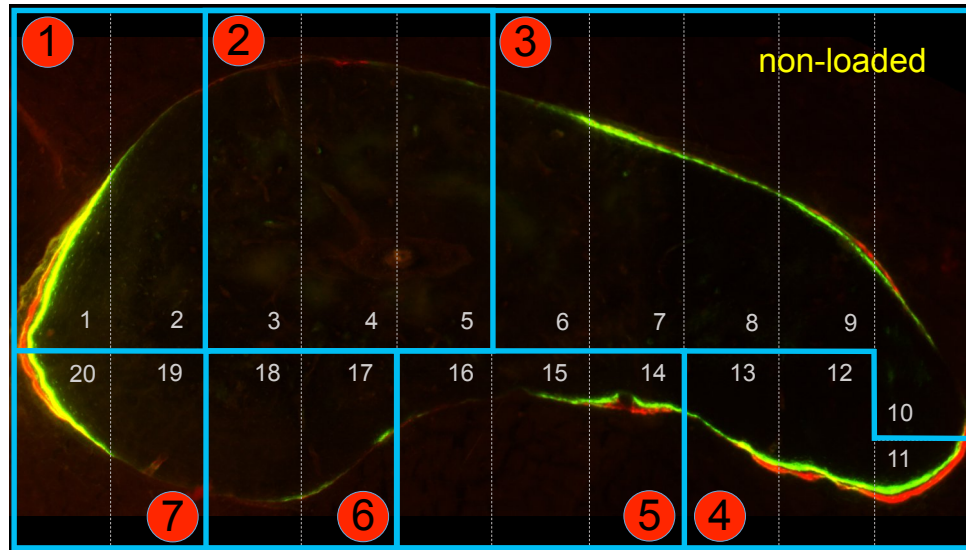


**Figure 3.7** Cross-sectional image of a non-loaded ulna with the 20-segment, 7-section grid overlaid.

### 3.5.6 MAR Determination

Captured images were imported into Powerpoint, aligned horizontally and overlaid with the 20-segment, 7-section grid template such that the edges of the grid aligned with the anterior and posterior tips of the bone section (Figure 3.6). The images with the overlaid grids were then saved as JPEG images. From these images with overlaid grids, double-label perimeter (dL.Pm) and double-label area (dL.Ar) were determined using ImageJ (<http://rsbweb.nih.gov/ij/>). The measurements were used to determine inter label thickness ( $Ir.L.Th = dL.Ar/dL.Pm; \mu m$ ) and mineral apposition rate ( $MAR = Ir.L.Th/inter\ label\ time\ (Ir.L.t)$ ). MAR was determined for each of the Sections individually (Figure 3.8). The MAR of each Section of the non-loaded left ulnas was compared to the MAR of the CON loaded right ulnas to determine which Sections contained lamellar bone formation induced by the mechanical loading. Sections in the

loaded ulnas that had a significantly greater MAR than the non-loaded ulnas were used to determine the timing effects of NSAID administration on MAR. Sections 1, 4 and 7 consistently exhibited bone formation associated with growth in the non-loaded ulnas and so it was decided to omit those sections from the main analyses (see *Results 4.1* for further explanation). The MAR for all Sections in each of the experiments can be found in the Appendix.

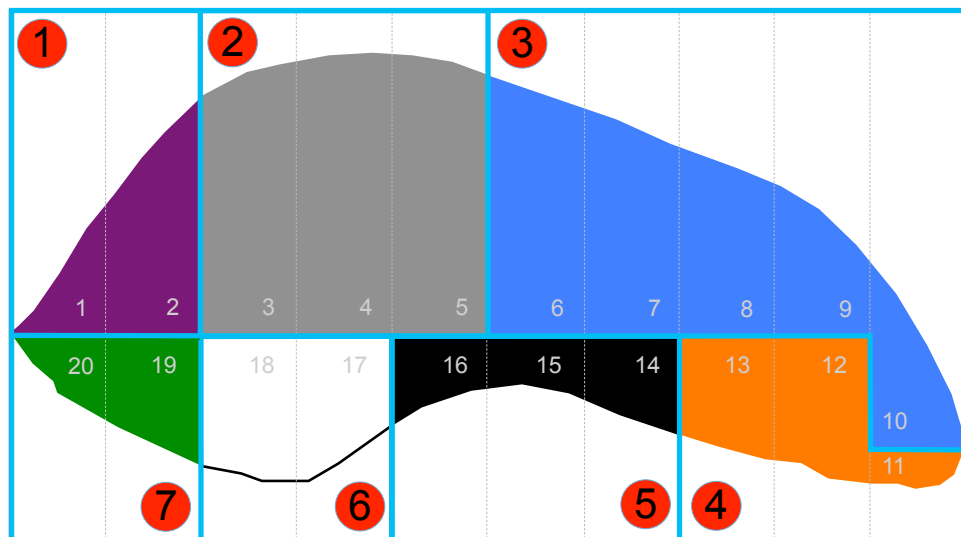


**Figure 3.8** Colour coded 7-Section grid of an ulna cross-section. The colours of each of the Sections correspond to the colours of the bars representing each Section on the graphs displaying MAR.

### 3.6 Statistics

To determine which Sections contained lamellar bone formation induced by the mechanical loading, an independent t-test was used to compare the MAR of each Section of the CON ulnas to the non-loaded LEFT ulnas (SPSS Inc., Chicago, IL, USA). An analysis of variance (ANOVA) with a Tukey post-hoc test was used to determine the

effects of NSAID administration and timing on MAR. A significance level of  $p < 0.05$  was used for all statistical tests.

## CHAPTER FOUR

### RESULTS: *IN VIVO* MECHANICAL LOADING

#### 4.1 1-Month Loading Protocol in Male Rats: Indomethacin

The effects of indomethacin on ulnar MAR were examined first using the 1-month loading protocol in male rats. Five ulnas were not included in the analyses of the indomethacin experiment. Two LEFT ulnas were not included because the cross-sectional images were cut-off when they were rotated for the MAR determination. One ulna from the H-POST group was not included because the image was missing. Two ulnas one from each of the L-PRE and L-POST groups developed woven bone and were therefore excluded from all analyses. Body mass did not differ between the CON group and the indomethacin experimental groups ( $p>0.05$ ) (Appendix XV).

The MAR was significantly greater in six of the seven sections in the CON ulnas compared to the LEFT ulnas ( $p<0.05$ ) (Figure 4.1). Only Section 4 ( $p=0.714$ ) (Figure 4.1D) exhibited a similar MAR between CON and LEFT ulnas. The MAR in the CON group did not differ compared to any of the indomethacin experimental groups for any of the seven Sections. Based on the analyses, the dose and timing of indomethacin administration did not have a significant effect on the MAR of the ulna for any of the Sections. See Figure 4.2A-G for the  $p$ -values determined by post-hoc analyses for each Section.

Based on the results of the indomethacin experiment, it was decided that Sections 1, 4 and 7 (Figure 4.1A, D, G) would not be included in further experimental analyses.

Section 4 was excluded because the MAR in that section was similar in the LEFT ulnas compared to the CON ulnas (Figure 4.1D). Sections 1 and 7 were not included because although those sections showed significantly greater MAR in the CON ulnas compared to the LEFT, they consistently showed bone formation in those sections. The MAR was similar ( $p>0.05$ ) in Sections 1, 4 and 7 and was greater ( $p<0.05$ ) in each of those sections compared to Sections 2, 3, 5 and 6 (Figure 4.1B, C, E, F).

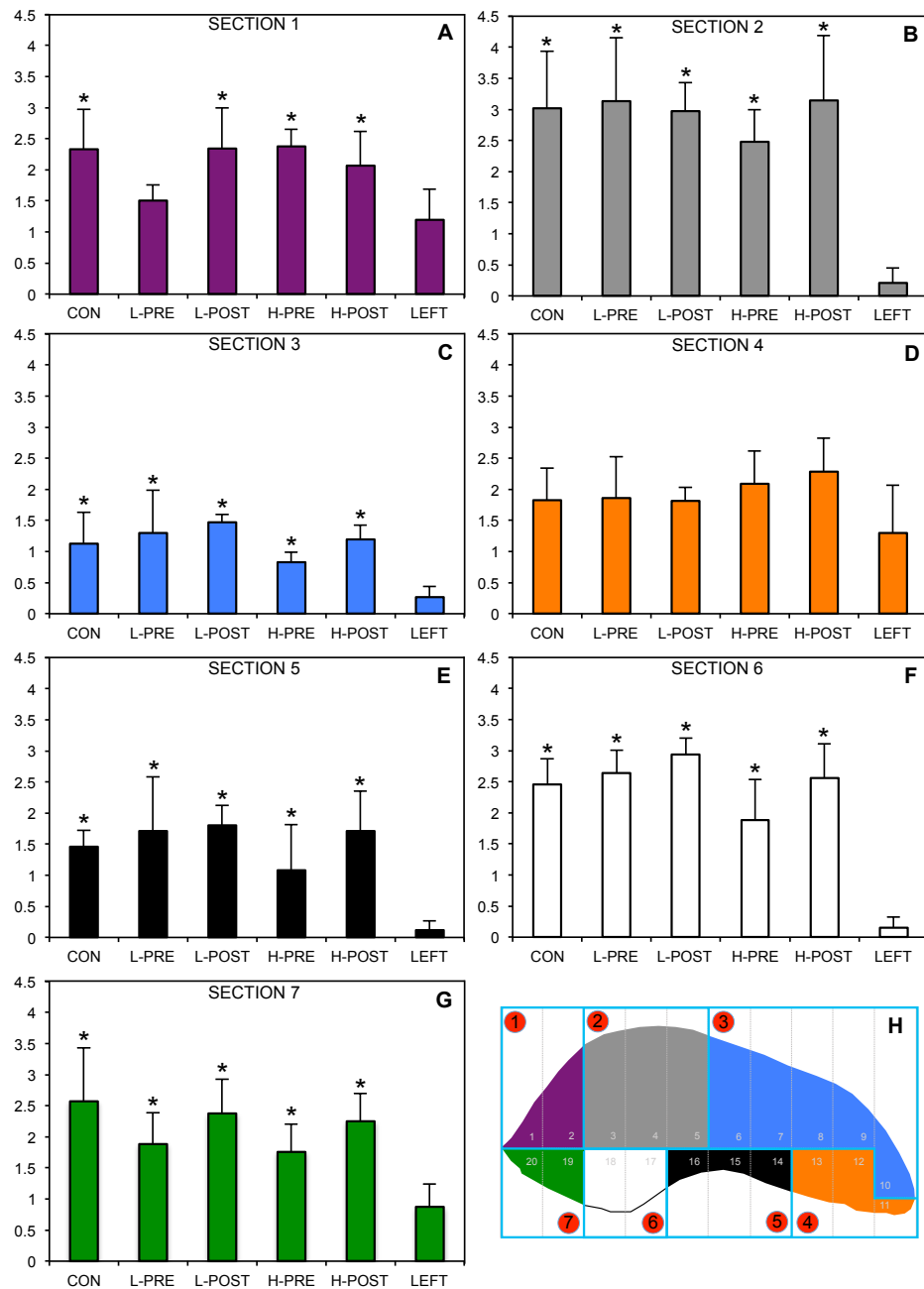


**Figure 4.1** MAR ( $\mu\text{m/day}$ ) of Sections 1-7 of the male ulnas that underwent the 1-month loading protocol in the indomethacin experiment. A-G) MAR of Sections 1-7, respectively. H) Colour coded 7-Section grid of ulna cross-section. Values are mean  $\pm$  STD. \*Different from LEFT. CON=no indomethacin dosing (n=4). L-PRE=low dose before (n=3); L-POST=low dose after (n=3); H-PRE=high dose before (n=4); H-POST=high dose after (n=3); LEFT=non-loaded ulnas (n=18). low dose=0.2mg/kg; high dose=2mg/kg.

<b>A</b>	<b>SECTION 1</b>	<b>L-PRE</b>	<b>L-POST</b>	<b>H-PRE</b>	<b>H-POST</b>	<b>LEFT</b>
	CON	0.278	1.00	1.00	0.983	0.003
	L-PRE		0.324	0.224	0.727	0.915
	L-POST			1.00	0.983	0.010
	H-PRE				0.963	0.002
	H-POST					0.081

<b>B</b>	<b>SECTION 2</b>	<b>L-PRE</b>	<b>L-POST</b>	<b>H-PRE</b>	<b>H-POST</b>	<b>LEFT</b>
	CON	1.00	1.00	0.827	1.00	<0.0005
	L-PRE		1.00	0.752	1.00	<0.0005
	L-POST			0.902	0.999	<0.0005
	H-PRE				0.738	<0.0005
	H-POST					<0.0005

<b>C</b>	<b>SECTION 3</b>	<b>L-PRE</b>	<b>L-POST</b>	<b>H-PRE</b>	<b>H-POST</b>	<b>LEFT</b>
	CON	0.971	0.649	0.681	1.00	<0.0005
	L-PRE		0.979	0.298	0.998	<0.0005
	L-POST			0.070	0.858	<0.0005
	H-PRE				0.561	0.015
	H-POST					<0.0005

<b>D</b>	<b>SECTION 4</b>	<b>L-PRE</b>	<b>L-POST</b>	<b>H-PRE</b>	<b>H-POST</b>	<b>LEFT</b>
	CON	1.00	1.00	0.994	0.95	0.714
	L-PRE		1.00	0.998	0.971	0.768
	L-POST			0.995	0.957	0.819
	H-PRE				0.999	0.312
	H-POST					0.215

<b>E</b>	<b>SECTION 5</b>	<b>L-PRE</b>	<b>L-POST</b>	<b>H-PRE</b>	<b>H-POST</b>	<b>LEFT</b>
	CON	0.961	0.870	0.793	0.961	<0.0005
	L-PRE		1.00	0.363	1.00	<0.0005
	L-POST			0.225	1.00	<0.0005
	H-PRE				0.363	0.002
	H-POST					<0.0005

<b>F</b>	<b>SECTION 6</b>	<b>L-PRE</b>	<b>L-POST</b>	<b>H-PRE</b>	<b>H-POST</b>	<b>LEFT</b>
	CON	0.983	0.454	0.183	0.999	<0.0005
	L-PRE		0.879	0.068	1.00	<0.0005
	L-POST			0.004	0.735	<0.0005
	H-PRE				0.129	<0.0005
	H-POST					<0.0005

<b>G</b>	<b>SECTION 7</b>	<b>L-PRE</b>	<b>L-POST</b>	<b>H-PRE</b>	<b>H-POST</b>	<b>LEFT</b>
	CON	0.446	0.994	0.196	0.950	<0.0005
	L-PRE		0.816	0.999	0.938	0.022
	L-POST			0.563	1.00	<0.0005
	H-PRE				0.766	0.025
	H-POST					0.001

$p < 0.05$

$p < 0.10$

**Figure 4.2** The  $p$ -values determined by post-hoc analyses for each Section of the indomethacin experiment. A-G)  $p$ -values of Sections 1-7, respectively.

#### **4.2 1-Month Loading Protocol in Male Rats: NS-398**

The effects of NS-398 (a COX-2 selective inhibitor) on ulnar MAR were examined in a 1-month loading experiment in male rats. Four ulnas were not included in the analyses of the NS-398 experiment. Two ulnas from the CON group and one from the PRE group were not included because the cross-sectional images were cut-off when they were rotated for the MAR determination. One of the POST ulnas was excluded because the cross-sectional image was not at an appropriate location along the length of the ulna; it was too distal. Body mass did not differ between the CON group and the PRE and POST groups ( $p>0.05$ ) (Appendix XV).

The MAR was significantly greater in Sections 2, 3, 5 and 6 in the CON ulnas compared to the LEFT ulnas ( $p<0.05$ ) (Figure 4.3A-D). The MAR in the CON group did not differ compared to the PRE or POST groups for Sections 2, 3, 5 or 6. NS-398, administered either before or after loading, did not affect MAR in the loaded rat ulna.

See Appendix VI for graphs of all seven sections and Appendix VIII for tables displaying the  $p$ -values determined by post-hoc analyses for each Section.

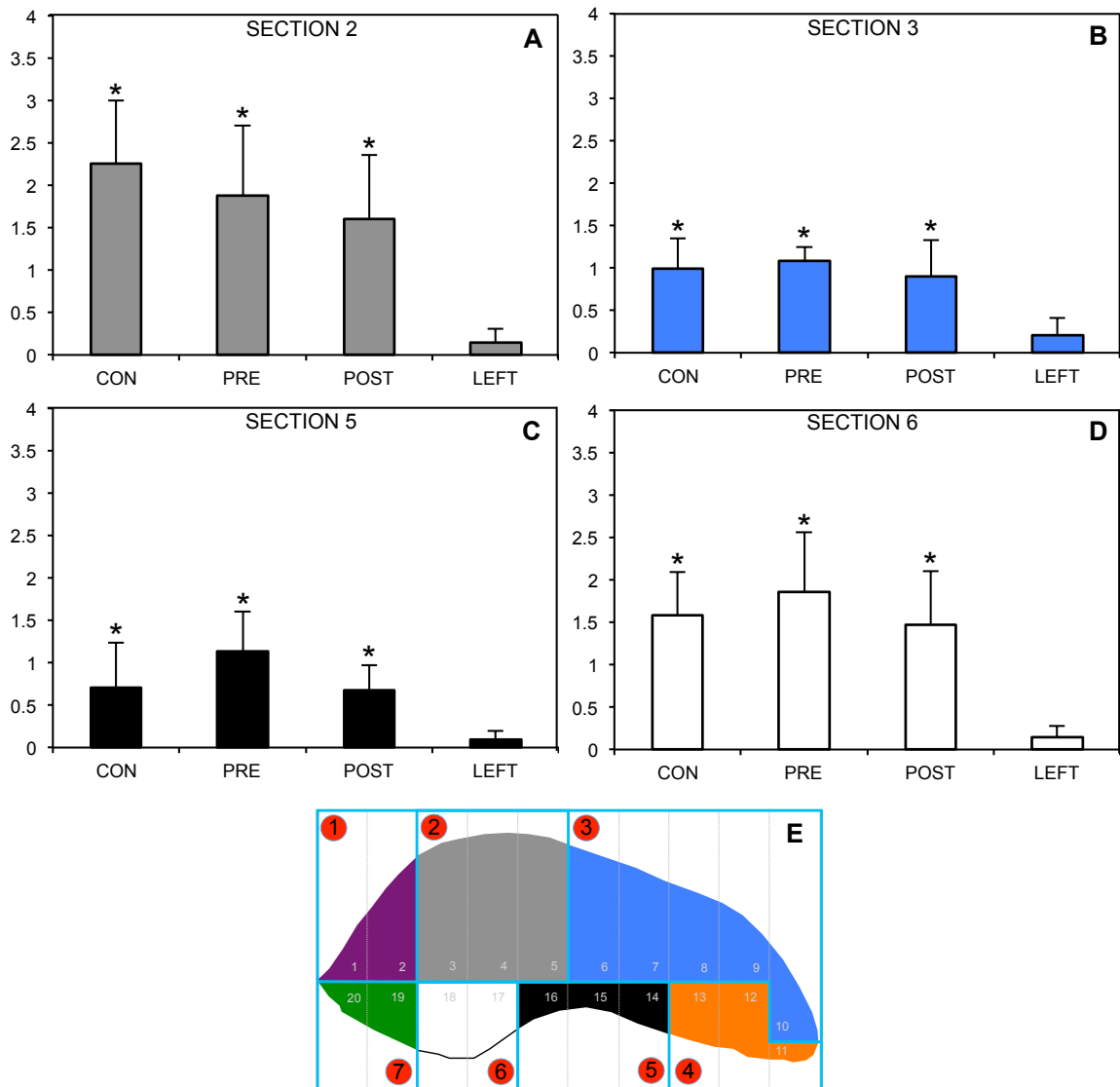


**Figure 4.3** MAR ( $\mu\text{m}/\text{day}$ ) of Sections 2, 3, 5 and 6 of the male ulnas that underwent the 1-month loading protocol in the NS-398 experiment. **A-D)** MAR of Sections 2, 3, 5 and 6, respectively. **E)** Colour coded 7-Section grid of ulna cross-section. Values are mean  $\pm$  STD. \*Different from LEFT. CON=no NS-398 dosing (n=8); PRE=dose before (n=9); POST=dose after (n=9); LEFT=non-loaded ulnas (n=15).

### **4.3 2-Week Loading Protocol in Female Rats: Ibuprofen and Celebrex**

The effects of ibuprofen (a non-selective inhibitor) and Celebrex (a COX-2 specific inhibitor) on ulnar MAR were examined using the 2-week loading protocol in female rats (Figure 4.4). In the 2-week loading experiment 11 of the 26 female ulnas exhibited woven bone formation so they were excluded from all analyses. In addition, one of the forelimbs in the IBU-POST group was broken during the loading. Only 14 ulnas were analyzed. The CBX-PRE group only had one ulna remaining after the exclusions, so it was excluded from all statistical analyses. Body mass did not differ between the CON group and the IBU and CBX experimental groups ( $p>0.05$ ) (Appendix XV).

The MAR was significantly greater in Section 2 in CON ulnas compared to the LEFT ulnas ( $p<0.05$ ) (Figure 4.4A). The MAR in the CON group did not differ ( $p>0.05$ ) compared to the IBU or CBX groups for Sections 2, 3, 5 or 6 (Figure 4.4A-D). Ibuprofen, administered either before or after loading, did not affect ulnar MAR in the female rats that underwent the 2-week loading protocol.

See Appendix IX for graphs of all seven sections and Appendix XI for tables displaying the  $p$ -values determined by post-hoc analyses for each Section.

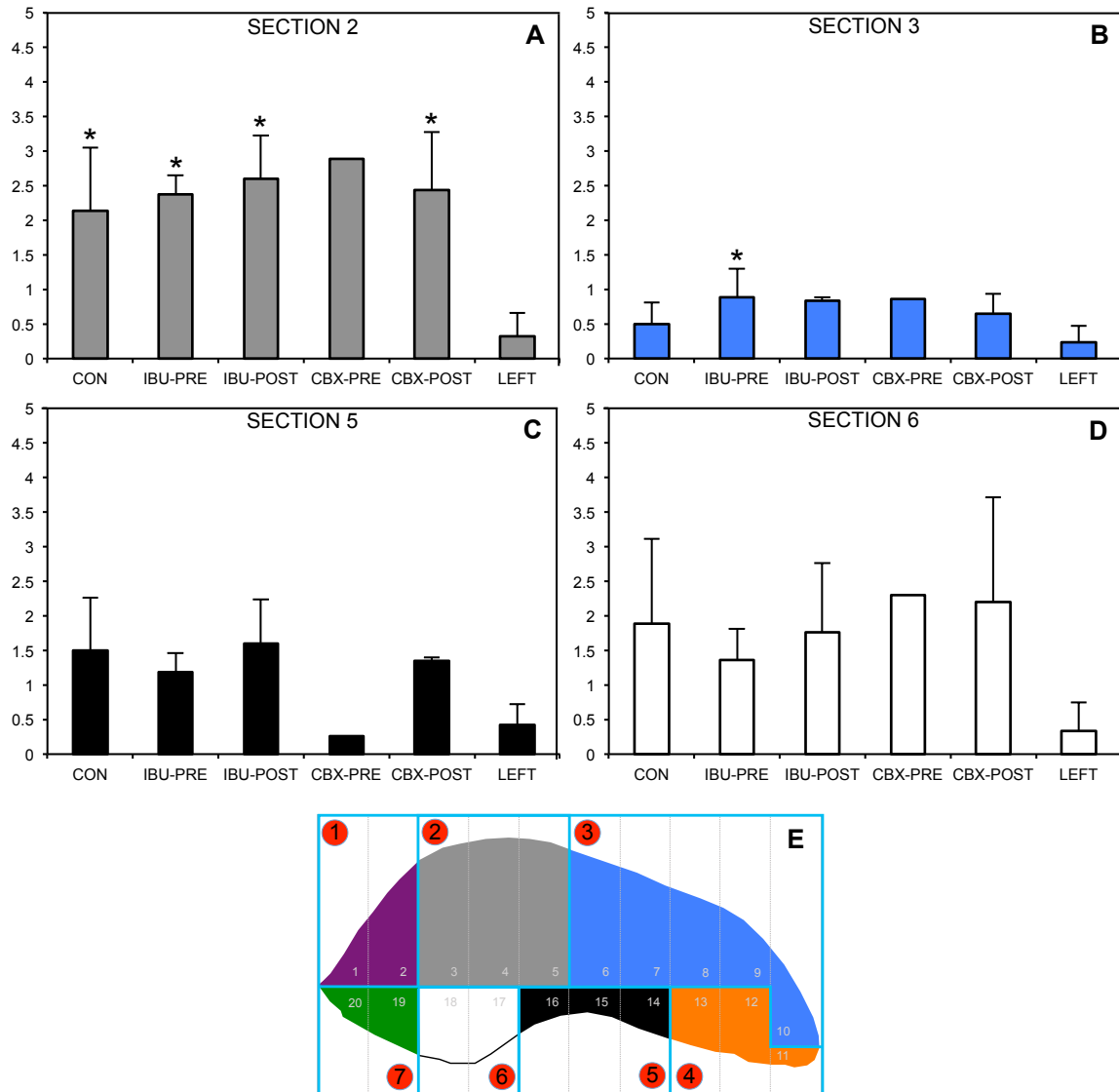


**Figure 4.4** MAR ( $\mu\text{m}/\text{day}$ ) of Sections 2, 3, 5 and 6 of the female ulnas that underwent the 2-week loading protocol in the IBU/CBX experiment. **A-D)** MAR of Sections 2, 3, 5 and 6, respectively. **E)** Colour coded 7-Section grid of ulna cross-section. Values are mean  $\pm$  STD. \*Different from LEFT. CON=no NSAID dosing (n=3); IBU-PRE=ibuprofen dosing before (n=4); IBU-POST=ibuprofen dosing after (n=3); CBX-PRE=Celebrex dosing before (n=1); CBX-POST= Celebrex dosing after (n=2); LEFT=non-loaded ulnas (n=5).

#### **4.4 1-Month Loading Protocol in Female Rats: Ibuprofen**

The timing effects of ibuprofen administration before loading on ulnar MAR were examined in female rats using the 1-month loading protocol. One animal was excluded from the 1HR group because she did not eat her flavoured gelatin. Body mass did not differ between the CON group and the ibuprofen experimental groups ( $p>0.05$ ) (Appendix XV).

The MAR was significantly greater in Section 2 in the CON ulnas compared to the LEFT ulnas ( $p<0.05$ ) (Figure 4.5A). The MAR in Sections 3, 5 and 6 did not differ ( $p>0.05$ ) between the CON and LEFT ulnas (Figure 4.5B-D). The MAR in the CON group did not differ ( $p>0.05$ ) compared to any of the IBU experimental groups for Sections 2, 3, 5 or 6 (Figure 4.5A-D). Ibuprofen administration before loading did not affect ulnar MAR in female rats that underwent the 1-month loading protocol.

See Appendix XII for graphs of all seven sections and Appendix XIV for tables displaying the  $p$ -values determined by post-hoc analyses for each Section.

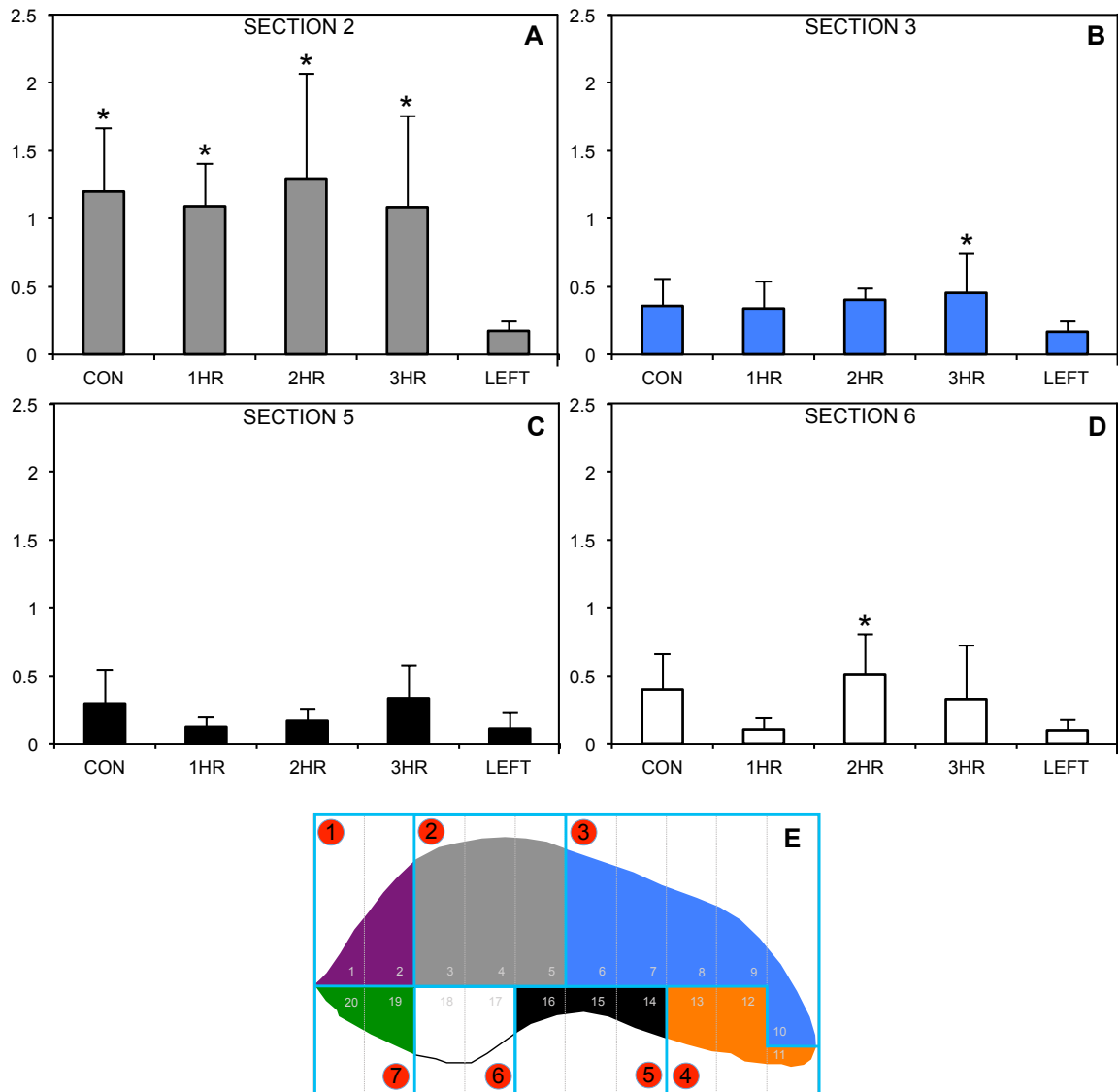


**Figure 4.5** MAR of ( $\mu\text{m}/\text{day}$ ) of Sections 2, 3, 5 and 6 of the female ulnas that underwent the 1-month loading protocol in the ibuprofen timing experiment. A-D) MAR of Sections 2, 3, 5 and 6, respectively. E) Colour coded 7-Section grid of ulna cross-section. Values are mean  $\pm$  STD. \*Different from LEFT. CON=no ibuprofen dosing (n=5); 1HR=ibuprofen dosing 1hr before (n=4); 2HR=ibuprofen dosing 2hrs before (n=6); 3HR=ibuprofen dosing 3hrs before (n=5); LEFT=non-loaded ulnas (n=8).

## CHAPTER FIVE

### DISCUSSION: *IN VIVO* MECHANICAL LOADING

#### 5.1 Discussion

The purpose of the *in vivo* experiments was to examine the timing-related effects of inhibiting mechanotransductive signals, specifically PGE<sub>2</sub> production, with NSAID administration, on lamellar bone formation induced by multiple loading events. The hypothesis was that NSAID administration before mechanical loading would impair bone formation, whereas administration following loading would enhance bone formation. The findings did not support the hypothesis. The loading protocols successfully induced the formation of lamellar bone in the ulna as measured by dynamic histomorphometric measures of bone mineral apposition rate (MAR). However, NSAID administration, either before or after loading, did not have a significant effect on MAR. MAR did not differ between male rats administered indomethacin or NS-398, before or after loading, and control rats that received no NSAID. Similarly, in female rats, there was no difference in MAR between rats administered ibuprofen, before or after loading, and rats not receiving ibuprofen. The results suggest that NSAID administration, either before or after loading, does not influence bone formation induced by multiple mechanical loading sessions.

Previous animal studies that examined NSAID administration prior to one loading event demonstrated inhibitory effects on lamellar bone formation indices [9–12,172]. More recent studies examined the effects of NSAID administration prior to multiple

loading events [13,170]; an inhibitory effect of NSAID administration was not shown.

The results of this project are in agreement with the studies examining repeated loading sessions; NSAIDs administered prior to loading do not impair bone formation. The results are also in agreement with two human studies, which demonstrated no impairment of bone mineral density adaptation to exercise when ibuprofen was administered before exercise in a 9 month exercise program [14,15]. Together these results suggest different signalling pathways and factors may be relied upon more for bone formation resulting from multiple days of loading compared to just one loading event.

Signalling pathways besides the COX-2/PGE<sub>2</sub> pathway may be active during the extended loading protocols. It was shown that a functional COX-2 gene was not required for bone adaptation to two days of mechanical loading in female mice with a null mutation of the COX-2 gene [215]. The authors suggested that there may be compensatory pathways in the COX-2 deficient mice and that these may not develop when COX-2 is simply blocked with NSAIDs, as shown in previous studies. However, the studies the authors referred to [10,12] only examined one loading event.

Alam et al. [215] suggested that compensation from COX-1 and non-COX compensatory pathways was possible in the COX-2 deficient mice. In this project, compensation through COX-1 may have occurred in the animals receiving NS-398, a COX-2 selective NSAID, but the results of the experiments examining indomethacin and ibuprofen, non-selective NSAIDs inhibiting COX-1 and COX-2 approximately equally, suggest it is more likely that other compensatory pathways were active. Further investigation is needed to determine if other early response pathways, such as calcium, or nitric oxide

signalling, were more active and/or relied upon more and if there were changes in gene expression that compensated for inhibition of the COX-2/PGE<sub>2</sub> pathway during loading protocols that extended over a period of time.

## **5.2 NSAID Administration Before and After Loading**

Prostaglandins are one of the key intermediaries responsible for bone mechanotransductive signalling. It is believed that COX-2 produced by the early upregulation of mRNA is not responsible for the immediate rise in PG production in response to mechanical loading [81]. COX-2 protein synthesis does not begin until 1-4 hours post loading and peaks at 3-12 hours [96]. Since the mechanically induced COX-2 production is delayed after loading, the early release of PGs (within the first hour) seems to be a result of constitutive COX activity and not induced COX-2. Therefore, the PGs responsible for signalling mechanically induced bone formation are likely a result of constitutive COX enzymes. Induced COX-2 expression occurs when a prolonged period of PGs is required, as is the case when mechanical loading triggers bone adaptation and various cell responses, including differentiation and replication [81]. Induced COX-2 produces large amounts of PGs that can then induce bone formation. Chow and Chambers [11] showed that daily administration of indomethacin for 7 days after a single loading session inhibited bone formation, indicating that induced COX activity is required for the subsequent bone response to mechanical loading.

NSAID administration around the time of loading, either before or after, targets COX enzyme activities differently. NSAID administration before mechanical loading is

thought to inhibit the constitutive COX activity, which is responsible for producing PGs required for mechanotransductive signalling. NSAID administration before a single mechanical loading event has been shown to diminish the bone formation induced by the loading [9–12]. Li et al. [12] administered NS-398 with intraperitoneal injection 3 hours or 30 minutes (time of peak plasma concentration) before a single loading session or 30 minutes after in female rats. They found that an injection 3 hours or 30 minutes before loading impaired periosteal bone formation rate (BFR) to a similar extent whereas an injection 30 minutes after loading only slightly suppressed BFR [12]. They suggested that the primary cellular mechanism of bone formation following a single loading event involves the secretion of intracellular constitutive PGs, not new PG synthesis associated with increased COX-2 activity. Therefore, PG synthesis must be suppressed with NSAIDs for a period of time before loading to reduce the intracellular PG stores and inhibit the subsequent secretion at the time of loading. The presence of NS-398 for 30 minutes reduced intracellular PGE<sub>2</sub> levels of MC3T3-E1 osteoblasts *in vitro* by 80% compared to controls and suppressed the release of PGE<sub>2</sub> after mechanical stimulation [172]. It is also possible that it takes time for the bone cells to take up the NSAID from the serum. However, Paulson et al. [188] found that celecoxib reached maximum concentrations in the bone and bone marrow 1 hour after oral administration in male rats. Tissue distribution would take longer after oral administration so that does not seem as likely.

NSAID administration before each loading session, when there are multiple loading sessions, does not appear to affect bone formation. In this project, the MAR in the

PRE group did not differ from the CON group. These results are in agreement with the only two studies in the literature that examined the effects of NSAID administration before loading on bone formation induced by multiple loading sessions [13,170].

Sugiyama et al. [13] found that NS-398 did not affect bone formation. However, the hindlimb axial loading model used in that study induced both lamellar and woven bone formation [13]. Cunningham [170] found no effect of ibuprofen administration before multiple simulated resistance training exercise sessions in rats on periosteal lamellar BFR, mineralizing surface (MS/BS) or MAR. However, woven bone was also induced in that model. It is difficult to compare a model without woven bone formation to one that induced woven bone because different bone formation signals are responsible for the different responses. It could be that PG mediated mechanotransductive signalling is not essential for bone formation induced by multiple mechanical loading sessions; other pathways may be more important. In addition, the induced COX-2 expression would still have occurred after each loading event, producing large amounts of PGs, important for bone formation.

NSAID administration after loading may suppress induced COX-2 activity. Peak NSAID activity would occur approximately during COX-2 protein synthesis. Therefore, although mechanotransduction would still have occurred normally, the induced COX-2 synthesis of PGs, required for bone formation, would likely have been inhibited. PGE<sub>2</sub> synthesis from induced COX-2 may be inhibited with NSAID administration after loading, but it does not appear to affect bone formation; in this project the MAR in the POST group did not differ from the CON group. The increased PGE<sub>2</sub> production before

loading may be enough to trigger bone formation. These results are in agreement with a study that found no effect of ibuprofen administration, after multiple simulated resistance training exercise sessions, on periosteal lamellar BFR, MS/BS or MAR in rats [170].

However, woven bone was also induced in that model. Chow and Chambers [11] found no effect of indomethacin on bone formation when it was administered orally six hours after a single loading session but Li et al. [12,172] found that intraperitoneal injection of NS-398, 20 or 30 minutes after a single loading session, did suppress bone formation, although not significantly. They suggested that PG synthesis occurring just after or a few hours after loading does contribute to bone formation. The lack of difference in MAR between the CON and POST group suggests that the key time may have been missed. Oral administration would take longer to reach peak levels than intraperitoneal injection. As stated previously however, other pathways may be more important when there are multiple loading events or the activity of other pathways may increase to compensate for the lack of PGE<sub>2</sub>.

Rissing and Buxton [216] developed a rat model of experimental osteomyelitis in the tibia. Interestingly, they showed that tibial bone PGE<sub>2</sub> concentrations were similar in rats that did not receive ibuprofen and rats that received oral doses of ibuprofen (30 mg/kg) every 8 hours for 12 days. They did find that ibuprofen decreased PGE<sub>2</sub> concentrations in infected tibiae and so they proposed that the ibuprofen may differentially affect the sources of PGE<sub>2</sub> and may reflect variable susceptibility of COX enzyme inhibition. NSAIDs were likely reaching the bone [188], but whether or not they inhibited PGE<sub>2</sub> production once there is not known. However, once again, the single

loading event studies showed an effect of NSAIDs on bone formation [9–12,172], suggesting that PGE<sub>2</sub> production was in some way altered. In this project, if PGE<sub>2</sub> concentrations were unaltered at the bone level, in the presence of NSAIDs, then bone mechanotransduction and formation would have been unaffected by NSAIDs.

Determining PGE<sub>2</sub> concentrations in the bone is difficult and animals would have needed to be sacrificed at various time points to determine the time course of PGE<sub>2</sub> production. Such an experiment would have required a large number of animals and resources. As a result, this was not examined *in vivo*. Instead, an *in vitro* approach was taken to examine the time course of PGE<sub>2</sub> production following mechanical stimulation.

The lack of effect of NSAID administration, either before or after loading, on bone formation, suggests that the COX-2/PGE<sub>2</sub> pathway is not essential for bone formation induced by multiple mechanical loading sessions. Further investigation is needed to determine which factors and pathways are responsible for inducing bone formation following multiple loading events, not just a single event, particularly the contributions that various pathways make when one is impaired.

### **5.3 Potential Factors Influencing NSAID Effects on Bone Adaptation**

NSAID effects on bone adaptation appear to be very complicated, likely due to the complicated nature of the COX-2/PGE<sub>2</sub> pathway. A number of factors likely contribute to the effect of NSAIDs including: the NSAID in use and the corresponding pharmacokinetics, the age and sex of the subjects examined and the overall state of the bone environment. Further investigation is needed to determine how to best manage

NSAID administration to limit adverse effects on bone and even possibly encourage positive outcomes.

### **5.3.1 NSAID Pharmacokinetics**

NSAID pharmacokinetics depend on a number of factors including: the type of NSAID, the route of administration, the dose, the subject studied as well as the age and sex of the subjects [187]. NSAID pharmacokinetics in rats differs from humans and the sex of the rat also influences how NSAIDs are metabolized. So translating NSAID doses and administration times between studies is complicated. It is important to understand how the selected NSAID will behave in the chosen model so as to be able to understand how it will affect COX inhibition and subsequent PG production.

#### **5.3.1.1 Type of NSAID**

The type of NSAID administered may influence its effect on mechanically induced bone formation. COX-2 has been acknowledged as the key enzyme responsible for PGE<sub>2</sub> production during mechanical loading. However, it is believed that the upregulation of COX-2 mRNA is not responsible for the immediate prostaglandin response to mechanical stimulation because it occurs too quickly [81]. Transient increases in COX-2 mRNA expression were shown not to occur until 2 hours after a mechanical loading event in rat osteocytes *in vivo* [217]. COX-2 mRNA expression was increased in rat tibiae 2 hours after bending and returned to pre-loading levels by 24 hours [81]. Immediately after loading COX-2 mRNA was similar in loaded and non-loaded

tibiae [81]. COX-1 mRNA expression was not influenced by loading and as a result remained similar immediately after loading, 2 hours and 24 hours after [81]. COX-1 mRNA expression was almost twice as great as COX-2 expression immediately after loading and 24 hours after and was similar to COX-2 expression at 2 hours [81].

Bakker et al. [169] showed that both constitutive COX-1 and COX-2 contributed to PGE<sub>2</sub> production following 1 hour of fluid flow. Li et al. [12] suggested that the secretion of intracellular constitutive PGs, not new PG synthesis is important for bone formation, suggesting a role for both COX-1 and COX-2 for the initial PG release.

Both constitutive COX-1 and COX-2 seem to be involved in the immediate prostaglandin release following mechanical stimulation. Forwood et al. [218] showed that 10 minutes after tibia bending in the rat, the number of osteocytes positive for COX-1 and COX-2 were significantly greater than in non-loaded tibias. This difference was no longer evident 6 and 24 hours after loading. The increased number of osteocytes labeled for both COX-1 and COX-2 following loading may indicate a need for both enzymes for the production of PGE<sub>2</sub> for initial mechanotransductive signalling. Subsequent signalling and bone formation may be more reliant upon induced COX-2. Forwood et al. [218] suggested that the transient increase was likely not a result of increased gene expression but rather an alteration in enzyme availability necessary for PGE<sub>2</sub> synthesis. The constitutive forms of COX-1 and COX-2 are typically bound to the cell membrane [218] and therefore may be available for mechanotransduction involving G proteins. G protein linked mechanotransducers are one of the potential pathways responsible for PG production [84] and mechanical stimulation of the mechanotransducer may release the

COX enzymes for PG production. Nitric oxide can also activate COX-1 and COX-2 [219], resulting in increased PGE<sub>2</sub> production.

The activities of both COX-1 and COX-2 appear to be important for initial mechanotransductive signalling. Non-selective NSAIDs may impair the immediate response more than COX-2 selective NSAIDs, since they inhibit COX-1-mediated events preferentially or inhibit COX-1 and COX-2-mediated events approximately equally. In contrast, COX-2 selective NSAIDs would likely influence the delayed induced COX-2 response more, the response responsible for promoting long-term PG effects. The type of NSAID administered before a single loading bout has been shown to differentially affect bone formation indices, but the results are not consistent. Forwood [10] showed that NS-398 administration prior to one tibial bending event impaired endocortical BFR, MAR and MS/BS in rats, but indomethacin only impaired BFR. Using a very similar model, Li et al. [12] showed that both NS-398 and indomethacin impaired endocortical BFR and MS/BS but had no effect on MAR. NS-398 did impair BFR more than indomethacin, however. The effects of NS-398 and indomethacin on periosteal bone formation indices were similar; both impaired BFR and had no effect on MS/BS and MAR [12]. In this project, periosteal MAR was not influenced by NS-398, indomethacin or ibuprofen. In agreement with this project, the two studies that examined multiple loading events showed that both NS-398 [13] and ibuprofen [170] did not affect bone formation. Taken together, all of these results suggest that non-selective and COX-2 selective NSAIDs have a similar effect or lack of effect on mechanically induced bone formation.

### **5.3.1.2 Timing of NSAID Administration**

The specific timing of NSAID administration relative to loading may influence NSAID effects on bone adaptation. NSAID administration before loading was intended to inhibit the PGE<sub>2</sub> mechanotransductive signalling at the time of loading. Therefore, the timing of administration before loading was chosen so that peak plasma concentrations would occur at the time of loading.

Previous studies examining the effects of NSAIDs on bone formation in response to a single loading event, used female rats [10,12,172]. However, they based their timing of NSAID administration on NSAID pharmacokinetics in male rats [197,198,203]. Whether sex differences exist in the pharmacokinetics of those particular NSAIDs was likely not known. Indomethacin and NS-398 pharmacokinetics in female rats do not appear to be present in the literature and some of the literature does not state the sex of the rats used. Indomethacin and NS-398 pharmacokinetics in female rats are unknown and therefore it is difficult to evaluate the validity of establishing the timing of their administration in female rats based on male rat pharmacokinetics. However, Forwood et al. [10] and Li et al. [12,172] found bone formation to be inhibited in female rats with indomethacin and NS-398 administration, with the administration timing based upon male rat pharmacokinetics. Inhibition of bone formation in these studies suggests the NSAIDs were indeed active and inhibiting PG production at the key times around the time of loading. NSAID pharmacokinetics should be determined for each individual model to determine optimal dosing times.

The motivation behind examining NSAID effects on bone formation in both male and female rats in this project stems from the potential sex differences in NSAID pharmacokinetics. The timing of NSAID administration in the male rats was based on the literature but there does not appear to be any literature describing NSAID pharmacokinetics in female rats. The NSAID timing before loading should have been appropriate for the males based on the pharmacokinetics described in the literature. The previous studies that examined NSAID effects on bone formation did not examine ibuprofen. Thus, the timing of ibuprofen administration in the female rats was based on the male pharmacokinetics while taking into account that females may metabolize the NSAIDs more slowly. The female ibuprofen timing experiment was designed to identify the optimal administration time before loading that would impair bone formation, as this was the hypothesis, NSAID administration before loading impairs bone formation. Three dosing times were examined; none of the ibuprofen administration times implemented, 1, 2 or 3 hours, impaired MAR. The lack of difference in MAR between the CON group and the 1HR, 2HR and 3HR groups suggests ibuprofen dosing before multiple loading events does not affect bone formation. In addition, since multiple administration times were examined, it is likely that peak plasma concentrations did occur near the time of loading in one of the groups.

In this project, NSAID administration occurred immediately following loading. The timing was based on the human exercise study that found that ibuprofen administration immediately after exercise enhanced the BMD response to exercise in premenopausal women [14]. All of the NSAIDs were administered immediately after

loading in this project. However, pharmacokinetics differ between NSAIDs and therefore the effects on the time course of PGE<sub>2</sub> production likely also differ, which could affect bone formation responses to loading. Administration of ibuprofen immediately after loading in the human exercise study [14] may have resulted in an “ideal” time course of PGE<sub>2</sub> production. The time course in this project may not have been conducive to bone formation because of different NSAID pharmacokinetics. However, the mechanism responsible for the increased BMD is not known and PG inhibition may not have a direct effect on bone formation. Exercise stimulates increases in inflammatory cytokines and in the human exercise study, ibuprofen may have acted indirectly on the bone by suppressing inflammatory-mediated bone resorption [14]. Examination of various NSAID administration times after loading may help to identify if and when NSAIDs can enhance bone formation.

### **5.3.1.3 NSAID Dosing**

The NSAID doses chosen for this project were based on previous literature showing that at those doses, new bone formation was impaired or physiological effects were observed. The indomethacin and NS-398 doses used had previously been shown to impair lamellar bone formation induced by a single loading event [10,12]. The Celebrex dose was chosen because it had been shown to impair ligament healing [205] and decrease the concentration of PGE<sub>2</sub> in muscle tissue and decrease heterotopic ossification [207]. The dose of ibuprofen used had previously been shown to impair stress fracture healing in the rat ulna [211]. Based on the literature, the NSAID doses selected

were likely effective at inhibiting PG production. However, NSAID plasma concentrations were not determined in this project. Therefore, although the NSAID doses showed an effect in previous studies, the doses in this study may not have reached effective concentrations. The lack of effect of NSAIDs on mechanically induced bone formation may therefore be due to insufficient dosing and consequently a lack of PG inhibition.

Compared to human NSAID doses, the doses administered to the rats, on a milligram/kilogram basis, were on the higher end of the maximum daily dose suggested, not a single dose. However, translating drug doses between animals based on a milligram/kilogram basis is not the most accurate method. There are a number of methods available to assist in scaling drug doses between animals, some are much more complex and require much more information about the animal and drug pharmacokinetics than others. The metabolic rate and drug pharmacokinetics can differ between animals [220], producing different effects with the same dose scaled to animal mass. It is less accurate to compare the actual doses across animals because doses are derived from pharmacokinetic modeling [220]. It is better to compare a drug's pharmacokinetic parameters, since these depend on physiological parameters [220]. These are not always known and therefore doses must be estimated using other means. Metabolic rate is one of the main size-dependent animal differences affecting drug dosage [221]. When extrapolating doses among species of widely varying body weights, it is suggested to take metabolic rate into account. To account for metabolic rate, a calculation based on milligram/kilogram<sup>0.75</sup> should be used instead of a calculation based on just milligram/kilogram dose to help

improve accuracy [221–223]. Larger animals require smaller drug doses on a milligram/kilogram basis.

The NSAID doses in rats based on the typical human doses and the milligram/kilogram<sup>0.75</sup> calculation, suggest that the doses administered in this project were actually on the lower end of the human dose equivalents (Table 5.1). Those doses are typical of a single dose of an NSAID, a dose likely consumed around the time of exercise. Doses can also be scaled using allometry, but it only deals with size; it does not account for metabolic rate differences between animals. The best way to determine the appropriate drug dose in a study is to determine the pharmacokinetics of that drug in the animal model used. However, this can be time consuming and costly, but likely provides the most accurate information.

**Table 5.1 Typical human NSAID doses and corresponding doses in rats using the milligram/kilogram<sup>0.75</sup> scaling calculation.**

<b>NSAID</b>	<b>Human Dose<sup>a</sup> (mg/kg)</b>	<b>Rat Dose<sup>*,b</sup> (mg/kg)</b>	<b>Project Dose (mg/kg)</b>
<b>Celebrex</b>	1.4 - 11.4	4.6 - 37.5 males 5.5 - 44.5 females	10.0
<b>indomethacin</b>	0.4 - 2.1	1.3 - 6.9 males 1.5 - 8.2 females	2.0
<b>ibuprofen</b>	2.9 - 30	9.5 - 98.7 males 11.3 - 117.2 females	30.0

<sup>a</sup>The human dose was based on a 70 kg person. <sup>\*</sup>The rat dose was calculated using the milligram/kilogram<sup>0.75</sup> scaling. <sup>b</sup>The male rat dose was based on an average body mass of 600 g and the female rat dose was based on an average body mass of 300 g.

### 5.3.2 Sex of the Subjects

NSAID effects on bone formation may differ depending upon the sex of the subjects examined, but there is more likely a role for the state of the bone environment influencing NSAID effects on bone rather than sex [14,161]. In the Canadian Multicentre Osteoporosis Study, COX-2 inhibitor use was associated with lower BMD in men but showed positive effects on BMD in postmenopausal women not on hormone therapy and no effect in postmenopausal women using hormone therapy [161]. In pro-inflammatory and high turnover states, like those that occur in postmenopausal women, NSAIDs may help to decrease inflammation and subsequently inhibit resorptive activities. In more normal conditions, in men for example, NSAIDs may act differently, even inhibiting bone formation. Similar effects have been shown *in vitro* [154–156]. Under certain inflammatory conditions, such as estrogen deficiency, NSAIDs have been shown to inhibit bone resorption and osteoclastogenesis induced by inflammatory cytokines; but under more normal conditions, non-inflammatory states, NSAIDs did not have an effect on resorption or osteoclastogenesis [154–156].

In animal models, the effects of NSAIDs on mechanically induced bone formation have only been examined in female animals. This project examined males and females and did not find a difference between sexes. NSAID effects on BMD adaptations to exercise in humans have shown that ibuprofen administration after exercise can enhance the BMD response to exercise in premenopausal women [14], but did not have an effect in elderly men and postmenopausal women [15,171]. Ibuprofen administration before exercise had no effect on BMD in elderly men, premenopausal or postmenopausal women

[14,15,171]. These results do not suggest a sex effect or an effect of the bone environment. An age effect may be present. The adaptive response of bone to loading is impaired with age [224] and therefore the influence of NSAIDs on bone adaptation may vary.

Sex hormones such as estrogen and testosterone have been shown to influence COX enzymes and prostaglandin production [225,226]. The effects of NSAIDs on stable, experimental inflammation have shown considerable intra- and inter- subject variability but no sex differences have been shown [227]. However, COX gene disablement has shown sex effects on adjuvant-induced arthritis and inflammation, suggesting that the effects of COX inhibitors may have some sex dependence [226]. A study by Sibonga et al. [182] found that ibuprofen may partly act on the skeleton by antagonizing antiresorptive actions of estrogens, leading to detrimental effects. Their findings suggest that the COX pathway is essential for estrogen associated bone remodeling. Estrogen may inhibit the production of PGE<sub>2</sub> [228] or stimulate it [229]. Estrogen likely acts through COX-2; the estrous cycle of the rat has been shown to influence PG production through COX-2 [230]. Further investigation is needed to determine if there are sex and age effects of NSAIDs on bone adaptation.

#### **5.4 Differential Effects of NSAIDs on BFR, MAR and MS/BS**

The bone formation indices commonly reported in studies examining mechanically induced bone formation include mineralizing surface (MS/bone surface (BS)), mineral apposition rate (MAR) and bone formation rate (BFR).

MS/BS is the percentage of bone surface actively forming bone and is considered to be an index of osteoblast activity, both proliferation and/or differentiation [231]. MAR is considered to be an index of osteoblast vigor [231]. BFR, the product of MS/BS and MAR, represents the cumulative bone formation activity, including both the number of sites undergoing active formation and the rate at each site [231]. As such, minimal changes in both MS/BS and MAR can result in significant changes in BFR, given the mathematical relationship. A strong correlation has been shown between bone strain and BFR, but relatively weak correlations have been shown between strain and MS/BS, and strain and MAR [232,233]. A dose response relationship has been shown, however, between periosteal BFR and MS/BS and mechanical strain [234–236]. It appears that MAR is not closely related to bone strain. Interestingly, NSAID administration before a single loading session impaired only periosteal BFR, not MS/BS or MAR [12]. Endocortical BFR and MS/BS were inhibited by NSAID administration before a single loading session, but not MAR [12]. These results suggest that MAR may not be the best bone formation index to evaluate the effects of NSAIDs on bone formation. MAR was the bone formation index examined in this project. However, the method chosen to evaluate bone formation in this project essentially eliminated the need to calculate BFR. Individual sections were analyzed and it was decided to only focus on Sections 2, 3, 5 and 6, given the bone formation in non-loaded ulnas in the other Sections. The MS/BS in these Sections in most ulnas was 100% and therefore BFR would have been equal to MAR. Further analyses beyond MAR, was therefore deemed unnecessary. Previous studies examining NSAID effects on bone formation determined the BFR, MS/BS and MAR of

the whole ulna, not different sections of it, as was done in this project; therefore it is difficult to compare the indices.

## **5.5 Lamellar and Woven Bone Formation**

Forwood [10] and Li et al. [12,172] used the rat tibial bending model to examine the effects of NSAIDs on bone formation induced by a single loading event. This model induces woven bone formation on the bone periosteal surface and lamellar bone on the endosteal surface. Forwood [10] found that in female rats NS-398 administered orally 3 hours before loading inhibited endosteal lamellar BFR, MAR and MS/BS but indomethacin only inhibited BFR. Li et al. [12], using a very similar model, found that both indomethacin and NS-398 administered before loading inhibited endosteal lamellar BFR and MS/BS but not MAR, and NS-398 inhibited BFR more than indomethacin. Li et al. [12] also used to the rat forelimb compression model to examine the effects of indomethacin and NS-398 on periosteal lamellar bone formation. Both indomethacin and NS-398 inhibited BFR, and to the same extent, but neither affected MAR or MS/BS [12]. Li et al. [12] also examined the effects of NS-398 intraperitoneal injections before loading on bone formation. They found that NS-398 impaired endosteal lamellar BFR and MS/BS, induced by tibial bending, but only impaired periosteal BFR (not MS/BS), induced by forelimb loading. The results of these studies suggest NSAIDs have a differential effect on endosteal and periosteal lamellar bone formation; or NSAIDs may act differently when woven bone and lamellar bone formation are induced vs. only lamellar bone formation.

Sugiyama et al. [13] examined the effects of NSAIDs on bone formation induced by multiple loading sessions using the hindlimb axial loading model. The load applied in their model induced both lamellar and woven bone formation. The only area in the tibia or fibula that formed lamellar bone was the cortical region of the middle of the fibula [13]. Using microCT, they found that NS-398 did not affect bone volume in that area [13], suggesting that NS-398 had no effect on lamellar bone formation.

Cunningham [170] used multiple simulated resistance training exercise sessions to induce bone formation in rat tibiae and found no effect of ibuprofen administration, either before or after the sessions, on lamellar BFR, MS/BS or MAR. However, woven bone was also induced in that model.

A loading regime that induces both lamellar and woven bone formation, as is implemented in the studies by Forwood [10], Li et al. [12,172], Sugiyama et al. [13] and Cunningham [170], would create a multitude of signals within the bone environment, thus the different bone formation responses. Woven and lamellar bone form in response to different osteogenic signals and the subsequent responses vary. Woven bone formation is associated with earlier and greater upregulation of osteogenic genes [56]. For example, after a single loading event, designed to induce lamellar bone formation using the rat forelimb compression model, COX-2 expression exhibited a 1.1 fold, 1.9 fold and 1.4 fold change 1 hour, 1 day and 3 days after loading, respectively [237]. The only significant difference in the change in COX-2 expression between loaded and non-loaded ulnas was found 1 day after loading. However, in a model designed to induce woven bone after one loading event, the change in COX-2 expression was 16.4, 16.9 and 8.6 fold, 1

hour, 1 day and 3 days after loading, respectively [237]. If both bone types are being formed at the same time, the signals responsible for woven bone formation may dominate the bone environment. The results of Li et al. [12] suggest that there are differential effects of NSAIDs in the two different situations, woven and lamellar bone formation vs. just lamellar. However, it may also be due to the bone surface on which the lamellar bone is forming. Nonetheless, it appears that the effect of NSAIDs on bone formation varies depending upon the model of mechanical loading.

## **5.6 Exogenous Bone Mechanical Loading vs. Exercise**

Bone formation is induced by a mechanical stimulus. Both exercise and animal exogenous bone mechanical loading models provide a mechanical strain stimulus, but a number of differences exist between the two models. Bone mechanical loading models apply one controlled and well-defined load and they are passive, there is no muscle activity. Mechanical loading in animals applies a load in the range of 5-7 times the animal's body weight to the bones being loaded and only in the direction of the load application. In exercise models it is difficult to measure and control the load [238,239] and the load imparted on the bone is a function of both gravity and muscle activity. Exercise that benefits bone involves both body weight and muscle loading. Exercise also induces a number of physiological changes that bone mechanical loading does not. These include increased blood flow and tissue oxygenation [240], local muscular contraction and the release of endocrine and local paracrine factors [241,242]. Post exercise, there are large increases in inflammatory cytokines [243] and these can stimulate bone resorption

activity via enhanced osteoclast differentiation and increased activity of mature osteoclasts [244]. Kohrt et al. [14] suggested that one potential reason for the increase seen in BMD in a group of women taking ibuprofen after exercise, may have been a reduction in inflammatory cytokines produced during high-intensity exercise.

Meakin et al. [224] found no beneficial effects of systemic and local muscular physiological changes induced by exercise on bones' adaptive response to strain. They suggested that the beneficial effects of exercise on bone mass and architecture are likely to reflect bones' adaptation to changes in local mechanical strain alone rather than any additional physiological response [224]. Local, exogenous bone mechanical loading could induce systemic changes, but likely not, and not to the same extent as exercise. Bone mechanical loading has one main advantage over physical activity interventions, it enables precise control and quantification of the applied mechanical loads. It also allows for the elimination of any contribution of systemic effects, as the mechanical load is solely responsible for inducing any changes in bone formation. The methods of bone loading in the exercise and bone mechanical loading models vary greatly, and therefore the bodily processes and the bone signalling pathways induced likely also vary.

The effect of NSAID administration, before or after exercise, on BMD has been examined in humans. In premenopausal women, ibuprofen dosing immediately after participating in weight-bearing exercise three times per week, for nine months, increased bone mass more than in women exercising and receiving a placebo [14]. Ibuprofen administration before exercise did not impair the BMD response to exercise compared to taking a placebo [14]. A different outcome was shown in elderly men and

post-menopausal women undergoing a very similar exercise protocol; ibuprofen did not beneficially affect BMD when it was administered either before or after exercise [15]. Similarly, in another study, ibuprofen administration immediately following resistance exercise three times per week, for 9 months did not benefit BMD in healthy post-menopausal women [171]. Our results are in agreement with the two studies examining elderly men and post-menopausal women [15,171]; no beneficial affect of NSAIDs following mechanical loading. All three human studies used the same ibuprofen dose, 400 mg/kg, and a similar exercise protocol. The two studies examining post-menopausal women found no benefit of taking ibuprofen following exercise [15,171], but the study in premenopausal women did [14]. Ibuprofen administration after exercise had no effect on BMD in elderly men [15]. Together, these results suggest ibuprofen may have differential effects on BMD depending upon age; ibuprofen does not appear to benefit BMD in elderly subjects. Further investigation is needed to corroborate these findings and to understand how NSAIDs may benefit younger subjects so that NSAIDs could also be utilized in elderly subjects.

## **5.7 Limitations**

### **5.7.1 Sample Size**

One of the main limitations of the *in vivo* experimentation was the small number of animals in each group, in each of the experiments. The power to detect a change in MAR between groups is smaller when fewer animals are used. The lack of differences in MAR between control animals and animals receiving NSAIDs, either before or after

loading, may have been due to a Type II error because of the small sample sizes. A Type II error is made when a false null hypothesis is accepted. The easiest way to avoid a Type II error is to increase the sample size, which in turn increases the power of the statistical analysis.

The indomethacin experiment was designed as a pilot project to examine the effects of NSAIDs on bone formation induced by multiple mechanical loading events. There were no trends seen in the data and so it was thought that the choice of a COX-2 selective NSAID, NS-398, may show more of an effect than indomethacin, a non-selective NSAID. The animal numbers were increased to  $n=10/\text{group}$  to help increase the power of the experiment. A formal sample size calculation was not completed as there were no indications of an effect of indomethacin on bone formation and a different NSAID was examined. The sample size for the NS-398 experiment was similar to those used previously in the literature to examine NSAID effects on bone formation. Those studies did not provide justification for their sample size selection of  $n=8/\text{group}$  [10,12,13]. The studies examining a single loading event showed significant effects of NSAIDs on bone formation with that sample size [10,12]. The study examining multiple loading events did not find an effect of NSAIDs on bone formation with that sample size [13]. Based on those previous studies, the sample size in the NS-398 experiment was likely adequate to find a difference between groups if it had existed.

An *a priori* power analysis, the most common way of determining sample size, may have provided a more accurate estimate of the required sample size [245]. The sample size calculation depends on the: effect size, standard deviation, chosen

significance level, chosen power, and alternative hypothesis [245]. The significance level and power are chosen by convention and the alternative hypothesis is determined by the research question. But, the expected effect size and standard deviation require some knowledge of the expected outcome. The most similar study examining NSAID effects on bone adaptation in the literature did not evaluate bone formation using histomorphometry and examined mice not rats using a different loading model [13]. Since the *in vivo* loading experiments in this project involved different NSAIDs and different sexes, it was difficult to determine what the effect of the NSAIDs would be on bone formation based on the previous experiments. The results of each of the previous experiments suggested that NSAIDs did not have an effect on bone formation; so it was difficult to determine what effect might have been observed.

In the studies examining one loading event, bone formation was 1.4-1.9 times greater in the animals not administered NSAIDs before loading [12] and based on that study an effect size of  $f=0.9$  was calculated, which is considered very large [246]. If this was the effect size to be expected in a study examining NSAID effects on bone formation induced by multiple loading events, then a sample size of  $n=6/\text{group}$  would be required, with a power of 0.8 and a significance of 0.05. In the NS-398 experiment, however, MAR was only 1.1-1.3 times greater in the rats not administered NSAIDs before or after loading, corresponding to an effect size of  $f=0.33$ , considered a medium effect [246]. The sample size needed to detect that effect size, with a power of 0.8 and a significance of 0.05, is  $n=33/\text{group}$ .

Next to the research question, the effect size may be the most important factor to define when designing a study. It is the difference in means that the investigator wants the experiment to be able to detect. It will determine what the results of the study mean. Significance testing provides a statistical significance based on predefined factors, some based simply on convention, but it does not provide an indication of the practical or biological significance. That is, if there is a statistical difference in MAR between the CON group and the PRE or POST group, it should represent a real difference in bone adaptation to loading that could subsequently affect bone health. If there is a statistical difference but the actual difference between means is small (a small effect size) it may not be of importance in terms of the overall impact on bone. So the effect size should be chosen so as to mean something biologically. However, defining what is of biological significance is difficult, especially without prior knowledge of the effects of NSAIDs on bone formation induced by multiple loading events.

Determining an appropriate effect size in the experiments in this project depends upon defining a difference in MAR between the CON and PRE and POST groups that would indicate a difference that affects bone integrity. The mechanical loading model used in this project induces bone formation on the medial periosteal surface of the ulna, the area of greatest compressive strain [42]. Adding bone on the periosteal surface increases the cross-sectional moment of inertia of the bone, which is a measure of the distribution of material within the bone cross section. The moment of inertia is proportional to the bending and torsional rigidity of the bone and so an increase in the moment of inertia increases bone strength. Bone rigidity can increase exponentially by

adding bone to the periosteal surface, even when the bone volume and bone mineral density do not change [22]. A small increase in periosteal MAR may have a large effect on bone strength.

In addition, Robling et al. [43] showed that even small changes in BMD, induced by ulnar compressive loading, greatly increased biomechanical properties if the new bone formation was localized to the most biomechanically relevant sites. Thus, it may be possible to enhance bone strength and fracture resistance, with only slight changes in BMD, through targeted mechanical loading or exercise. Most exercise intervention studies yield differences in BMD of only a few percent at most [14,15,247], but it is not known how such intervention affects fracture susceptibility. Small changes in BMD could enhance bone strength if the bone was added to mechanically appropriate sites, the areas of highest strain. Bone is optimized for daily loading activities but if the loading environment changes, so too does the bone. Bone formation would occur in the areas of highest strain to maintain structural integrity. Targeted loading or exercise could aim to enhance bone formation in known areas of weakness to potentially improve bone strength and subsequently fracture resistance. If NSAIDs could even enhance BMD by a percent or two, it may have a large effect on bone strength and fracture resistance, especially if it occurred in a vulnerable area. Kohrt et al. [14] showed that ibuprofen administration after exercise increased BMD by approximately 1.5% compared to a placebo and so NSAIDs may be able to enhance bone strength but it remains to be seen how that affects fracture resistance.

A small effect size may be of biological importance in this project. It would likely be best to determine how a change in MAR affects bone strength. If a small change in MAR affects bone strength greatly, then a small effect size may be of interest. However, a small effect size requires a large sample size to detect a difference between groups if significance testing is the method of analysis. So, determining how MAR affects bone strength is of importance.

A simple method based on the law of diminishing returns can be used to determine sample size when the standard deviation and/or effect size is not known [248]. It may also be useful in exploratory experiments where testing hypotheses is not the main objective, but rather the interest is finding any difference between groups. It is known as the resource equation method [245]. A value of E, which is the degrees of freedom of analysis of variance (ANOVA), is calculated using the following equation [248]:

$$E = \text{total \# of animals} - \text{total \# of groups} \qquad \textbf{Equation 5.1}$$

The value of E should be between 10 and 20. If E is less than 10 then adding more animals will increase the chance of finding a significant difference between groups, but if it is more than 20 then adding more animals will not help to increase the chance of finding a significant difference [245]. A sample size that keeps E between 10 and 20 should be adequate. This method seems to work well for whole animal experiments, but it tends to assume quite large effect sizes and is not as robust as a power analysis method [245]. According to the resource equation method the number of animals for the

indomethacin and ibuprofen experiments were adequate and there were more than enough animals for the NS-398 experiment (Table 5.2).

**Table 5.2 E values calculated using the resource equation for each of the *in vivo* loading experiments.**

<b>Experiment</b>	<b>Total # of Animals</b>	<b>Total # of Groups</b>	<b>E</b>	<b>E (with exclusions)</b>
<b>INDO</b>	20	5	15	12
<b>NS-398</b>	30	3	27	23
<b>IBU timing</b>	21	4	17	16

### 5.7.2 Standard Deviations

The large standard deviations in MAR in each of the Sections, in each of the groups and in all of the experiments presents a problem when trying to detect differences between groups. The small sample sizes may have contributed to the large variations in MAR within a group. However, the large standard deviations were seen in each of the experiments, even the NS-398 experiment, suggesting that there may have also been an issue with the method of MAR analysis or the loading protocol or possibly just variation in the animal responses to loading.

The MAR analysis itself was fairly robust and produced similar results for each ulna cross-section when completed multiple times and by two different evaluators. One issue with the analysis that may have contributed to the large variations in MAR within a group, were the ulna cross-sectional images themselves. The length of each embedded forelimb was measured and a cut was made 1 mm distal to the midpoint. Once the forelimbs were embedded in the resin it was difficult to ensure the exact midpoint was

located. As such, not all of the ulna cross-sectional images were at the exact same location along the length of the forelimb. However, all of the images were examined to ensure the location was appropriate and as consistent as possible across all ulnas. The images that were not in an appropriate location were excluded from the statistical analyses.

The method of loading may have contributed to the variation. The ADMET material testing system (eXpert 5601, ADMET, MA, USA) used during the forelimb loading had significant overshoot and therefore the target load was approximate. For example, the target load in the male rats in the NS-398 experiment was 20 N. To achieve this load at a frequency of 2 Hz, an input load of approximately 9.5 N was used. The input load was adjusted for each rat so that the target load was always 20 N. So, some rats received a greater load according to the ADMET input parameters but the output/target load of the ADMET, recorded by a load cell, suggested that the load actually reached was the same for each rat, approximately 20 N. The input loads ranged from 9 N to 10.5 N. A Pearson's product-moment correlation revealed a significant moderate linear correlation ( $r=0.61$ ) between the MAR in Section 2 and input load in the NS-398 experiment [249], suggesting that the input load may influence MAR. However, statistical differences were not found between the CON and POST groups for any of the Sections after adjusting for input load. Statistical differences were also not found between the CON and PRE groups after adjusting for input load, except in Section 5. The 1.5 N range (7.4-8.6 N) of input loads was similar in the female IBU timing experiment. Once again a significant moderate linear correlation ( $r=0.62$ ) was found between the MAR in Section 2 and input

load. However, statistical differences were not found between the CON and IBU groups for any of the Sections after adjusting for input load.

Adjusting the input load for each rat to achieve the same target load is not ideal, but given the limitations of the mechanical test system, it was deemed necessary in order to try to apply the same load to each animal. Applied load has a linear relationship with bone strain and therefore to induce the same amount of bone strain in each rat the load should also be the same. There are individual differences amongst rats in terms of body mass and overall body size however, so under a given load there will be some individual differences in the amount of strain a bone experiences. This may then influence the bone formation response. However, most of the rats in these experiments likely experienced similar strains under a given load given their similar size. The forelimb strain gauging performed in this project suggests only small variations in strain under a given load (see Figure 3.5, in *Materials and Methods: In vivo Mechanical Loading*).

The variation in MAR between animals may just be inherent of the loading protocol. Hsieh et al. [52] loaded female rats using the forelimb compression model and a similar multiple event loading protocol as this project, 10 days of loading over a 12 day period at a load of 14.5 N at 2 Hz for 360 cycles/day. They had a sample size of 14 and found an average MAR of 2.13  $\mu\text{m}/\text{day}$  with a standard deviation of 1.14  $\mu\text{m}/\text{day}$ . This is a large standard deviation and the coefficient of variation (CV) is over 50%. The CV in Section 2 of the CON groups in the indomethacin, NS-398 and ibuprofen timing experiments ranged from 30% to 39%. The large standard deviations in each study may be a result of multiple loading sessions. In a study examining one loading event the CV

was approximately 17% [12]. The variation in MAR in each experiment and the consistent CV amongst experiments and a similar study [52] may be expected with this type of loading protocol.

This project has limitations. However, the consistency amongst the experiments and the lack of observable trends in the experimental data suggest the conclusions of this project are appropriate. In addition, the experimental results of this project are in agreement with the studies in the literature examining NSAID effects on bone adaptation in animal models of repeated loading [13,170]. Despite the limitations, the results of each experiment are in agreement; NSAID administration before or after loading does not affect bone formation induced by multiple loading events.

## CHAPTER SIX

### MATERIALS AND METHODS: *IN VITRO* MECHANICAL LOADING

#### 6.1 MLO-Y4 Cell Line

The murine long bone osteocyte Y4 (MLO-Y4) cells were used in the *in vitro* fluid flow experiments. The MLO-Y4 osteocyte-like cell line is a well-characterized cell line representing an early osteocyte phenotype that shares numerous characteristics with primary osteocytes [250]. MLO-Y4 cells have been used to study osteocyte communication with each other and with other bone cells and to examine the response of osteocytes to mechanical stimulation, including fluid flow [69,72,251–254].

The MLO-Y4 osteocyte-like cell line, developed by Kato et al. [255], was established from long bones that respond to increased mechanical stress with an increase in bone formation. Osteocytes and osteoblasts share many markers but differences exist in the levels of expression of some of these markers. Osteocytes produce large amounts of osteocalcin, which is greater in osteocytes compared with osteoblasts [250]. Osteocalcin maintains an unmineralized area around osteocyte cell bodies and cell processes so nutrients and waste can diffuse to and from the cell [250]. Kato et al. [255] used bone cells from transgenic mice overexpressing T-antigen driven by an osteocalcin promoter to produce immortalized cells of the osteocyte phenotype. They used cellular morphology, specifically the expression of dendritic processes, a characteristic morphologic feature of osteocytes, to initially clone the cell line.

Once the MLO-Y4 clonal cells were established they were compared with known properties of primary osteocytes, osteoblasts and other cells. MLO-Y4 cells express proteins that are also expressed by osteoblasts such as osteocalcin, osteopontin, connexin-43 (Cx43), alkaline phosphatase (ALP), and type I collagen, but in relative amounts described for osteocytes. The low expression of ALP and high expression of osteocalcin by MLO-Y4 cells supports the hypothesis that the MLO-Y4 cell line is osteocyte-like as this pattern of expression in primary osteocytes has been shown previously [256]. MLO-Y4 cells also express very large amounts of Cx43 protein, like osteocytes do. However, there are known differences between primary osteocytes and MLO-Y4 cells. For example, MLO-Y4 cells express low to undetectable levels of sclerostin (Sost), whereas osteocytes are known to express Sost *in vivo* [257]. Despite the differences that exist between MLO-Y4 cells and osteocytes, MLO-Y4 cells remain a very useful tool for examining osteocyte behavior *in vitro*.

## **6.2 MLO-Y4 Cell Culturing and Seeding**

MLO-Y4 osteocyte-like cells (a gift to Dr. Lidan You from Dr. Lynda Bonewald, University of Missouri-Kansas City, MO, USA) were cultured on rat tail collagen I (BD Biosciences, Bedford, MA) coated culture dishes with  $\alpha$ -Modified Eagle's Medium ( $\alpha$ -MEM, GIBCO/Invitrogen, CA, USA) supplemented with 2.5% fetal bovine serum (FBS, Hyclone, UT, USA), 2.5% calf serum (CS, Hyclone, UT, USA), and 1% penicillin and streptomycin (PS, GIBCO/Invitrogen, CA, USA). Cultured cells were maintained at 37°C in a 5% CO<sub>2</sub> atmosphere and subcultured at 70% confluence.

For the parallel plate flow chamber experiments, MLO-Y4 cells were seeded on type I rat tail collagen-coated glass slides 48 hours prior to fluid flow exposure at 150,000 cells/slide to ensure 70–80% confluence.

For the orbital shaker experiments, MLO-Y4 cells were seeded on type I rat tail collagen-coated 6-well culture plates at 20,000 cells/well 48 hours prior to fluid flow.

### **6.3 Indomethacin Administration**

The concentration of indomethacin (Indomethacin – CAS 53-86-1, Cayman Chemical Company, MI, USA) used in all experiments was  $1 \times 10^{-5}$  M [146,173]. Dimethyl sulfoxide (DMSO) was the solvent used to put the indomethacin into solution. The concentration of DMSO in the media was 0.036%; media DMSO concentrations less than 0.1% have been shown to have no affect cells [258]. To ensure the effects were the same in all groups, DMSO was added to the control media at the same concentration. There were no visible effects of the DMSO on the cells.

The media in the control (CON) group contained no indomethacin. In the pre-loading (PRE) groups, indomethacin ( $1 \times 10^{-5}$  M) was introduced into the media 30 minutes prior to loading and was present during the loading and for 30 minutes after (Table 6.1). In the post-loading (POST) groups, indomethacin was added to the media 30 minutes after loading and was present for 3 hours before being replaced with fresh media at the 3.5hrs time point (Table 6.1).

Fresh media was added 30 minutes prior to loading to give the cells time to accommodate to the new media and conditions. It was not changed until 30 minutes after

loading so that indomethacin would be present in the media for 3 hours. To make sure both the PRE and POST groups were in the presence of indomethacin for the same amount of time, the indomethacin was present in the media in the POST group for 3 hours. The 3 hours was chosen with the intent to mimic NSAID levels *in vivo*. The peak plasma concentration of indomethacin occurs approximately 1-2 hours after oral administration in humans with a half life ranging from 2 hours to 11 hours [200–202]. In rats, the peak plasma concentration occurs approximately 2-6 hours after oral administration with a half life of approximately 4-6.5 hours [197,198]. Based on the pharmacokinetics, the 3 hour time period was chosen to try to mimic the length of time that indomethacin plasma concentrations are greatest, suggesting they are most effective at inhibiting PGE<sub>2</sub> production.

**Table 6.1** *In vitro* mechanical loading experimental groups.

<b>Group</b>	<b>Flow</b>	<b>Timing of NSAID Administration</b>
control - CON-S	Static (S)	N/A
control - CON-F	Flow (F)	N/A
indomethacin - PRE-S	S	30 minutes prior to, during and 30 minutes after loading
indomethacin - PRE-F	F	30 minutes prior to, during and 30 minutes after loading
indomethacin - POST-S	S	30 minutes after loading for 3 hours
indomethacin - POST-F	F	30 minutes after loading for 3 hours

## **6.4 Development of Fluid Flow Protocol**

To generate fluid shear stress in the *in vitro* experiments, parallel plate flow chambers were first used. After a number of experiments, it was determined that the orbital shaker was a better model for producing fluid shear stress and controlling for PGE<sub>2</sub> levels in the experiments.

### **6.4.1 Parallel Plate Flow Chamber Model**

Parallel plate flow chamber systems have been used extensively to study *in vitro* bone mechanotransduction [33,63,76]. The flow chambers are used to apply a well-defined shear stress and can decouple flow rate from flow frequency [77]. However, due to the complexity and expense of these systems only a limited number of samples can be evaluated in a single experiment. In addition, the cells undergo a large amount of manipulation when they are loaded into these systems, and as explained later, this is a problem for controlling for PGE<sub>2</sub> expression.

Briefly, cells are seeded onto glass slides and placed into parallel plate flow chambers (Figure 6.1A). Fluid is pumped through the chamber over the cells in the desired flow profile using a syringe pump or actuator. The shear stress experienced by the cells in the chambers is related to the flow rate of the circulating media through the chamber, the chamber width and the distance between the two plates [259].

The shear stress ( $\tau$ ) at the cell layer is estimated using the equation [259]:

$$\tau = \frac{6\eta Q}{bh^2} \quad \text{Equation 6.1}$$

where  $\eta$  is fluid viscosity,  $Q$  is flow rate,  $b$  is the width of the chamber and  $h$  is the distance between plates.

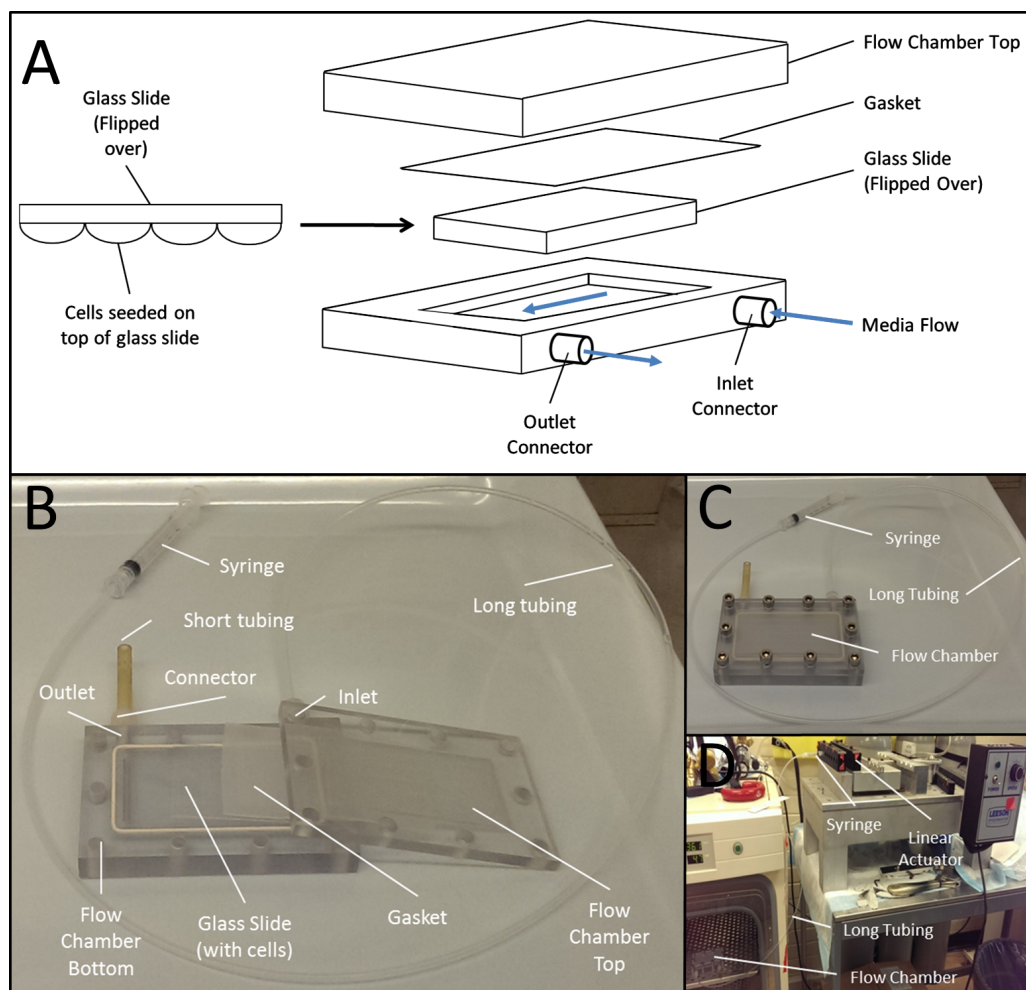


**Figure 6.1** Parallel plate flow chamber system. **A)** Schematic of the flow chamber setup. **B)** A pre-assembled flow chamber. **C)** An assembled flow chamber before placement into the incubator. **D)** The flow chamber placed in the incubator and attached to the linear actuator, which provides the fluid flow. (Image courtesy of Yu-Heng (Vivian) Ma, Dr. Lidan You's Lab, University of Toronto).

#### **6.4.2 Parallel Plate Flow Chamber System**

MLO-Y4 seeded slides were placed in the parallel plate flow chambers and placed in a 5% CO<sub>2</sub> incubator at 37°C for the entire duration of the flow experiment. The custom parallel plate flow chamber system, previously established (Figure 6.1) [66], applied oscillatory fluid flow to the cells. The flow was driven by 3 ml syringes mounted on and driven by an electromechanical loading device. The oscillatory flow pattern, based on previous studies, generated a sinusoidal shear stress of 1-2 Pa at 1 Hz [66,69]. The flow was applied for 2 hours [69]. The chambers sat static 30 minutes pre and post flow. Cells that were seeded on slides, placed in the flow chambers, but not exposed to flow, were the static controls.

Thirty minutes post flow completion, the chambers were removed and media samples were taken from the flow chambers to assess PGE<sub>2</sub> production at 30 minutes. The slides were then transferred to culture dishes, with new media, with or without indomethacin, to assess PGE<sub>2</sub> production over the next 24 hours.

#### **6.4.3 Parallel Plate Flow Chamber Limitations**

Parallel plate flow chambers were first used to generate fluid shear stress in this study. This method of loading requires the manipulation of glass slides seeded with MLO-Y4 cells. The slides were removed from petri dishes, flipped over and lowered into a chamber. The slide manipulation required to set up this experiment can apply unwanted stimulation to the cells and as a result may activate signalling pathways. All of the cells,

whether they were exposed to fluid flow or not, were placed into the chambers to include all steps of the experimental set up except the application of fluid flow.

The results of the parallel plate flow chamber experiments in this study, suggested that the cell manipulation that occurred during the experimental setup affected signalling in and amongst the cells. The media PGE<sub>2</sub> concentrations were similar in the flow (CON-F) and static (CON-S) control samples (Figure 6.2). The media PGE<sub>2</sub> concentration was significantly greater in the CON-S group compared to the concentration measured in the media of static petri dishes each containing a slide of cells (DISH-S) (Figure 6.2). Fresh media was added to the petri dishes 3 hours prior to taking the sample, which corresponds to the 3 hours that the slides were present in the flow chambers in the CON-S group. The similar media PGE<sub>2</sub> concentrations in the CON-S and CON-F groups, as well as significantly greater media PGE<sub>2</sub> concentrations in the CON-S group compared to the DISH-S group, suggested that the cells in the static condition were stimulated. The stimulation likely occurred during the flow chamber set up. Due to the lack of difference in media PGE<sub>2</sub> concentrations, an orbital shaker was used in place of the parallel plate flow chambers to generate fluid flow shear stress. Media PGE<sub>2</sub> concentrations were greater in the flow controls compared to the static controls when the orbital shaker was used for fluid flow stimulation. The use of the orbital shaker and 6-well plates eliminated the cell manipulation during the experimental setup and therefore likely prevented the activation of some acute signalling pathways, including PGE<sub>2</sub> production.

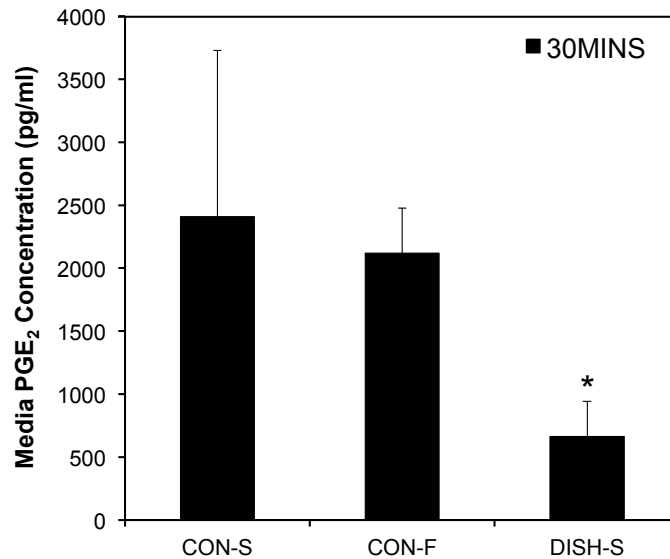


**Figure 6.2 Media PGE<sub>2</sub> concentration 30 minutes after fluid flow in the parallel plate flow chambers.** Values are mean STD. \*Different from CON-S. CON-S=static slides in chambers; CON-F=flow slides in chambers; DISH-S=static slides in petri dishes. n=4/group.

#### 6.4.4 Orbital Shaker Model

Orbital shakers can be used to impart fluid shear stress on cells. They address some of the limitations of parallel plate flow chambers, most importantly the manipulation needed to set up the flow chamber. Orbital shakers are simple to use and allow a number of experimental groups to be run simultaneously. Generating fluid flow with the orbital shaker lessens the inadvertent activation of acute signalling pathways that can occur when loading the cells into the flow chambers [260].

Orbital shakers generate fluid flow in a cylinder of an oscillatory nature [261,262]. The flow is generated by a wave whose peak rotates around the round dish at an angular velocity corresponding to the orbital velocity of the dish or shaker. The shear stresses, created by the wave, oscillate around the dish as the shaker rotates but the fluid flow itself

is not oscillatory per se. That is, the flow does not reverse directions like the flow does in the parallel plate flow chambers or as is thought to occur *in vivo*. The fluid flow in each well should be thought of as more pulsatile than oscillatory in this case [77]. Nonetheless, orbital shakers have been used to study bone cell responses to fluid shear stress [77,260,263,264].

The magnitude of shear stress on the bottom of an orbiting dish can be calculated using [265]:

$$\tau_{max} = a\sqrt{\eta\rho(2\pi f)^3} \quad \text{Equation 6.2}$$

where  $a$  is the orbital radius of rotation of the shaker (cm),  $\eta$  is the viscosity of the culture media (poise),  $\rho$  is the density of the culture media (g/ml) and  $f$  is the frequency of rotation (rotations/sec).

#### 6.4.5 Orbital Shaker System

An orbital shaker (Junior Orbit Shaker 3520, Lab-Line Instruments Inc, IL, USA) was used to generate oscillatory fluid flow in the orbital shaker experiments (Figure 6.3A). Using appropriate values for the experimental setup and Stokes' approximation (Equation 2), where  $a$  is the orbital radius of rotation of the shaker (1.9 cm),  $\eta$  is the viscosity of the culture media (~0.01 poise),  $\rho$  is the density of the culture media (~1.0 g/ml) and  $f$  is the frequency of rotation (200 rotations/min), the shear stress generated was calculated to be approximately 1.8 Pa on the bottom of each well. This shear stress falls within the range of 0.8 to 3 Pa predicted by theoretical models of

*in vivo* physiological shear stresses [62]. The cells were exposed to fluid shear stress for 2 hours.

The shaker was placed in a 5% CO<sub>2</sub> incubator at 37°C for the entire duration of the flow experiment. Six-well culture plates containing cells subjected to shear stress were placed on the shaker and static non-loaded plates of cells were placed on a shelf in the incubator (Figure 6.3B).

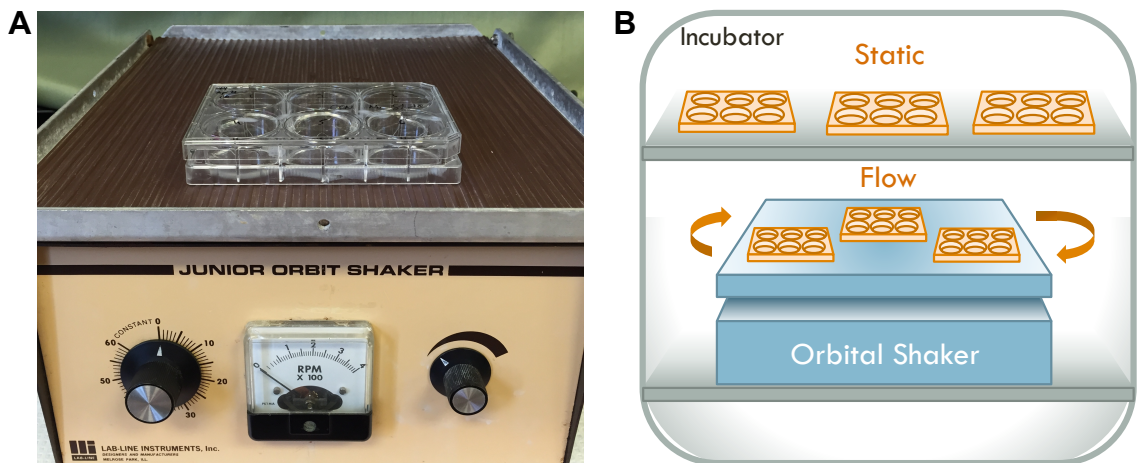


**Figure 6.3** A) Orbital shaker used to generate fluid shear stress with a 6-well culture plate in position. B) Schematic of the orbital shaker setup in the incubator (Image courtesy of Madeleine Bateau, Dr. Lidan You's Lab, University of Toronto).

## 6.5 *In vitro* Mechanical Loading Experimental Timelines

A number of fluid flow experiments were conducted to examine the effects of media changes on media PGE<sub>2</sub> concentrations (Figure 6.4). In all of the orbital shaker fluid flow experiments, regardless of the number of media changes, media was removed from the wells and replaced with 1 ml of fresh media 30 minutes prior to loading. The cells were then loaded (F) for 2 hours or sat static (S) for 2 hours. Following loading, all

of the cells sat static for 30 minutes. Media was changed at various time points, depending upon the experiment conducted. Each time the media was changed all of the media was collected and it was replaced with fresh media. If the media was sampled, then a 100 µl sample of media was taken from each well, but the media was not changed.

Some of the experiments were terminated at 24hrs because different findings have been shown regarding COX-2 mRNA expression at 24hrs *in vivo* vs. *in vitro*. COX-2 mRNA expression has been shown to return to pre-loading levels by 24 hours *in vivo* [81]. However, both COX-2 mRNA expression and media PGE<sub>2</sub> concentrations have been shown to remain elevated 24 hours after fluid flow *in vitro* [169]. Therefore, the effects of fluid flow and NSAID administration, in this model, on media PGE<sub>2</sub> concentrations at 24hrs were examined.

Two of the experiments were terminated at 12hrs to determine how the media PGE<sub>2</sub> concentrations varied between the groups before the 24hrs point and if the additional 12 hours of incubation altered PGE<sub>2</sub> production.

### **6.5.1 Three Media Changes at 30mins, 3.5hrs and 6.5hrs**

Experiments with three media changes at 30mins, 3.5hrs and 6.5hrs (Figure 6.4A) were the first set of experiments conducted. The media change 30 minutes after loading was implemented to remove the indomethacin from the PRE group and the media change 3.5 hours after loading occurred to remove the indomethacin from the POST group. A media change 6.5 hours after loading also occurred to examine the PGE<sub>2</sub> production after

the removal of indomethacin in the POST group. These experiments were terminated at 24hrs.

### **6.5.2 Two Media Changes at 30mins and 3.5hrs**

Experiments with two media changes were also conducted with media changes occurring at 30mins and 3.5hrs (Figure 6.4B). These experiments were terminated at 12hrs.

### **6.5.3 One Media Change at 30mins**

The influence of only one media change was also examined (Figure 6.4C). The only media change occurred 30mins after, so only the CON and PRE groups were included in this experiment. The POST group was not included because the indomethacin would not have been removed from the media with only one media change occurring at 30mins. The experiments were terminated at 24hrs.

### **6.5.4 No Media Changes**

Experiments with just the CON group and no media changes were also conducted to examine the effect of accumulating media PGE<sub>2</sub> on subsequent PGE<sub>2</sub> production (Figure 6.4D, E). A media sample (100 µl) was taken 30 minutes after loading, with no media change, and the experiments were terminated at either 12hrs or 24hrs.

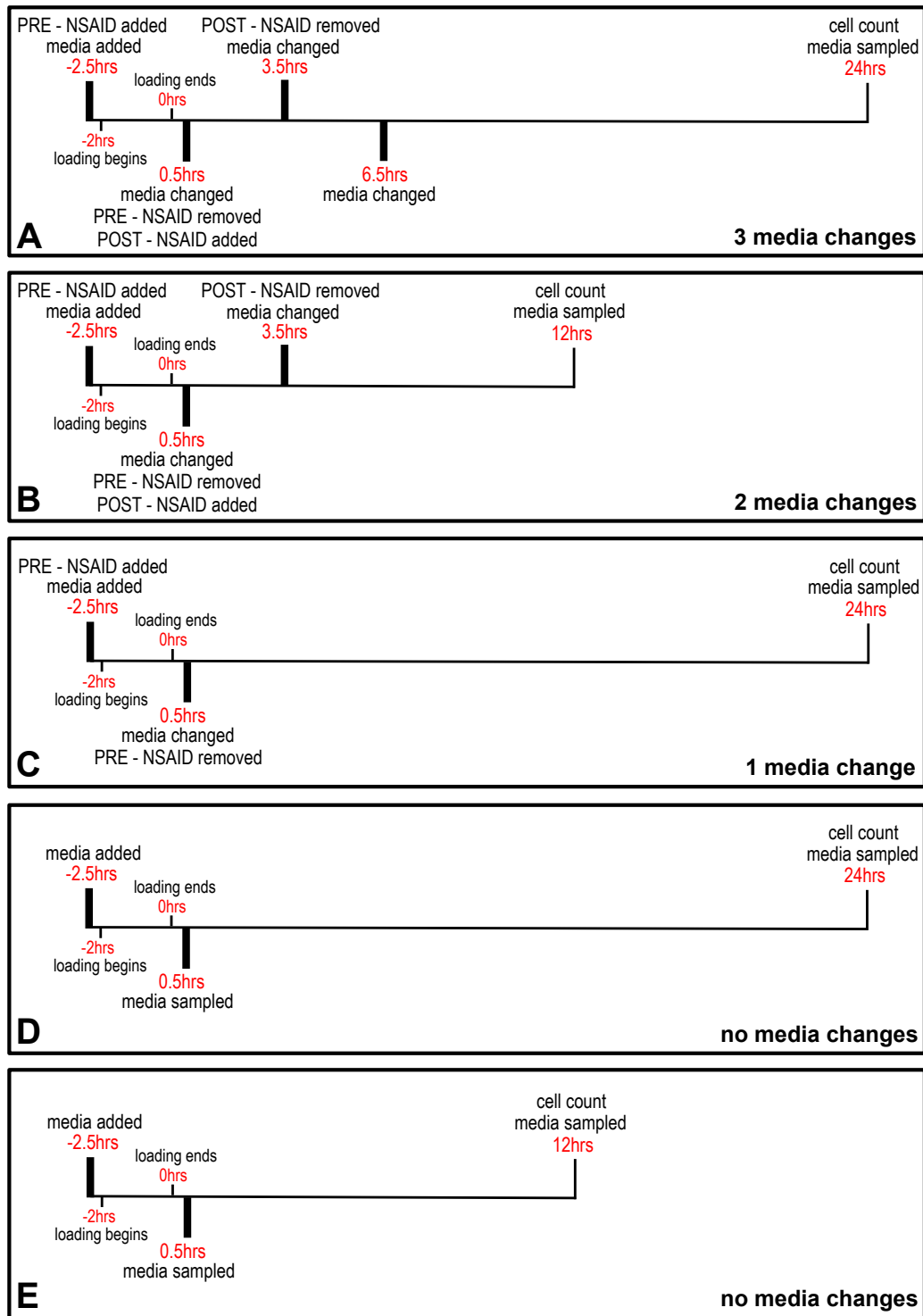


**Figure 6.4** *In vitro* mechanical loading experimental timelines. **A)** Three media changes. **B)** Two media changes. **C)** One media change. No media changes and termination at **D)** 24hrs and **E)** 12hrs.

## **6.6 Cell Count Determination**

At the termination of each experiment, either 12 or 24 hours after loading depending upon the experiment, cells were collected and counted. Briefly, trypsin was added to the culture wells to detach the cells, followed by the addition of media before the suspension was collected and placed in 4 ml sample cups. The cells were then counted using an automated cell counter (ViCELL-XR, Beckman Coulter, CA, USA).

## **6.7 Media PGE<sub>2</sub> Concentration Determination**

Media PGE<sub>2</sub> concentrations were measured using a commercially available enzyme immunoassay (Prostaglandin E2 EIA Kit – Monoclonal 514010, Cayman Chemical Company, MI, USA). The assay is based on the competition between the PGE<sub>2</sub> in the media samples and a PGE<sub>2</sub>-acetylcholinesterase (AChE) conjugate (PGE<sub>2</sub> Tracer) for a limited amount of PGE<sub>2</sub> Monoclonal Antibody [266]. Because the concentration of PGE<sub>2</sub> varies in the media samples, the amount of PGE<sub>2</sub> Tracer that is able to bind to the PGE<sub>2</sub> Monoclonal Antibody will be inversely proportional to the concentration of PGE<sub>2</sub> in the media samples [266]. To perform the assay, standards and samples were diluted with the same culture media, containing DMSO, as was used in the flow experiments. The media samples, PGE<sub>2</sub> Tracer and PGE<sub>2</sub> Monoclonal Antibody were then added to a 96-well plate coated with goat polyclonal anti-mouse IgG. The plate was incubated for 18 hours at 4°C in which time the antibody-PGE<sub>2</sub> complex bound to the coated plate. The plate was washed to remove unbound reagents and then Ellman's Reagent (which contains the substrate AChE) was added to the wells. The product of that enzymatic

reaction has a yellow colour that absorbs at 412 nm [266]. The intensity of the colour was determined with a microplate reader; it is proportional to the amount of PGE<sub>2</sub> Tracer bound to the plate, which is inversely proportional to the amount of PGE<sub>2</sub> in the media samples [266]. The detection limit of the assay was 15 pg/ml [266]. The absorbance data was analyzed using an Excel spreadsheet provided by Cayman Chemical Company ([www.caymanchem.com/analysis/eia](http://www.caymanchem.com/analysis/eia)) to determine the concentration of PGE<sub>2</sub> in the media samples. A curve was constructed from the standards and the PGE<sub>2</sub> concentration of the media samples was determined using the absorbance for each sample and the equation of the standard curve plot. Media PGE<sub>2</sub> concentrations were normalized to the number of cells in each well.

## **6.8 Statistics**

To determine the effects of flow and indomethacin on media PGE<sub>2</sub> concentration in the experiments with one, two and three media changes, a two-way ANOVA was used (SPSS Inc., Chicago, IL, USA). Where statistically significant ( $p < 0.05$ ) interactions were found, simple main effects were determined with Bonferroni adjustment. Where statistically significant ( $p < 0.05$ ) main effects were found, post-hoc analyses with Bonferroni adjustment were carried out. An independent t-test was used to determine the effect of flow on media PGE<sub>2</sub> concentrations in the CON group in the experiment with no media changes. A significance level of  $p < 0.05$  was used for all statistical tests.

## CHAPTER SEVEN

### RESULTS: *IN VITRO* MECHANICAL LOADING

#### 7.1 Parallel Plate Flow Chamber Experiments

##### 7.1.1 CON and PRE Groups

The parallel plate flow chamber experiment with the non-NSAID control (CON) and pre-load NSAID administration (PRE) groups examined media PGE<sub>2</sub> concentrations 30 minutes after loading (Figure 7.1). Media PGE<sub>2</sub> concentrations did not differ between the CON-S and CON-F groups at 30mins ( $p=0.562$ ). Indomethacin inhibited PGE<sub>2</sub> production in both the PRE-S and PRE-F groups at 30mins, resulting in similar concentrations between the two groups ( $p=0.769$ ) and significantly lower PGE<sub>2</sub> concentrations than the CON-S ( $p<0.05$ ) and CON-F ( $p<0.05$ ) groups.

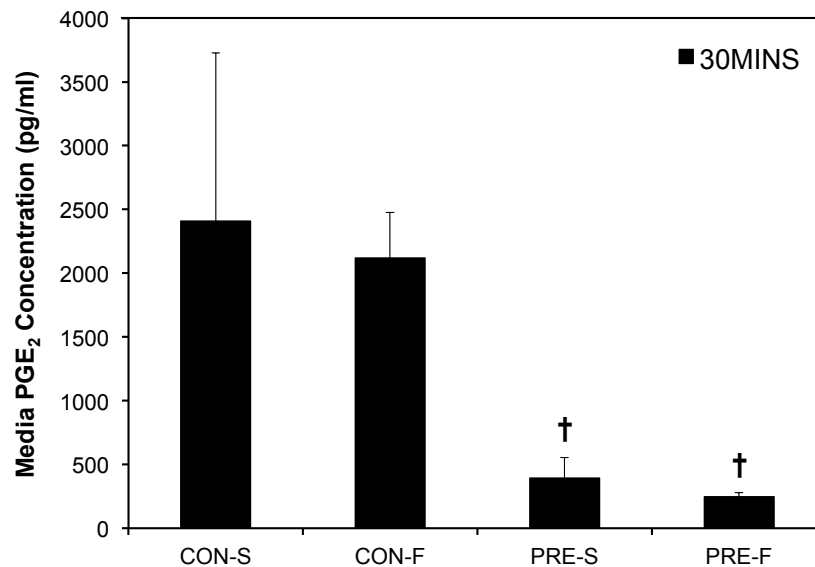


**Figure 7.1** Media PGE<sub>2</sub> concentrations in the CON and PRE groups at 30mins in the parallel plate flow chamber experiments. Values are mean  $\pm$  STD. †Different from CON. CON=no indomethacin; PRE=indomethacin administered prior to loading. S=static; F=flow. n=4/group.

### 7.1.2 CON and POST Groups

The parallel plate flow chamber experiment with the non-NSAID control (CON) and post-load NSAID administration (POST) groups examined media PGE<sub>2</sub> concentrations 30 minutes and 3.5 hours after loading (Figure 7.2). Media PGE<sub>2</sub> concentrations did not differ between the CON-S and CON-F groups at 30mins ( $p=0.151$ ) or 3.5hrs ( $p=0.581$ ). Media PGE<sub>2</sub> concentrations did not differ between the POST-S and POST-F groups at 30mins ( $p=0.098$ ). The media PGE<sub>2</sub> concentration was significantly greater in the CON-S group compared to the POST-S group at 30mins ( $p<0.05$ ). Indomethacin inhibited PGE<sub>2</sub> production in both the POST-S and POST-F groups at 3.5hrs, resulting in similar concentrations between the two groups ( $p=0.968$ ) and significantly lower PGE<sub>2</sub> concentrations than the CON-S ( $p<0.001$ ) and CON-F ( $p<0.001$ ) groups.

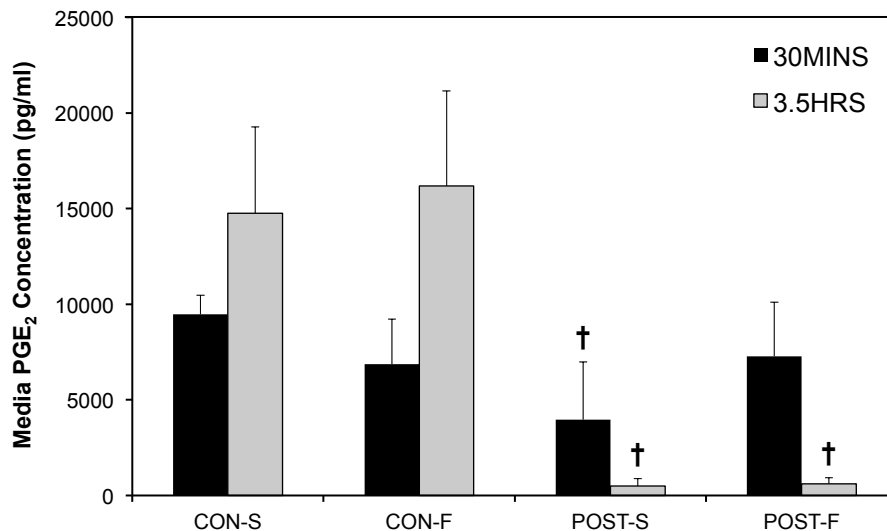


**Figure 7.2** Media PGE<sub>2</sub> concentrations in the CON and POST groups at 30mins and 3.5hrs in the parallel plate flow chamber experiments. Values are mean  $\pm$  STD. †Different from CON. CON=no indomethacin; POST=indomethacin administered after loading. S=static; F=flow. n=4/group.

## 7.2 Orbital Shaker Experiments

### 7.2.1 Three Media Changes at 30mins, 3.5hrs and 6.5hrs

The flow experiment with three media changes after loading examined media PGE<sub>2</sub> concentrations in the non-NSAID control (CON), pre-load NSAID administration (PRE) and post-load NSAID administration (POST) groups 30 minutes and 24 hours after loading (Figure 7.3A). Fluid shear stress caused significantly greater PGE<sub>2</sub> production from the MLO-Y4 cells at 30mins in the CON-F and POST-F groups compared to their respective static controls (Figure 7.3B). At 30mins the media PGE<sub>2</sub> concentration was greater in the CON-F group compared to the CON-S group ( $p<0.001$ ) and in the POST-F group compared to the POST-S group ( $p<0.001$ ). There was no difference between the CON-S and POST-S ( $p=0.926$ ) groups at 30mins but the POST-F group had a greater media PGE<sub>2</sub> concentration than the CON-F group ( $p<0.05$ ). Indomethacin inhibited PGE<sub>2</sub> production in both the PRE-S and PRE-F groups at 30mins, resulting in similar concentrations between the two groups ( $p=0.978$ ) and significantly lower PGE<sub>2</sub> concentrations than the CON-S ( $p<0.05$ ) and CON-F ( $p<0.001$ ) groups.

At 24hrs, the media PGE<sub>2</sub> concentrations were much greater in the CON and PRE groups and were similar between the CON-S and CON-F groups ( $p=0.592$ ) (Figure 7.3B). The media PGE<sub>2</sub> concentrations in the PRE-S and PRE-F groups were similar at 24hrs ( $p=0.961$ ) and did not differ from the CON-S ( $p=0.502$ ) and CON-F ( $p=0.248$ ) groups. At 24hrs, media PGE<sub>2</sub> concentrations were similar in the POST-S and POST-F groups ( $p=0.751$ ) and were significantly lower than the CON-S ( $p<0.001$ ) and CON-F ( $p<0.001$ ) groups.

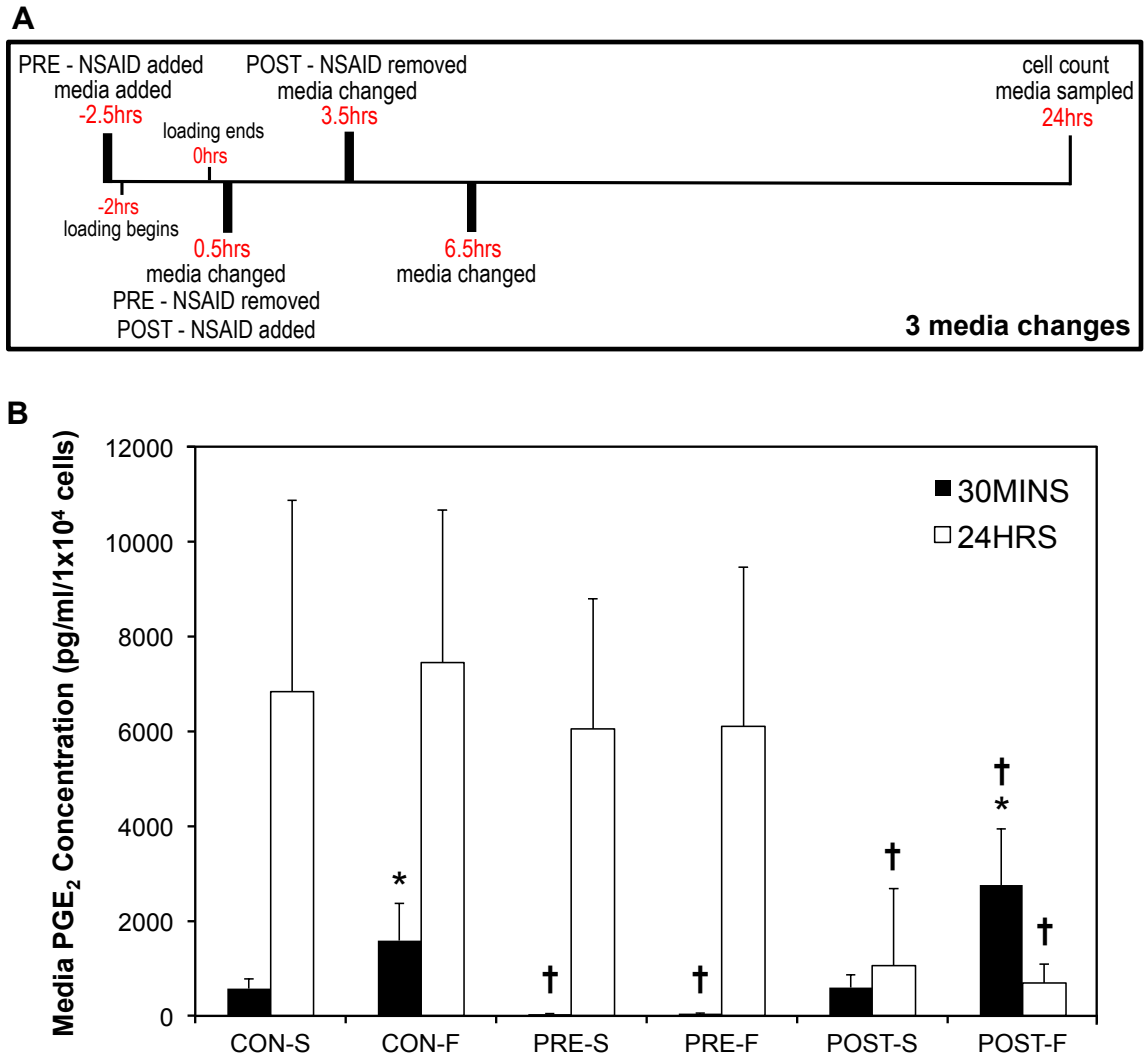


**Figure 7.3** **A) Experimental timeline for the three media change experiment.** **B) Media PGE<sub>2</sub> concentrations at 30mins and 24hrs in the three media change experiment.** Values are mean ± STD. \*Different from static. †Different from CON. CON=no indomethacin; PRE=indomethacin administered prior to loading; POST= indomethacin administered after loading. S=static; F=flow. n=12/group.

### 7.2.2 Two Media Changes at 30mins and 3.5hrs

In the flow experiment with two media changes, media PGE<sub>2</sub> concentrations were determined 30 minutes and 12 hours after loading in the CON, PRE and POST groups (Figure 7.4A). At 30mins the media PGE<sub>2</sub> concentration was greater in the CON-F group compared to the CON-S group ( $p<0.001$ ) and in the POST-F group compared to the POST-S group ( $p<0.001$ ) (Figure 7.4B). There were no differences between the CON-S and POST-S ( $p=0.862$ ) groups or the CON-F and POST-F groups ( $p=0.071$ ). Indomethacin inhibited PGE<sub>2</sub> production in both the PRE-S and PRE-F groups at 30mins, resulting in similar concentrations between the two groups ( $p=0.975$ ) and significantly lower than the CON-S ( $p<0.05$ ) and CON-F ( $p<0.001$ ) groups.

At 12hrs, the media PGE<sub>2</sub> concentrations were similar between the CON-S and CON-F groups ( $p=0.892$ ) (Figure 7.4B). The media PGE<sub>2</sub> concentrations in the PRE-S and PRE-F groups were similar at 12hrs ( $p=0.684$ ) and significantly lower than the CON-S ( $p<0.001$ ) and CON-F ( $p<0.001$ ) groups. At 12hrs, media PGE<sub>2</sub> concentrations were similar in the POST-S and POST-F groups ( $p=0.998$ ) and were significantly lower than the CON-S ( $p<0.001$ ) and CON-F ( $p<0.001$ ) groups.

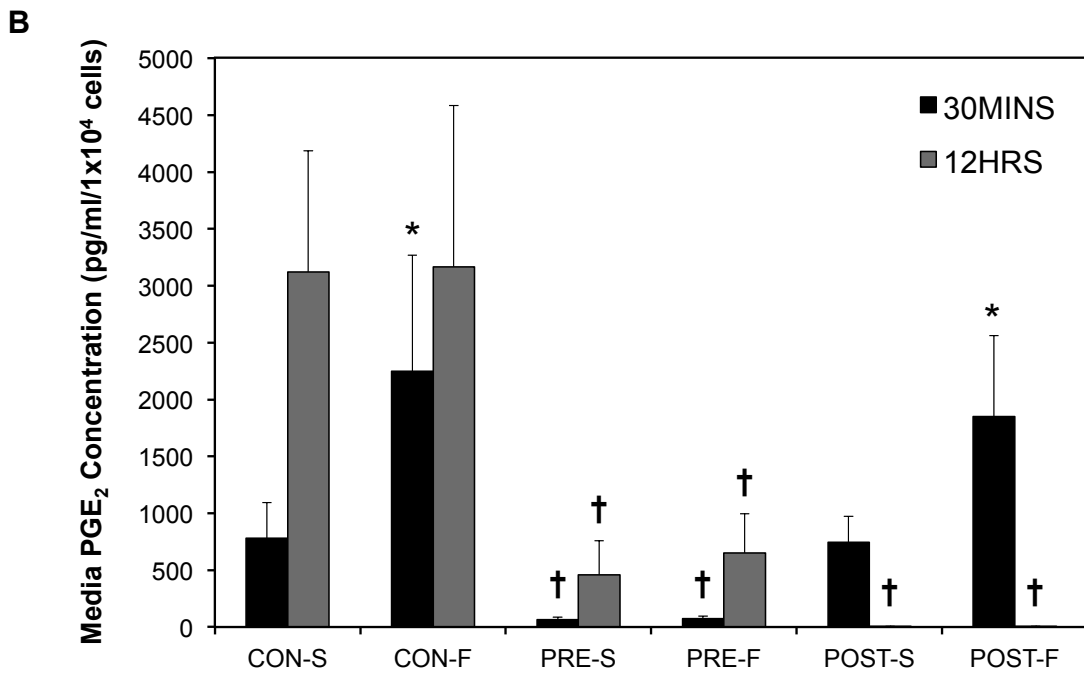
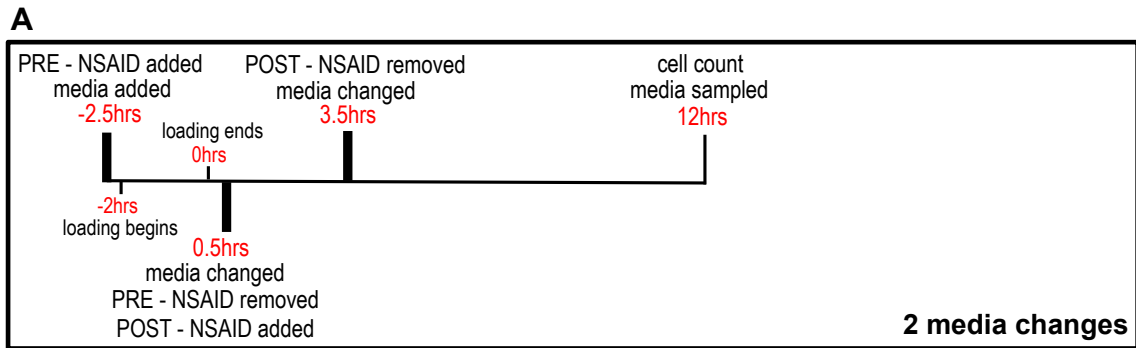


**Figure 7.4** A) Experimental timeline for the two media change experiment. B) Media PGE<sub>2</sub> concentrations at 30mins and 12hrs in the two media change experiment. Values are mean ± STD. \*Different from static. †Different from CON. CON=no indomethacin; PRE=indomethacin administered prior to loading; POST= indomethacin administered after loading. S=static; F=flow. n=12/group.

### 7.2.3 One Media Change at 30mins

The flow experiment with one media change after loading examined media PGE<sub>2</sub> concentrations in the CON and PRE groups 30 minutes and 24 hours after loading (Figure 7.5A). The media PGE<sub>2</sub> concentration was greater in the CON-F group compared to the CON-S group ( $p<0.001$ ) at 30mins (Figure 7.5B). Media PGE<sub>2</sub> concentrations were similar in the PRE-S and PRE-F ( $p=0.987$ ) groups at 30mins. Indomethacin inhibited PGE<sub>2</sub> production in the PRE groups and as a result media PGE<sub>2</sub> concentrations were significantly lower in the PRE-S ( $p=0.029$ ) and PRE-F ( $p<0.001$ ) groups compared to the CON groups at 30mins. At 24hrs, media PGE<sub>2</sub> concentrations were similar in the CON-S and CON-F ( $p=0.833$ ) groups and were significantly greater than the PRE-S ( $p<0.001$ ) and PRE-F ( $p<0.001$ ) groups, which had similar concentrations ( $p=0.688$ ).

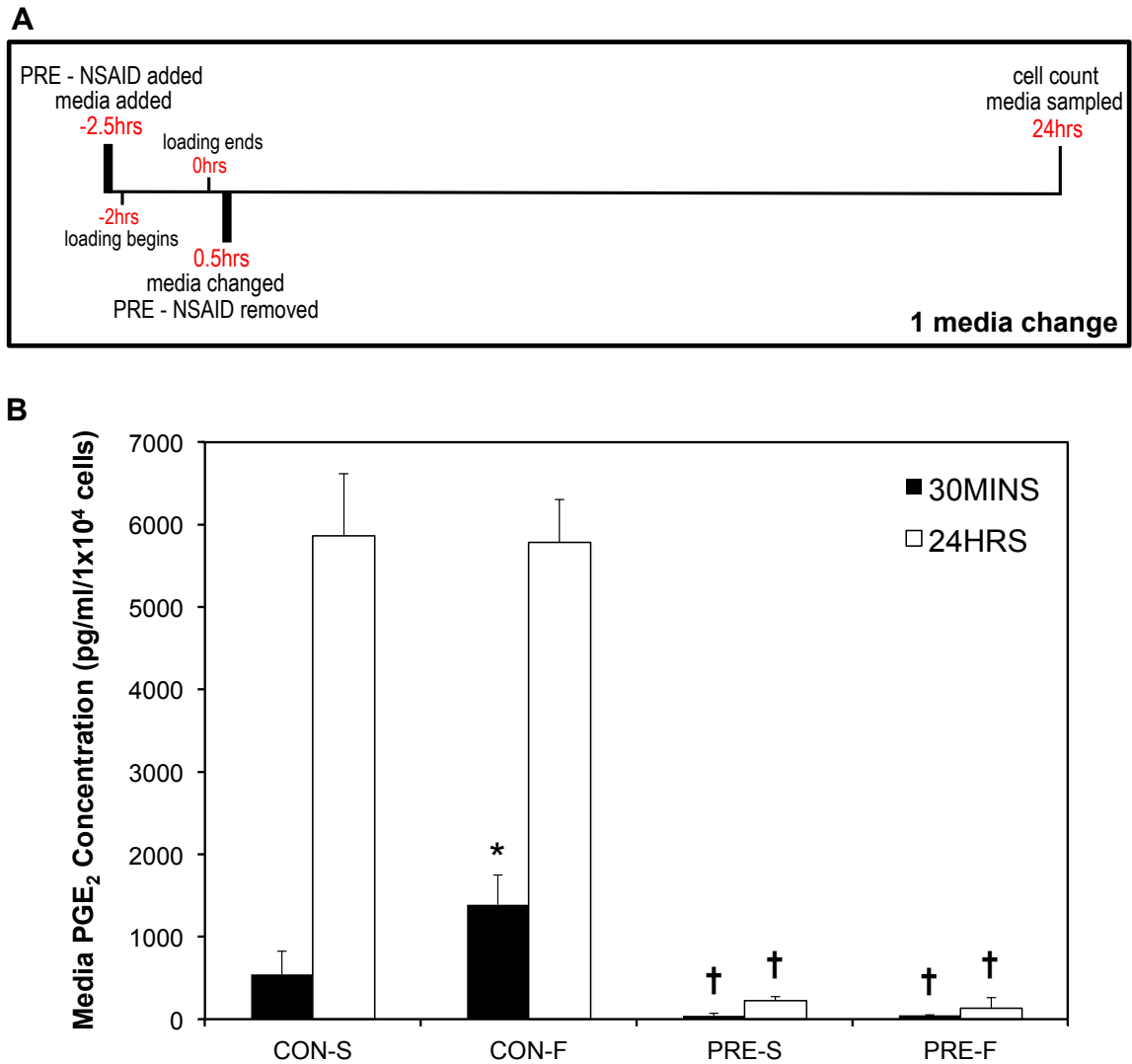


**Figure 7.5** A) Experimental timeline for the one media change experiment. B) Media PGE<sub>2</sub> concentrations at 30mins and 24hrs in the one media change experiment. Values are mean ± STD. \*Different from static. †Different from CON. CON=no indomethacin; PRE=indomethacin administered prior to loading. S=static; F=flow. n=4/group.

#### **7.2.4 No Media Changes**

In the flow experiments with no media changes after loading, media PGE<sub>2</sub> concentrations were only examined in the CON group 12 hours and 24 hours after loading in two separate experiments (Figure 7.6A). Only the CON groups were included because media changes would need to have occurred to remove the indomethacin from the media in the PRE and POST groups. Fluid shear stress increased the PGE<sub>2</sub> production of MLO-Y4 cells at 12hrs and 24hrs (Figure 7.6B). As a result, media PGE<sub>2</sub> concentrations were significantly greater in the CON-F group compared to the CON-S at 12hrs and 24hrs ( $p < 0.05$ ).

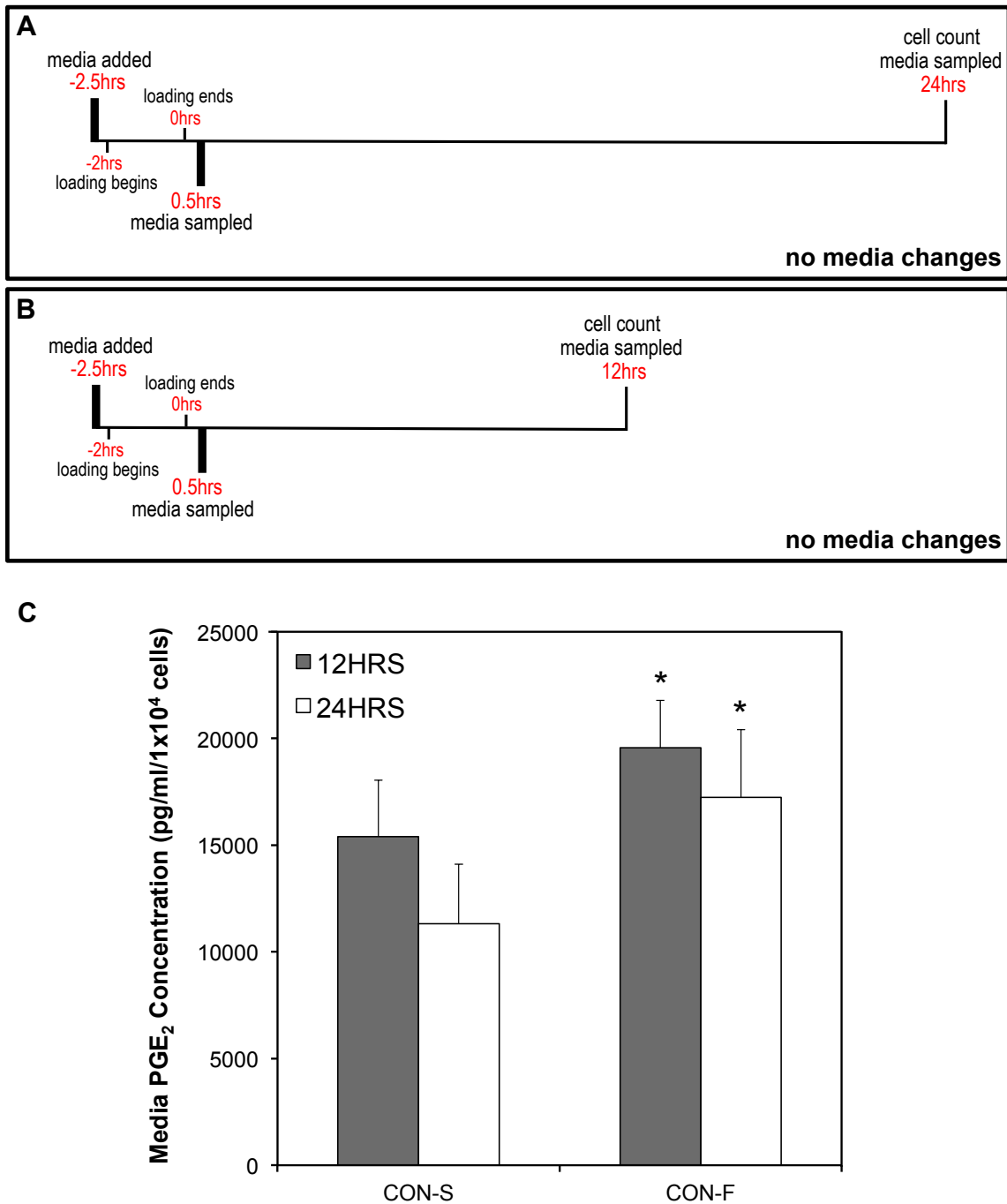


**Figure 7.6** Experimental timeline for the no media change experiment at A) 24hrs and B) 12hrs. C) Media PGE<sub>2</sub> concentrations at 12hrs and 24hrs in the no media change experiment. Values are mean ± STD. \*Different from static. CON=no indomethacin. S=static; F=flow. n=6/group.

### 7.2.5 Media Changes in the CON Group

The effect of media changes on media PGE<sub>2</sub> concentrations was examined in the CON group by comparing across the flow experiments with different numbers of media changes (Figure 7.7). At 24hrs the CON-S and CON-F groups that underwent no media changes after loading had significantly greater ( $p<0.05$ ) media PGE<sub>2</sub> concentrations than the CON-S and CON-F groups that experienced one and three media changes. The CON-S and CON-F groups that experienced one media change had similar media PGE<sub>2</sub> concentrations as the CON-S ( $p=0.649$ ) and CON-F ( $p=0.432$ ) groups that underwent three media changes.

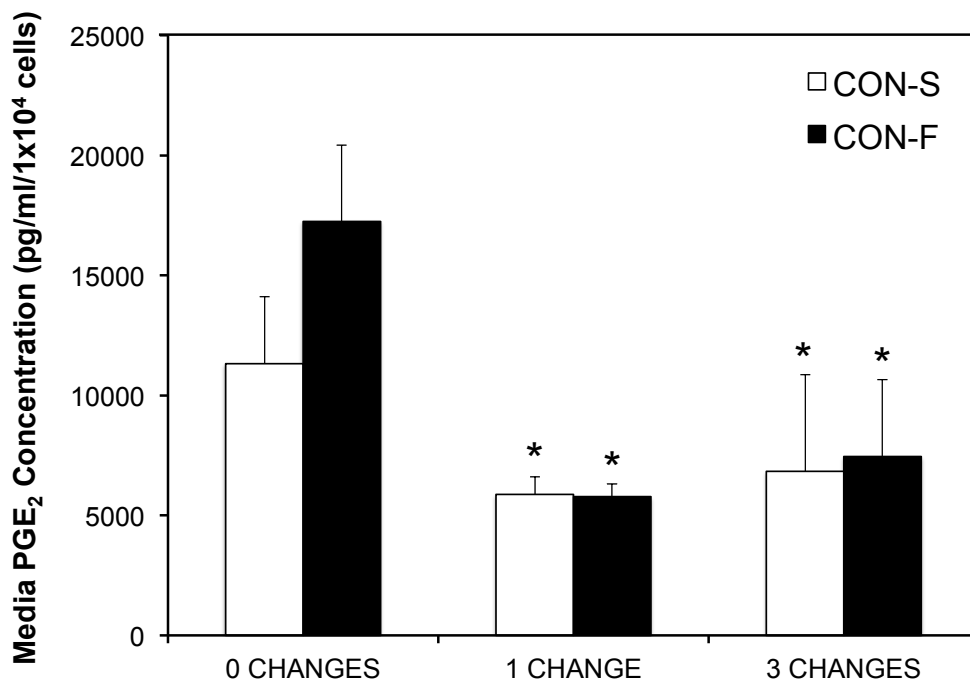


**Figure 7.7** Media PGE<sub>2</sub> concentrations at 24hrs in the CON group in the experiments with no, one and three media changes. Values are mean ± STD. \*Different from 0 CHANGES. 3 CHANGES=3 media changes after loading (n=12); 1 CHANGE=one media change after loading (n=4); 0 CHANGES=no media changes after loading (n=6).

## CHAPTER EIGHT

### DISCUSSION: *IN VITRO* MECHANICAL LOADING

#### 8.1 Parallel Plate Flow Chambers

The first method of fluid flow generation implemented in this study, the parallel plate flow chambers, did not produce consistent results. The media PGE<sub>2</sub> concentrations in the static control groups (CON-S) were similar to those of the flow groups (CON-F). The release of PGE<sub>2</sub> by bone cells has long been known to be one of the responses to mechanical stimuli [76,82]. The lack of difference in media PGE<sub>2</sub> concentrations suggested that the cells were being stimulated in both the static and flow conditions. The set up of the flow chambers involved a large amount of cell manipulation and all of the cells whether they were exposed to fluid flow or not, were placed into the chambers. Previous studies examining PG production placed static controls in dishes, not the flow chambers [76,95,103,169]; this was likely done to avoid any inadvertent stimulation when placing the slides into the chambers. In this study, all of the cells were placed into chambers to try to keep all of the conditions similar between the static and flow groups. MLO-Y4 cells are very sensitive to movement and placing them into parallel plate flow chambers can activate acute signalling mechanisms, which may interfere with the study outcomes [103]. This appears to have occurred in the flow chamber experiments. As a result, the orbital shaker, which almost completely eliminated any cell manipulation, was used to generate fluid shear stress in the experiments examining NSAID effects on PGE<sub>2</sub> production.

## 8.2 Orbital Shaker

The purpose of the *in vitro* experiments was to gain a better understanding of the results from the *in vivo* experiments that examined the effects of NSAIDs on mechanically induced bone formation. The hypothesis was that NSAID administration would differentially affect PGE<sub>2</sub> production from MLO-Y4 cells depending on the timing of delivery, either before or after loading. NSAID administration before loading would impair the immediate increase in PGE<sub>2</sub> production whereas NSAID administration after loading would impair the longer term production of PGE<sub>2</sub>. The *in vitro* experiments were designed to examine the effects of NSAIDs on cellular and molecular signalling in response to fluid flow induced shear stress but unfortunately due to the complexities of trying to mimic *in vivo* conditions in the *in vitro* setup, the results, although very informative, did not provide a clear picture of NSAID timing effects *in vivo*.

Fluid flow induced shear stress, generated by the orbital shaker increased the PGE<sub>2</sub> production from MLO-Y4 cells. Media PGE<sub>2</sub> concentrations were greater in the CON-F group compared to the CON-S group 30 minutes after loading. Indomethacin inhibited the PGE<sub>2</sub> production from MLO-Y4 cells. Indomethacin administration prior to fluid flow (PRE) lowered the media PGE<sub>2</sub> concentration three hours later, in both the static and fluid flow groups, and to a similar degree. This was expected, as indomethacin is a non-selective COX inhibitor designed to inhibit PGE<sub>2</sub> production and has been shown to do so in *in vitro* fluid flow experiments [169,175]. Similar to the PRE group, when indomethacin was delivered after the fluid flow (POST), it impaired PGE<sub>2</sub> production in both the static and flow groups and to a similar degree in both groups. This result was

expected, as the presence of indomethacin in the media will impair any COX activity, constitutive or induced. One of the confounding effects of the model was that media PGE<sub>2</sub> concentrations in the PRE and POST groups in the hours following indomethacin removal were dependent upon the number of media changes. The media changes also influenced media PGE<sub>2</sub> concentrations in the CON groups. The media changes made it difficult to differentiate between the effects of the media changes on PGE<sub>2</sub> production vs. the timing effects of indomethacin administration on PGE<sub>2</sub> production.

Previous studies examining the effects of NSAIDs on PGE<sub>2</sub> production *in vitro* have implemented various NSAID administration time courses. NSAID administration before fluid flow has been shown to impair PGE<sub>2</sub> production [169,175]. Similar to this study, Bakker et al. [169] showed that NS-398 administration 30 minutes prior to 1 hour of fluid flow, inhibited the stimulating effect of fluid flow on PGE<sub>2</sub> production in primary mouse long bone cells immediately after loading. However, they found that in the static, no flow group, NS-398 only slightly reduced PGE<sub>2</sub> production. This is in contrast to this study's findings; indomethacin inhibited PGE<sub>2</sub> production in the PRE static as well as the flow groups. However, Bakker et al. [169] found that in human bone cells from trabecular bone biopsies, NS-398 impaired PGE<sub>2</sub> production in both the flow and static groups. The contrasting results may suggest that different cells react differently to the NSAIDs.

The effects of NSAID administration following fluid flow have only been examined in one study previously. Westbroek et al. [95] subjected chicken calvarial osteocytes to one hour of pulsatile fluid flow and then incubated them for 2 hours in the presence of NS-398; it decreased the production of PGE<sub>2</sub>. These findings are in

agreement with the lower media PGE<sub>2</sub> concentration seen in the POST group in this study. Bakker et al. [169] showed that NS-398, a COX-2 selective inhibitor, impaired PGE<sub>2</sub> production when it was administered before fluid flow and in this study indomethacin, a non-selective NSAID, also impaired PGE<sub>2</sub> production. Similarly, both NS-398 [95] and indomethacin impaired PGE<sub>2</sub> production when they were administered following fluid flow. It appears that both non-selective and COX-2 selective NSAIDs have a similar effect on PGE<sub>2</sub> production both before and after fluid flow in the *in vitro* cell culture models.

The effects of NSAIDs on fluid flow induced PGE<sub>2</sub> production have mostly been examined immediately after fluid flow or within a few hours of fluid flow ending. Two studies did show inhibition of PGE<sub>2</sub> production 22 hours [173] and 24 hours [169] after flow, but the cells were incubated in media containing the NSAIDs for the entire duration of the experiment. These results are expected since NSAIDs are not metabolized by bone cells and therefore would continue to inhibit PGE<sub>2</sub> production as long as they were present within the media. In this study, indomethacin was removed from the media to more closely mimic *in vivo* conditions, where it would be metabolized and would not be present 24 hours after flow. However, the process of removing the NSAID involved a media change and created a number of issues with the experimental design and determining the effects of only NSAIDs on PGE<sub>2</sub> production was difficult. The results of the *in vitro* experiments brought to the forefront the complexity of modeling the timing effects of NSAIDs on MLO-Y4 PGE<sub>2</sub> production in response to fluid flow.

Translating these *in vitro* results to *in vivo* conditions is difficult. *In vivo* conditions vary greatly from the very simplified *in vitro* environment. The major obstacle is that the time course of PGE<sub>2</sub> production and metabolism *in vivo* remains largely unknown because it is difficult to measure PGE<sub>2</sub> concentrations *in vivo*. Thorsen et al. [94] did show however, that the concentration of PGE<sub>2</sub> in the proximal tibial metaphysis of females, was still increasing 2 hours after mechanical loading finished. This suggests that *in vivo* PGE<sub>2</sub> concentrations remain elevated and even continue to increase hours after loading; PGE<sub>2</sub> does not appear to be rapidly removed from the bone environment. Therefore eliminating the PGE<sub>2</sub> from the media 30 minutes after loading, likely does not simulate *in vivo* conditions. Unfortunately, the media needed to be changed to eliminate the indomethacin because it is not metabolized by bone cells and would have continued to inhibit PGE<sub>2</sub> production indefinitely if not removed. *In vivo*, indomethacin would have been metabolized and therefore the inhibition of COX would have diminished over time. Recognizing the limitations with *in vitro* models is important when discussing PGE<sub>2</sub> production in response to mechanical loading.

### **8.3 Effect of Media Changes on the Control (CON) Group**

The media changes in the *in vitro* experimental protocol were implemented to remove indomethacin from the culture media. Unfortunately the only way to eliminate indomethacin from the media was to remove the media and replace it with fresh media containing no indomethacin, as indomethacin is not broken down in bone cell culture. However, changing the media in the 6-well plates after loading affected the media PGE<sub>2</sub>

concentrations over the 24 hours that followed. The media changes introduced a couple of potential confounding factors: the removal of PGE<sub>2</sub> and the addition of fresh serum.

PGs are not stored in cells and are rapidly metabolized once they are secreted into the peripheral circulation *in vivo* [78]. *In vitro*, however, PGE<sub>2</sub> is stable and accumulates in the media [78]. The *in vivo* time course of PGE<sub>2</sub> production and metabolism in bone in response to mechanical loading is not well understood, and is therefore challenging to mimic *in vitro*. The removal of PGE<sub>2</sub> with media changes *in vitro* may or may not be appropriate, but it does influence future media PGE<sub>2</sub> concentration and potentially PGE<sub>2</sub> production and therefore is important to consider. PGE<sub>2</sub> accumulation may be an issue because PGE<sub>2</sub> has been shown to induce COX-2 mRNA [92,95]. Therefore, when PGE<sub>2</sub> is left to accumulate in the media, an increase in PGE<sub>2</sub> production is likely to be seen. If however, the PGE<sub>2</sub> is removed when the media is changed, it will no longer stimulate COX-2 mRNA expression. The addition of fresh media also involves the introduction of fresh serum, which has also been shown to induce COX-2 mRNA and therefore increase PGE<sub>2</sub> production [92,95]. It is likely that both the elimination of PGE<sub>2</sub> and the addition of fresh media are important factors in this experimental setup. It is therefore very challenging to translate *in vitro* PGE<sub>2</sub> production in response to loading to an *in vivo* model.

The media changes affected media PGE<sub>2</sub> concentrations in the CON groups. A media change at 30mins, whether followed by additional media changes (the two and three media change experiments) or not (the one media change experiment), eliminated the effect of flow on media PGE<sub>2</sub> concentrations at the final time points. The media

change at 30mins, eliminating any PGE<sub>2</sub> in the media that was induced by fluid flow, appeared to level the playing field between the flow and static conditions. The CON-S and CON-F groups were both “reset” 30 minutes after flow resulting in similar media PGE<sub>2</sub> concentrations in the CON-S and CON-F groups at 12hrs or 24hrs. When the media was not changed, however, the CON-S group did not “catch up” to the CON-F group; the CON-S media PGE<sub>2</sub> concentration remained statistically lower than the CON-F at 12hrs or 24hrs. The observed “catch up” effect that resulted from eliminating the PGE<sub>2</sub> from the media, may have disrupted the autoamplification effect and/or may have decreased the cumulative amount of PGE<sub>2</sub>, resulting in lower media PGE<sub>2</sub> concentrations at the end of the experiments.

Further support for the importance of the first media change at 30mins can be found by examining the CON groups that underwent one and three media changes. The media PGE<sub>2</sub> concentrations at 24hrs in the CON groups undergoing one or three media changes were similar, suggesting that the initial PGE<sub>2</sub> accumulation during the loading and 30 minutes afterward (before the first media change) was important for determining the concentration 24 hours later. The media PGE<sub>2</sub> concentrations at 24hrs in the CON groups were similar whether there was only one media change at 30mins or there were three, at 30mins, 3.5hrs and 6.5hrs.

The lack of difference in media PGE<sub>2</sub> concentrations in the CON-S and CON-F groups at 24hrs is in contrast to Bakker et al. [169]. They showed that the media PGE<sub>2</sub> concentration remained elevated in fluid flow stimulated cells 24 hours after loading compared to static cells. Bakker et al. [169] used parallel plate flow chambers to provide

fluid flow and so after the fluid flow the slides containing the cells were removed from the chambers and placed into dishes containing fresh media. Similar to the experimental setup in this study, the PGE<sub>2</sub> produced during the fluid flow would not have been present in the dishes the cells were transferred to, and therefore would not have contributed to the PGE<sub>2</sub> concentrations at 24hrs. Brighton et al. [173] also found that media PGE<sub>2</sub> concentrations were elevated 22 hours after cyclic biaxial strain of rat calvarial cells, but the media was not changed after stimulation. The contrasting results may be attributed to a different method of fluid flow stimulation and/or the cell type used. As discussed previously, MLO-Y4 cells are very sensitive to movement [103]. Not all types of bone cells respond the same way to all fluid flow profiles and not all fluid flow profiles elicit the same response in a given bone cell type [254].

COX-2 mRNA expression is increased by fluid flow [76,169,267]. It has been suggested that COX-1 mRNA expression may be sensitive to nutrient conditions in bone cells [169], but flow-induced COX-2 mRNA expression in bone cells appears to be independent of serum-factors [76,267]. Bakker et al. [169] showed that COX-2 mRNA expression was increased in human bone cells 1 hour after pulsating fluid flow and remained elevated even 24 hours later. Kamel et al. [268] found that COX-2 mRNA expression was increased in MLO-Y4 cells immediately after 2 hours of pulsatile fluid flow, but 24 hours after flow the increased expression was no longer evident. Govey et al. [269] found that COX-2 mRNA expression was increased 1.37 fold and 1.45 fold, 2 hours and 8 hours after flow, respectively, in MLO-Y4 cells subjected to oscillatory fluid flow, but the expression was not significantly regulated. It appears that

COX-2 mRNA expression differs between studies and since it was not measured in this study, it is not known how the expression changed throughout the time course of the fluid flow experiments.

COX-2 mRNA expression may have been altered in the experiments in this study because of the removal of PGE<sub>2</sub> from the media. COX-2 mRNA induction has been shown to exhibit a biphasic pattern in response to stimulation. It is believed that the biphasic pattern, specifically the second peak, is likely the result of autoamplification by PGE<sub>2</sub>, as PGE<sub>2</sub> can induce COX-2 [92]. As PGE<sub>2</sub> increases, it stimulates COX-2, enhancing its own production. So, removing PGE<sub>2</sub> from the media may have affected COX-2 mRNA expression in this study. However, Bakker et al. [169] showed that the media PGE<sub>2</sub> concentration and COX-2 mRNA expression remained elevated 24 hours after fluid flow, even though the media was removed after loading. It does not appear that the removal of PGE<sub>2</sub> from the media affected PGE<sub>2</sub> production or COX-2 mRNA expression in that study. Kamel et al. [268] found, however, that COX-2 mRNA expression was not increased in MLO-Y4 cells 24 hours after flow even though the cells remained in the same flow media after loading. Despite the presence of the PGE<sub>2</sub> produced during the flow in the post-flow incubation media, COX-2 mRNA expression did not remain elevated 24 hours after flow. As discussed above, Govey et al. [269] found that COX-2 mRNA expression was not significantly regulated in MLO-Y4 cells in the 24 hours following flow. The contrasting results may be attributed to a different method of fluid flow stimulation and/or the cell type used. The mechanisms and kinetics of responses to loading could vary substantially in different bone cell types [268].

Bakker et al. [169] found that during 24 hours of post-flow incubation, PG production was much lower than after 1 hour of flow or sitting static. This was in contrast to the results in this study, where PGE<sub>2</sub> production was much greater after fluid flow than during fluid flow, suggesting that there are differences between the studies. Only certain time points were examined in each study and therefore key time points of COX-2 mRNA expression may have gone undetected. Further investigation is needed to determine how the presence and/or absence of PGE<sub>2</sub> affects the time course of COX-2 mRNA expression.

The addition of fresh media may have affected media PGE<sub>2</sub> concentrations in the CON-S and CON-F groups undergoing three media changes. Media PGE<sub>2</sub> concentrations were similar in the CON-S and CON-F groups with one and three media changes at 24hrs, despite 6 hours less for PGE<sub>2</sub> to accumulate in the CON-S and CON-F groups undergoing three media changes. Media changes may have stimulated PGE<sub>2</sub> production. However, the CON-S and CON-F groups that had no media changes had a statistically greater media PGE<sub>2</sub> concentration than the groups with three changes and the groups experiencing just one change. So, the introduction of fresh media does not appear to dominate PGE<sub>2</sub> production but may play a role.

The media PGE<sub>2</sub> concentration was approximately two times greater in the CON-S group in the no media change experiment compared to the CON-S group in the one media change experiment, despite only a difference of 3 hours in the time available for the PGE<sub>2</sub> to accumulate. Based on that observation, it appears that media PGE<sub>2</sub> concentrations are also dependent upon the time allowed for PGE<sub>2</sub> accumulation and the

presence of PGE<sub>2</sub> in the media. PGE<sub>2</sub> has been shown to induce COX-2 mRNA and subsequently increase PGE<sub>2</sub> production so removing the media essentially removes all PGE<sub>2</sub> from the media and also reduces the autoamplification effect. Therefore although the time difference was only 3 hours between the no media change and one media change experiment, it would theoretically take an additional 3 hours for the CON-S group from the one media change experiment to get back up to where it was before the media change, let alone to where the CON-S group with no media changes was at (at the same time point). The removal of media, and consequently removal of PGE<sub>2</sub> appears to hinder the autoamplification effect, resulting in lower media PGE<sub>2</sub> concentrations. Different media PGE<sub>2</sub> concentrations between the experiments may also be due to inherent differences between the experiments. However, the large differences (approximately two fold) seem more likely to be a consequence of the removal of PGE<sub>2</sub>.

#### **8.4 Effect of Media Changes on the PRE and POST Groups**

The effect of the media changes was also evident in the PRE group. With the three media changes occurring, the PRE groups had similar media PGE<sub>2</sub> concentrations as the CON groups, both static and flow, at 24hrs. The media changes, and likely the removal of PGE<sub>2</sub> from the CON groups, allowed the PRE groups to “catch up” to the CON groups at 24hrs, in terms of media PGE<sub>2</sub> concentration. At the 6.5hrs time point, when the last media change was made in the three media change experiment, the CON and the PRE groups would have been essentially at the same level; that is, there was no PGE<sub>2</sub> present in the new media, it was removed with the media change, and the indomethacin had been

cleared from the PRE groups. So, similar media PGE<sub>2</sub> concentrations 17.5 hours later at the 24hrs time point was not unexpected. Because the indomethacin and PGE<sub>2</sub> were removed from the media, the CON and PRE groups were essentially the same after the 6.5hrs media change. Any effect of an NSAID or lack thereof, was erased. *In vivo*, PGE<sub>2</sub> would not have been completely eliminated from the bone, as occurred *in vitro*, and so the PGE<sub>2</sub> concentration likely differs *in vivo* in the time following loading, where there is likely autoamplification effects. The addition of fresh media occurred in both the CON and PRE groups so any effect on subsequent PGE<sub>2</sub> production should have been similar in both groups. However, Pilbeam et al. [92] showed that inhibiting PGE<sub>2</sub> production with indomethacin decreased the serum induction of COX-2 mRNA, and so there may have been less of an affect of fresh media stimulation on the PRE groups. Nonetheless, after the 6.5hrs media change the CON and PRE groups were essentially the same. Media changes and consequently the removal of PGE<sub>2</sub> from the media disrupted the examination of indomethacin effects on PGE<sub>2</sub> production following fluid flow.

Despite the role that accumulating media PGE<sub>2</sub> may play in autoamplification or any effect of fresh serum, the media PGE<sub>2</sub> concentrations remained statistically lower in the PRE groups, both static and flow, in the one and two media change experiments compared to the CON groups. The PRE-S group media PGE<sub>2</sub> concentration did “catch up” to the CON-S group at 24hrs in the three media change experiment however, suggesting once again that the number of media changes influenced the media PGE<sub>2</sub> concentrations. The media changes were designed to remove the indomethacin from the media to mimic *in vivo* NSAID metabolism. Examination of the media PGE<sub>2</sub>

concentrations in the PRE groups across the experiments suggests that indomethacin was not completely removed from the media unless the media was changed three times. With three media changes, the media PGE<sub>2</sub> concentration in the PRE-S group was similar to that of the CON-S group at 24hrs. However, when there were only one or two media changes, the media PGE<sub>2</sub> concentrations were statistically lower in the PRE-S groups compared to the CON-S groups. The likely explanation is that the indomethacin was not being completely eliminated from the cells and media with less than three washes.

Further support for this theory can be found by examining the POST-S group. Theoretically the only differences between the PRE-S and POST-S groups were a 3 hour difference in the timing of indomethacin administration and one less media change in the POST-S groups. As discussed above, a 3 hour time difference in the time allowed for PGE<sub>2</sub> to accumulate in the media could affect subsequent PGE<sub>2</sub> production; however, a media change did take place 3 hours after the indomethacin was removed, which would have essentially set the CON-S, PRE-S and POST-S groups all back to the same point. And yet the POST-S group did not “catch up” to the CON-S or PRE-S groups by 24hrs. So, it is unlikely that the 3 hour delay in indomethacin administration was the reason for the statistically lower media PGE<sub>2</sub> concentration in the POST-S groups at 24hrs or even 12hrs, in the two media change experiment, compared to the CON-S groups. This then suggests that the one less media change in the POST groups affected media PGE<sub>2</sub> concentrations. The PRE groups experienced three media changes whereas the POST groups only received two, in the three media change experiment. The results suggest that the indomethacin was washed away in the PRE groups, as media PGE<sub>2</sub> concentrations

were similar in the PRE-S and CON-S groups at 24hrs, but not the POST-S group, where media PGE<sub>2</sub> concentrations remained statistically lower at 24hrs compared to the CON-S group. Any remaining indomethacin in the POST groups would have continued to inhibit PGE<sub>2</sub> production, leading to the statistically lower media PGE<sub>2</sub> concentration seen in the POST group compared to both the CON and PRE groups at 24hrs.

An alternative explanation as to why the POST group may have exhibited lower media PGE<sub>2</sub> concentrations at 24hrs compared to the CON group, besides a lack of indomethacin elimination, may have involved the inhibition of PGE<sub>2</sub> production resulting from induced COX-2 synthesis. COX-2 protein synthesis is believed to start 1-4 hours post loading and peak at 3-12 hours [96]. Based on that observation, indomethacin administration after loading would be active during that time period of near maximum to maximum COX-2 synthesis and therefore PGE<sub>2</sub> production. This may help to explain why the POST-F group does not appear to “catch up” to the CON-F group in terms of media PGE<sub>2</sub> concentrations at 24hrs. Inhibiting PGE<sub>2</sub> production when it was greatest would have greatly affected media PGE<sub>2</sub> concentrations. The media PGE<sub>2</sub> concentrations in the POST-S group however, suggest a lack of removal of indomethacin as the more likely cause of lower media PGE<sub>2</sub> concentrations in the POST groups at 24hrs.

The dependency of the media PGE<sub>2</sub> concentrations on the number of media changes suggests that if the media was changed less than three times, then the indomethacin was not washed away and continued to inhibit PGE<sub>2</sub> production. Further investigation is needed to determine for certain if indomethacin was still present in the

media collected at 24hrs, or if the lower media PGE<sub>2</sub> concentration at 24hrs was a result of indomethacin administration following fluid flow.

## **8.5 Limitations**

### **8.5.1 *In vitro* vs. *In vivo***

*In vitro* experiments, typically two-dimensional, attempt to mimic the three-dimensional *in vivo* bone environment and cell organization of the lacuna-canalicular system. However, there are several differences between fluid-flow stimulation of bone cells *in vivo* and *in vitro*. Most notably are cell morphology and substrate attachment and the actual flow environment [270]. *In vivo*, cells are attached to the mineralized matrix via tethering filaments or integrin-based focal adhesions but *in vitro* there is no matrix surrounding the cells so the attachments to the substrate are all integrin-based [270]. As well, osteocytes seeded on flat surfaces spread out and build strong attachments to the substrate [270]. This flat adherent shape has been shown to be less sensitive to mechanical stimuli than round non-adherent osteocytes [271]. The differences in morphology between *in vitro* and *in vivo* cells may affect their mechanosensitivity. Perhaps the largest and most significant difference between *in vitro* and *in vivo* models is the actual flow environment. The lack of three-dimensional structure means that the spatial arrangement of the cells is not that of the *in vivo* environment. As well, since the spatial arrangement of the cells is lacking, so too is the real time interaction and communication with other cells, a limitation with many *in vitro* experiments. Recreating the *in vivo* bone environment is difficult given the complex

nature of the lacunar-canalicular system and the mechanotransductive processes. It is likely difficult to determine the many complexities of mechanotransduction using simplified *in vitro* models. However, *in vitro* experiments do provide insight into the cellular and molecular signalling involved in bone mechanical stimulation.

One of the main differences between the *in vitro* and *in vivo* experiments is the cell environment. The drastic differences in the environments means that the interaction with NSAIDs likely varies. *In vitro*, there is immediate and direct contact with NSAIDs in the media. *In vivo*, it takes time for NSAIDs to reach the bone and the concentration of NSAID that makes it to the bone does not appear to be great. Paulson et al. [188] found that the bone was one of the tissues with the lowest exposure to celecoxib after oral administration in male rats. The concentration of indomethacin used in the *in vitro* experiments almost shut down PGE<sub>2</sub> production completely, which likely does not occur *in vivo*. The amount of NSAID that reached the bone *in vivo* is not known but based on the finding by Paulson et al. [188], it was likely not equivalent to the concentration used *in vitro*. The concentration used in the *in vitro* experiments ( $1 \times 10^{-5}$  M or 3.5 µg/ml) was based on previous experiments that had shown that at that concentration, PGE<sub>2</sub> production was impaired *in vitro* and there were no adverse effects on cells [146,173]. In humans, oral indomethacin doses of 50 mg resulted in an average peak plasma concentration of 2.2 µg/ml but there was considerable variation among individuals, with concentrations ranging from 0.5-4.95 µg/ml [272]. Another study found that a 50 mg dose resulted in an average peak plasma concentration of 4.2 µg/ml [273]. So, the dose used in the *in vitro* experiments falls within the range of indomethacin plasma concentrations

observed. How the plasma concentration relates to the concentration at the bone is not known. Paulson et al. [188] did show however that celecoxib levels in the plasma were about 1.5 times greater than those in the bone, suggesting the concentration of indomethacin used *in vitro* was greater than what would occur *in vivo*. The effect of various levels of PGE<sub>2</sub> inhibition on subsequent PGE<sub>2</sub> production and bone formation are not known, and would likely not be able to be determined from the *in vitro* model used in this study.

In addition to differences in the *in vivo* and *in vitro* environments, the cells themselves differ in each model. Different cell types have been used to study osteocyte responses to fluid flow *in vitro* and different cell types have been shown to respond differently to fluid flow [254]. Osteocytes are terminally differentiated osteoblasts that have become embedded in the bone matrix as it is being secreted. They sit in lacunae deep within the bone, an ideal location to sense mechanical strain, but making it difficult for *in vivo* observation and examination. Primary osteocytes are also difficult to study *ex vivo* as they are not easy to obtain, especially those from long bones. Primary osteocytes have been isolated but are most commonly from very young (a few days old to a few weeks old) calvaria [37,95,274] as they are easier to obtain. Studies have isolated osteocytes from murine long bones [169,274,275] but these are also usually from young animals. While these studies may provide information about the behaviour of osteocytes during development, they do not provide insight into the behaviour of osteocytes from skeletally mature animals, an age that may be of more importance in some studies, such as this one.

Although primary osteocytes are the ideal strategy for studying osteocyte behavior *ex vivo*, the methodology for isolating and studying them is still difficult and time consuming and therefore most studies choose to use established cell lines. Cell lines are convenient and useful and due to their large presence in the literature, easier to compare with and validate. The MLO-Y4 cell line is a well-characterized cell line representing an early osteocyte phenotype which shares numerous characteristics with primary osteocytes [250]. MLO-Y4 cells have been used extensively to study osteocyte communication with each other and with other bone cells and to examine the response of osteocytes to mechanical stimulation, including fluid flow [69,72,251–254]. They exhibit low expression of ALP and high expression of osteocalcin, similar to the pattern of expression in primary osteocytes [256] and express very large amounts of connexin 43 protein, like osteocytes do. There are known differences between primary osteocytes and MLO-Y4 cells. For example, MLO-Y4 cells express low to undetectable levels of sclerostin (Sost), whereas osteocytes are known to express Sost *in vivo* [257]. MLO-Y4 cells do however respond to mechanical stimuli *in vitro* similarly to mouse osteocytes *in vivo* [276]. Despite the differences that exist between MLO-Y4 cells and primary osteocytes, MLO-Y4 cells remain a very useful model for examining osteocyte behavior *in vitro*.

### **8.5.2 Orbital Shaker**

Several *in vitro* cell stimulation models have been implemented in the literature to study osteocyte responses to fluid shear stress. The models use different cells and

mechanical stimulation methods. The method of fluid flow generation and flow parameters, including flow profile, flow rate, shear stress amplitude, frequency and duration of flow also vary amongst the studies. All of these factors influence cell responses to fluid flow [63,66–70], making it difficult to compare findings between studies and ultimately to determine what the responses of osteocytes are *in vivo*.

The orbital shaker was chosen as the model of fluid flow stimulation for this study because it almost eliminated any manipulation of the cells during the experimental procedures. This is important because MLO-Y4 cells are very sensitive to movement and can become inadvertently stimulated, leading to the activation of acute signalling pathways which may interfere with the outcomes of the study [103,260]. Previous studies examining PGE<sub>2</sub> production placed the static controls in petri dishes under similar conditions as the experimental groups, but not within the actual flow chambers used for fluid flow application [76,95,103,169]. The orbital shaker model ensured all of the cells underwent the same procedures, whether in the static or flow groups, ensuring the differences observed were a result of only fluid flow.

There are recognized limitations with the orbital shaker method of fluid flow; most notable is the fluid flow profile. The fluid flow is not oscillatory, that is the fluid does not move back and forth, but rather is continuously moving in one direction around the dish. Fluid flow *in vivo* is believed to be oscillatory. The bone matrix deforms when it is loaded creating a pressure gradient that fluid flows along [63]. The load is then removed reversing the gradient and subsequently the flow. This does not occur in an orbiting dish. Although the fluid flow profile differs in the orbiting dish compared to the

parallel plate flow chamber and the suspected *in vivo* environment, other studies have employed this method to stimulate bone cells [77,260,263,264] and suggest that the orbital shaking gives rise to similar bone cell responses for a range of outcomes [260]. Further studies are required to determine if the responses induced by the flow in this study agree with those induced by oscillatory fluid flow.

Although the flow profile is not truly oscillatory the other flow parameters implemented were similar to other studies examining osteocytes responses to fluid flow. The shear stress induced by the shaker was approximately 1.8 Pa, which falls within the 0.8 and 3 Pa range predicted by theoretical models of *in vivo* physiological shear stresses within the lacuna-canalicular system [62]. In general, studies have implemented fluid shear stresses between 1 and 2 Pa [70–74]. The frequency of fluid flow in this study was 3.3 Hz. Oscillating frequencies vary amongst studies, but generally 1 Hz is the frequency most used [70,73–75], which is typical of locomotion [64]. However, greater frequencies have been recorded during activity [65] and have been studied [66]. In general, most cell responses exhibit a dose responsive behaviour, with greater shear stresses, frequencies and durations, increasing the responses to fluid flow. As well, cells appear to respond to the parameters in a synergistic manner [66]. A flow duration of 2 hours was implemented in this study which is typical of the literature [70,73–75].

One drawback of the orbital shaker model, however, is that the magnitude of shear stress can only be estimated without the use of complex modeling.

Ley et al. [265] reported shear stress as a simplified constant value at the bottom of an orbiting dish as:

$$\tau_{max} = a\sqrt{\eta\rho(2\pi f)^3} \quad \text{Equation 6.2}$$

where  $a$  is the orbital radius of rotation of the shaker (cm),  $\eta$  is the viscosity of the culture media (poise),  $\rho$  is the density of the culture media (g/ml) and  $f$  is the frequency of rotation (rotations/sec).

The equation is a two dimensional extension of Stokes' second problem for an infinite plate beneath a fluid layer of large height undergoing uniaxial oscillatory motion [262,277]. This equation has been used extensively for estimating shear stress values on the bottom of rotating plates [77,260,278]. The equation is greatly simplified compared to the complexity of the actual motion occurring in orbiting dishes. The Stokes' approximation assumes that the entire bottom surface of the plate experiences the same steady, constant shear stress. However, the cells experience an oscillating stress that varies with radial position due to the motion of the wave travelling around the dish [262]. The approximation does not take into account the influence of well walls or fluid volume/height. These are integral for calculating shear stress.

Compared to computational models of fluid motion in orbiting petri dishes, the equation set forth by Ley et al. [265] is a fairly good predictor of shear stress.

Thomas et al. [262] modeled the wall shear stress in an orbiting dish and shear stress magnitudes were calculated to be  $0.01 \pm 0.102$  Pa higher than the equation put forth by Ley et al. [265], over the full range of orbital speeds they modeled. Salek et al. [277]

developed a model of wall shear stress in orbiting 6-well plates; at 200 rpm they found that the shear stress was only constant near the centre of the well at 0.83 Pa. The average shear stress over the entire bottom surface was 0.87 Pa, which is similar to the predicted Stokes' approximation of 0.91 Pa. Salek et al. [277] suggested that the Stokes' approximation can lead to inaccurate conclusions when results are compared at different rotational rates or fluid heights. The shear stress does vary over the bottom surface of each well, depending upon radial position, and as the wave of fluid rotates around the well [277], but not completely unlike the distribution of shear stresses in a parallel plate flow chamber [279]. Based on the similar shear stress values calculated using the models and the Stokes' approximation, an approximation of the shear stress was deemed to be sufficient for the purpose of this study.

## CHAPTER NINE

### CONCLUSION

#### 9.1 Conclusion

The overall goal of this study was to better understand the mechanisms responsible for bone formation induced by multiple mechanical loading events, specifically the role that prostaglandins play in bone mechanotransduction and how NSAIDs influence that process. To accomplish this, the temporal effects of NSAID administration on bone formation, induced by multiple mechanical loading events, were examined *in vivo*. To provide further insight into the *in vivo* findings, the effects of NSAIDs on osteocyte PG production in response to fluid flow *in vitro* were also examined. NSAID administration either before or after mechanical loading did not affect bone formation induced by multiple loading events in rats. The *in vitro* experiments, although designed to examine the effect of NSAIDs on the time course of PG production following fluid flow, were not able to differentiate between NSAID timing effects and effects inherent in the experimental design.

Indomethacin administration before fluid flow impaired the PGE<sub>2</sub> production of MLO-Y4 cells, suggesting that *in vivo* mechanotransduction would be disrupted. However, the *in vivo* experimental results suggest that despite diminished PGE<sub>2</sub> production, bone mechanotransduction was not impaired, as shown by a lack of difference in MAR between the CON and PRE groups. Indomethacin administration following fluid flow impaired PGE<sub>2</sub> production as well. A decrease in PGE<sub>2</sub> production

after loading *in vitro*, may suggest an inhibitory affect on bone formation *in vivo*, as the large amounts of PGE<sub>2</sub> produced as a result of induced COX-2 activity are believed to contribute to bone formation [81]. However, the *in vivo* results do not corroborate the *in vitro* findings; NSAID administration following loading did not affect MAR. PGE<sub>2</sub> production *in vivo* was likely impaired by NSAID administration, as the *in vitro* results would suggest, but that did not influence bone adaptation to mechanical stimulation.

The results of the *in vivo* experimentation suggest that other signaling pathways and factors may compensate for the COX-2/PGE<sub>2</sub> pathway when bone formation is induced by multiple loading events in the presence of NSAIDs. Further investigation is needed to determine which pathways may be compensating for PGE<sub>2</sub> inhibition. However, examining those pathways would be difficult given the multiple loading sessions. Animals would need to be sacrificed at various time points throughout the four weeks to determine which pathways are more active after each of the loading sessions and how the expression of various genes differ over time. Previous studies have looked at gene expression at various time points over four and a half weeks in a rat forelimb compression model where loading took place each day [59,280]. Three primary clusters of gene expression were identified: genes upregulated early in the time course, genes upregulated during matrix formation, and genes downregulated during matrix formation [59]. Interestingly, mention was not made of the expression of COX-2 in the study, which reported genes that showed a greater than 1.4 fold change [59]. An *in vitro* study examining the effects of oscillatory fluid flow on gene expression in MLO-Y4 cells found that COX-2 was not significantly regulated [269]. It may be that the COX-2/PGE<sub>2</sub>

pathway is not relied upon as heavily as the many other pathways and genes involved in the bone formation response to mechanical loading. Further investigation is needed to examine how multiple loading sessions affect signaling pathways and gene expression and how NSAIDs may influence that.

The *in vitro* model used in this study could help to identify the contribution of other signaling pathways in the short term, before the media changes take place. The effect of media changes on the *in vitro* experiments would likely interfere with the examination of NSAID effects over the longer term but any early changes in the activation of other pathways and genes may provide valuable insight into *in vivo* processes. If a different model were implemented, that did not involve complete media changes, but was still able to remove the indomethacin from the media, it may be better able to demonstrate the effects of NSAIDs on PGE<sub>2</sub> production. Removing the indomethacin from the media without removing the PGE<sub>2</sub> would be difficult to accomplish and leaving all of the PGE<sub>2</sub> in the media would likely not mimic the *in vivo* environment. The *in vitro* model is likely better suited for examining the short-term effects of NSAIDs on PGE<sub>2</sub> production and other signaling pathways.

The *in vitro* model could be further used to examine effects of NSAIDs on osteocytes and how that subsequently influences osteoblast activity. Any factor that alters osteocyte release of paracrine signals, including mechanical stimuli and NSAIDs, could potentially affect bone adaptation. Indomethacin may have altered the expression of a number of factors related to osteoblast differentiation and mineralization by mechanically stimulated osteocytes. Indomethacin has been shown to affect the expression of insulin-

like growth factor-I (IGF-I) mRNA following mechanical loading *in vivo* [281] and NS-398 has been shown to affect IGF-I and osteocalcin expression following loading *in vitro* [90]. NSAIDs have also been shown to directly affect osteoblast activity [144–147,151]. Examining the effects of NSAIDs on osteocyte responses to mechanical stimulation and subsequent osteoblast activity may provide more information about the relationship of PGs and osteocyte signaling of osteoblasts.

Although the present data suggest that NSAID administration in rats, prior to or following mechanical loading, does not affect bone formation induced by multiple days of mechanical loading, NSAIDs have been shown to affect bone adaptation. NSAIDs impaired bone formation when administered before a single mechanical loading event in animal models [9–12,172]. Ibuprofen administration following exercise in premenopausal women enhanced the beneficial adaptation of BMD to exercise [14]. Further research is needed to determine the mechanisms responsible for the timing effects of NSAIDs on mechanically induced bone formation. Careful consideration should be taken when NSAIDs are taken around the time of exercise so as not to impair the adaptive response of bone to mechanical loading.

Mechanical loading is beneficial for bone not only because it can increase bone mass, but because it can also improve bone architecture, which contributes significantly to bone strength. Understanding the mechanisms that orchestrate bone formation in response to mechanical stimulation can provide a basis for future development of strategies to enhance bone mass following anabolic loading. We need to take advantage

of the intrinsic ability of bone to adapt to mechanical loading, a benefit over pharmacological agents, to help improve bone health.

## REFERENCES

- [1] Public Health Agency of Canada. Fast Facts from the 2009 Canadian Community Health Survey - Osteoporosis Rapid Response. 2009.
- [2] Osteoporosis Canada. Breaking barriers not bones: 2008 report on osteoporosis care. 2008.
- [3] Tarride J-E, Hopkins RB, Leslie WD, Morin S, Adachi JD, Papaioannou A, et al. The burden of illness of osteoporosis in Canada. *Osteoporos Int* 2012;23:2591–600.
- [4] Ferretti JL, COUNTRY GR, Capozza RF, Frost HM. Bone mass, bone strength, muscle-bone interactions, osteopenias and osteoporoses. *Mech Ageing Dev* 2003;124:269–79.
- [5] Greene DA, Naughton GA. Adaptive skeletal responses to mechanical loading during adolescence. *Sports Med* 2006;36:723–32.
- [6] Baxter-Jones ADG, Kontulainen SA, Faulkner RA, Bailey DA. A longitudinal study of the relationship of physical activity to bone mineral accrual from adolescence to young adulthood. *Bone* 2008;43:1101–7.
- [7] Rubin LA, Hawker GA, Peltekova VD, Fielding LJ, Ridout R, Cole DE. Determinants of peak bone mass: clinical and genetic analyses in a young female Canadian cohort. *J Bone Miner Res* 1999;14:633–43.
- [8] Hui SL, Slemenda CW, Johnston CC. The Contribution of Bone Loss to Postmenopausal Osteoporosis. *Osteoporos Int* 1990;1:30–4.
- [9] Pead M, Lanyon L. Indomethacin modulation of load-related stimulation of new bone formation in vivo. *Calcif Tissue Int* 1989;34–40.
- [10] Forwood M. Inducible cyclo-oxygenase (COX-2) mediates the induction of bone formation by mechanical loading In vivo. *J Bone Miner Res* 1996;11:1688–93.
- [11] Chow JW, Chambers TJ. Indomethacin has distinct early and late actions on bone formation induced by mechanical stimulation. *Am J Physiol* 1994;267:E287-92.
- [12] Li J, Burr DB, Turner CH. Suppression of prostaglandin synthesis with NS-398 has different effects on endocortical and periosteal bone formation induced by mechanical loading. *Calcif Tissue Int* 2002;70:320–9.
- [13] Sugiyama T, Meakin LB, Galea GL, Lanyon LE, Price JS. The cyclooxygenase-2 selective inhibitor NS-398 does not influence trabecular or cortical bone gain resulting from repeated mechanical loading in female mice. *Osteoporos Int* 2013;24:383–8.
- [14] Kohrt WM, Barry DW, Van Pelt RE, Jankowski CM, Wolfe P, Schwartz RS. Timing of ibuprofen use and bone mineral density adaptations to exercise training. *J Bone Miner Res* 2010;25:1415–22.
- [15] Jankowski CM, Shea K, Barry DW, Linnebur SA, Wolfe P, Kittelson J, et al. Timing of ibuprofen use and musculoskeletal adaptations to exercise training in older adults. *Bone Reports* 2015;1:1–8.
- [16] Fowler TO, Durham CO, Planton J, Edlund BJ. Use of nonsteroidal anti-inflammatory drugs in the older adult. *J Am Assoc Nurse Pract* 2014;26:414–23.

- [17] Alliance for Rational Use of NSAIDs. Advice for you and your family about taking nonsteroidal anti-inflammatory drugs (NSAIDs) for pain and/or inflammation. 2014.
- [18] Zhou Y, Boudreau DM, Freedman AN. Trends in the use of aspirin and nonsteroidal anti-inflammatory drugs in the general U.S. population. *Pharmacoepidemiol Drug Saf* 2014;23:43–50.
- [19] Friedewald VE, Bennett JS, Christo JP, Pool JL, Scheiman JM, Simon LS, et al. AJC Editor’s consensus: Selective and nonselective nonsteroidal anti-inflammatory drugs and cardiovascular risk. *Am J Cardiol* 2010;106:873–84.
- [20] Canada G of. *Canadians in Context - Aging Population 2015*.
- [21] Seeman E. Modelling and remodelling: the cellular machinery responsible for the gain and loss of bone’s material and structural strength. In: Bilezikian J, editor. *Princ. Bone Biol*. 3rd ed., San Diego, CA: Academic Press; 2008, p. 3–28.
- [22] Bruce M, Burr D, Sharkey N. *Skeletal Tissue Mechanics*. New York: Springer-Verlag; 1998.
- [23] Fritton SP, Weinbaum S. Fluid and solute transport in bone: flow-induced mechanotransduction. *Annu Rev Fluid Mech* 2009;41:347–74.
- [24] Baron R, Tross R, Vignery A. Evidence of sequential remodeling in rat trabecular bone: morphology, dynamic histomorphometry, and changes during skeletal maturation. *Anat Rec* 1984;208:137–45.
- [25] Martiniakova M, Omelka R, Grosskopf B, Mokosova Z, Toman R. Histological analysis of compact bone tissue in adult laboratory rats. *Slovak J Anim Sci* 2009;42:56–9.
- [26] Chapter 6: *Bones and Skeletal Tissue* n.d.
- [27] Frost HM. Bone “mass” and the “mechanostat”: a proposal. *Anat Rec* 1987;219:1–9.
- [28] Lee EJ, Long KA, Risser WL, Poindexter HB, Gibbons WE, Goldzieher J. Variations in bone status of contralateral and regional sites in young athletic women. *Med Sci Sports Exerc* 1995;27:1354–61.
- [29] Torrance AG, Mosley JR, Suswillo RF, Lanyon LE. Noninvasive loading of the rat ulna in vivo induces a strain-related modeling response uncomplicated by trauma or periosteal pressure. *Calcif Tissue Int* 1994;54:241–7.
- [30] Nakashima T, Hayashi M, Fukunaga T, Kurata K, Oh-Hora M, Feng JQ, et al. Evidence for osteocyte regulation of bone homeostasis through RANKL expression. *Nat Med* 2011;17:1231–4.
- [31] Nijweide P, Burger E, Klein-Nulend J. The Osteocyte. In: Bilezikian J, editor. *Princ. Bone Biol*. 2nd ed., San Diego, CA: Academic Press; 2002, p. 93–107.
- [32] Liu C, Zhao Y, Cheung WY, Gandhi R, Wang L, You L. Effects of cyclic hydraulic pressure on osteocytes. *Bone* 2010;46:1449–56.
- [33] Klein-Nulend J, van der Plas A, Semeins CM, Ajubi NE, Frangos JA, Nijweide PJ, et al. Sensitivity of osteocytes to biomechanical stress in vitro. *FASEB J* 1995;9:441–5.
- [34] Cowin SC, Weinbaum S, Zeng Y. A case for bone canaliculi as the anatomical site of strain generated potentials. *J Biomech* 1995;28:1281–97.

- [35] You L, Cowin SC, Schaffler MB, Weinbaum S. A model for strain amplification in the actin cytoskeleton of osteocytes due to fluid drag on pericellular matrix. *J Biomech* 2001;34:1375–86.
- [36] Schaffler MB, Cheung WY, Majeska R, Kennedy O. Osteocytes: Master orchestrators of bone. *Calcif Tissue Int* 2014;94:5–24.
- [37] Cherian PP, Siller-Jackson AJ, Gu S, Wang X, Bonewald LF, Sprague E, et al. Mechanical strain opens connexin 43 hemichannels in osteocytes: a novel mechanism for the release of prostaglandin. *Mol Biol Cell* 2005;16:3100–6.
- [38] Burger E. Experiments on cell mechanosensitivity: bone cells as mechanical engineers. In: Cowin S, editor. *Bone Mech. Handb.*, Boca Raton, Florida: CRC Press LLC; 2001, p. 1–16.
- [39] Bao G. Protein mechanics: A new frontier in biomechanics. *Exp Mech* 2009;49:153–64.
- [40] Jacobs CR, Temiyasathit S, Castillo AB. Osteocyte mechanobiology and pericellular mechanics. *Annu Rev Biomed Eng* 2010;12:369–400.
- [41] Hung CT, Allen FD, Pollack SR, Brighton CT. What is the role of the convective current density in the real-time calcium response of cultured bone cells to fluid flow? *J Biomech* 1996;29:1403–9.
- [42] Kotha SP, Hsieh Y-F, Strigel RM, Müller R, Silva MJ. Experimental and finite element analysis of the rat ulnar loading model-correlations between strain and bone formation following fatigue loading. *J Biomech* 2004;37:541–8.
- [43] Robling AG, Hinant FM, Burr DB, Turner CH. Improved bone structure and strength after long-term mechanical loading is greatest if loading is separated into short bouts. *J Bone Miner Res* 2002;17:1545–54.
- [44] Turner CH. Three rules for bone adaptation to mechanical stimuli. *Bone* 1998;23:399–407.
- [45] Robling AG, Castillo AB, Turner CH. Biomechanical and molecular regulation of bone remodeling. *Annu Rev Biomed Eng* 2006;8:455–98.
- [46] Lanyon LE, Rubin CT. Static vs dynamic loads as an influence on bone remodelling. *J Biomech* 1984;17:897–905.
- [47] Warden SJ, Turner CH. Mechanotransduction in the cortical bone is most efficient at loading frequencies of 5-10 Hz. *Bone* 2004;34:261–70.
- [48] Robling AG, Burr DB, Turner CH. Recovery periods restore mechanosensitivity to dynamically loaded bone. *J Exp Biol* 2001;204:3389–99.
- [49] Srinivasan S, Weimer DA, Agans SC, Bain SD, Gross TS. Low-magnitude mechanical loading becomes osteogenic when rest is inserted between each load cycle. *J Bone Miner Res* 2002;17:1613–20.
- [50] Schrieffer JL, Warden SJ, Saxon LK, Robling AG, Turner CH. Cellular accommodation and the response of bone to mechanical loading. *J Biomech* 2005;38:1838–45.
- [51] Saxon LK, Robling AG, Alam I, Turner CH. Mechanosensitivity of the rat skeleton decreases after a long period of loading, but is improved with time off. *Bone* 2005;36:454–64.

- [52] Hsieh YF, Robling a G, Ambrosius WT, Burr DB, Turner CH. Mechanical loading of diaphyseal bone in vivo: the strain threshold for an osteogenic response varies with location. *J Bone Miner Res* 2001;16:2291–7.
- [53] Saxon LK, Lanyon LE. Assessment of the in vivo adaptive response to mechanical loading. *Methods Mol Biol* 2008;455:307–22.
- [54] Mosley JR, March BM, Lynch J, Lanyon LE. Strain magnitude related changes in whole bone architecture in growing rats. *Bone* 1997;20:191–8.
- [55] Uthgenannt BA, Kramer MH, Hwu JA, Wopenka B, Silva MJ. Skeletal self-repair: stress fracture healing by rapid formation and densification of woven bone. *J Bone Miner Res* 2007;22:1548–56.
- [56] McKenzie J a, Silva MJ. Comparing histological, vascular and molecular responses associated with woven and lamellar bone formation induced by mechanical loading in the rat ulna. *Bone* 2011;48:250–8.
- [57] Zaman G, Sunters A, Galea GL, Javaheri B, Saxon LK, Moustafa A, et al. Loading-related regulation of transcription factor EGR2/Krox-20 in bone cells is ERK1/2 protein-mediated and prostaglandin, Wnt signaling pathway-, and insulin-like growth factor-I axis-dependent. *J Biol Chem* 2012;287:3946–62.
- [58] Zaman G, Saxon LK, Sunters A, Hilton H, Underhill P, Williams D, et al. Loading-related regulation of gene expression in bone in the contexts of estrogen deficiency, lack of estrogen receptor alpha and disuse. *Bone* 2010;46:628–42.
- [59] Mantila Roosa SM, Liu Y, Turner CH. Gene expression patterns in bone following mechanical loading. *J Bone Miner Res* 2011;26:100–12.
- [60] Burger EH, Klein-Nulend J. Responses of bone cells to biomechanical forces in vitro. *Adv Dent Res* 1999;13:93–8.
- [61] Kamioka H, Kameo Y, Imai Y, Bakker AD, Bacabac RG, Yamada N, et al. Microscale fluid flow analysis in a human osteocyte canaliculus using a realistic high-resolution image-based three-dimensional model. *Integr Biol (Camb)* 2012;4:1198–206.
- [62] Weinbaum S, Cowin SC, Zeng Y. A model for the excitation of osteocytes by mechanical loading-induced bone fluid shear stresses. *J Biomech* 1994;27:339–60.
- [63] Jacobs CR, Yellowley CE, Davis BR, Zhou Z, Cimbala JM, Donahue HJ. Differential effect of steady versus oscillating flow on bone cells. *J Biomech* 1998;31:969–76.
- [64] Wang L, Cowin SC, Weinbaum S, Fritton SP. Modeling tracer transport in an osteon under cyclic loading. *Ann Biomed Eng* 2000;28:1200–9.
- [65] Turner CH, Yoshikawa T, Forwood MR, Sun TC, Burr DB. High frequency components of bone strain in dogs measured during various activities. *J Biomech* 1995;28:39–44.
- [66] Li J, Rose E, Frances D, Sun Y, You L. Effect of oscillating fluid flow stimulation on osteocyte mRNA expression. *J Biomech* 2012;45:247–51.
- [67] Liu X, Zhang X, Lee I. A quantitative study on morphological responses of osteoblastic cells to fluid shear stress. *Acta Biochim Biophys Sin (Shanghai)* 2010;42:195–201.

- [68] Bacabac RG, Smit TH, Mullender MG, Dijcks SJ, Van Loon JJWA, Klein-Nulend J. Nitric oxide production by bone cells is fluid shear stress rate dependent. *Biochem Biophys Res Commun* 2004;315:823–9.
- [69] You L, Temiyasathit S, Lee P, Kim CH, Tummala P, Yao W, et al. Osteocytes as mechanosensors in the inhibition of bone resorption due to mechanical loading. *Bone* 2008;42:172–9.
- [70] Kim CH, You L, Yellowley CE, Jacobs CR. Oscillatory fluid flow-induced shear stress decreases osteoclastogenesis through RANKL and OPG signaling. *Bone* 2006;39:1043–7.
- [71] Xia X, Batra N, Shi Q, Bonewald LF, Sprague E, Jiang JX. Prostaglandin promotion of osteocyte gap junction function through transcriptional regulation of connexin 43 by glycogen synthase kinase 3/beta-catenin signaling. *Mol Cell Biol* 2010;30:206–19.
- [72] Cheng B, Zhao S, Luo J, Sprague E, Bonewald LF, Jiang JX. Expression of functional gap junctions and regulation by fluid flow in osteocyte-like MLO-Y4 cells. *J Bone Miner Res* 2001;16:249–59.
- [73] Lu XL, Huo B, Park M, Guo XE. Calcium response in osteocytic networks under steady and oscillatory fluid flow. *Bone* 2012;51:466–73.
- [74] Xu H, Zhang J, Wu J, Guan Y, Weng Y, Shang P. Oscillatory fluid flow elicits changes in morphology, cytoskeleton and integrin-associated molecules in MLO-Y4 cells, but not in MC3T3-E1 cells. *Biol Res* 2012;45:163–9.
- [75] Jeon OH, Yoo Y-M, Kim KH, Jacobs CR, Kim CH. Primary cilia-mediated osteogenic response to fluid flow occurs via increases in focal adhesion and Akt signaling pathway in MC3T3-E1 osteoblastic cells. *Cell Mol Bioeng* 2011;4:379–88.
- [76] Klein-Nulend J. Pulsating fluid flow stimulates prostaglandin release and inducible prostaglandin G/H synthase mRNA expression in primary mouse bone cells. *J Bone Miner Res* 1997;12:45–51.
- [77] Worton LE, Ausk BJ, Downey LM, Bain SD, Gardiner EM, Srinivasan S, et al. Systems-based identification of temporal processing pathways during bone cell mechanotransduction. *PLoS One* 2013;8:e74205.
- [78] Blackwell K, Raisz LG, Pilbeam CC. Prostaglandins in bone: bad cop, good cop? *Trends Endocrinol Metab* 2010;21:294–301.
- [79] Pilbeam C, Harrison J, Raisz L. Prostaglandins and bone metabolism. In: Bilezikian J, Raisz L, Rodan G, editors. *Princ. Bone Biol.* 2nd ed., New York: Academic Press; 2002, p. 979–94.
- [80] Weinreb M, Kelner A, Keila S. Inhibition of cyclo-oxygenase-2 activity does not abolish the anabolic effect of prostaglandin E2 in vivo or in vitro. *J Endocrinol* 2002;174:127–35.
- [81] Li L, Pettit AR, Gregory LS, Forwood MR. Regulation of bone biology by prostaglandin endoperoxide H synthases (PGHS): a rose by any other name... *Cytokine Growth Factor Rev* 2006;17:203–16.

- [82] Rawlinson SC, el-Haj AJ, Minter SL, Tavares IA, Bennett A, Lanyon LE. Loading-related increases in prostaglandin production in cores of adult canine cancellous bone in vitro: a role for prostacyclin in adaptive bone remodeling? *J Bone Miner Res* 1991;6:1345–51.
- [83] Pavalko FM, Chen NX, Turner CH, Burr DB, Atkinson S, Hsieh YF, et al. Fluid shear-induced mechanical signaling in MC3T3-E1 osteoblasts requires cytoskeleton-integrin interactions. *Am J Physiol* 1998;275:C1591-601.
- [84] Turner CH, Pavalko FM. Mechanotransduction and functional response of the skeleton to physical stress: the mechanisms and mechanics of bone adaptation. *J Orthop Sci* 1998;3:346–55.
- [85] Ajubi NE, Klein-Nulend J, Alblas MJ, Burger EH, Nijweide PJ. Signal transduction pathways involved in fluid flow-induced PGE2 production by cultured osteocytes. *Am J Physiol* 1999;276:E171-8.
- [86] Saunders MM, You J, Zhou Z, Li Z, Yellowley CE, Kunze EL, et al. Fluid flow-induced prostaglandin E2 response of osteoblastic ROS 17/2.8 cells is gap junction-mediated and independent of cytosolic calcium. *Bone* 2003;32:350–6.
- [87] Hughes-Fulford M. Signal transduction and mechanical stress. *Sci STKE* 2004;2004:RE12.
- [88] McGarry JG, Klein-Nulend J, Prendergast PJ. The effect of cytoskeletal disruption on pulsatile fluid flow-induced nitric oxide and prostaglandin E2 release in osteocytes and osteoblasts. *Biochem Biophys Res Commun* 2005;330:341–8.
- [89] Haugh MG, Vaughan TJ, McNamara LM. The role of integrin  $\alpha$ V $\beta$ 3 in osteocyte mechanotransduction. *J Mech Behav Biomed Mater* 2015;42:67–75.
- [90] Kawata A, Mikuni-Takagaki Y. Mechanotransduction in stretched osteocytes--temporal expression of immediate early and other genes. *Biochem Biophys Res Commun* 1998;246:404–8.
- [91] Nakagawa N, Yasuda H, Yano K, Mochizuki S i, Kobayashi N, Fujimoto H, et al. Basic fibroblast growth factor induces osteoclast formation by reciprocally regulating the production of osteoclast differentiation factor and osteoclastogenesis inhibitory factor in mouse osteoblastic cells. *Biochem Biophys Res Commun* 1999;265:158–63.
- [92] Pilbeam CC, Kawaguchi H, Hakeda Y, Voznesensky O, Alander CB, Raisz LG. Differential regulation of inducible and constitutive prostaglandin endoperoxide synthase in osteoblastic MC3T3-E1 cells. *J Biol Chem* 1993;268:25643–9.
- [93] Murakami M, Kuwata H, Amakasu Y, Shimbara S, Nakatani Y, Atsumi G, et al. Prostaglandin E2 amplifies cytosolic phospholipase A2- and cyclooxygenase-2-dependent delayed prostaglandin E2 generation in mouse osteoblastic cells. Enhancement by secretory phospholipase A2. *J Biol Chem* 1997;272:19891–7.
- [94] Thorsen K, Kristoffersson A. In situ microdialysis in bone tissue stimulation of prostaglandin E2 release by weight-bearing mechanical loading. *J Clin Invest* 1996;2:2–5.

- [95] Westbroek I, Ajubi NE, Alblas MJ, Semeins CM, Klein-Nulend J, Burger EH, et al. Differential stimulation of prostaglandin G/H synthase-2 in osteocytes and other osteogenic cells by pulsating fluid flow. *Biochem Biophys Res Commun* 2000;268:414–9.
- [96] Wadhwa S, Godwin SL, Peterson DR, Epstein MA, Raisz LG, Pilbeam CC. Fluid flow induction of cyclo-oxygenase 2 gene expression in osteoblasts is dependent on an extracellular signal-regulated kinase signaling pathway. *J Bone Miner Res* 2002;17:266–74.
- [97] Chen QR, Miyaura C, Higashi S, Murakami M, Kudo I, Saito S, et al. Activation of cytosolic phospholipase A2 by platelet-derived growth factor is essential for cyclooxygenase-2-dependent prostaglandin E2 synthesis in mouse osteoblasts cultured with interleukin-1. *J Biol Chem* 1997;272:5952–8.
- [98] Murakami M, Kambe T, Shimbara S, Kudo I. Functional coupling between various phospholipase A2s and cyclooxygenases in immediate and delayed prostanoid biosynthetic pathways. *J Biol Chem* 1999;274:3103–15.
- [99] Rochefort GY, Pallu S, Benhamou CL. Osteocyte: the unrecognized side of bone tissue. *Osteoporos Int* 2010;21:1457–69.
- [100] Liu X-H, Kirschenbaum A, Weinstein BM, Zaidi M, Yao S, Levine AC. Prostaglandin E2 modulates components of the Wnt signaling system in bone and prostate cancer cells. *Biochem Biophys Res Commun* 2010;394:715–20.
- [101] Bonewald LF, Johnson ML. Osteocytes, mechanosensing and Wnt signaling. *Bone* 2008;42:606–15.
- [102] Cherian PP, Cheng B, Gu S, Sprague E, Bonewald LF, Jiang JX. Effects of mechanical strain on the function of gap junctions in osteocytes are mediated through the prostaglandin EP2 receptor. *J Biol Chem* 2003;278:43146–56.
- [103] Lara-Castillo N, Kim-Weroha N a., Kamel M a., Javaheri B, Ellies DL, Krumlauf RE, et al. In vivo mechanical loading rapidly activates  $\beta$ -catenin signaling in osteocytes through a prostaglandin mediated mechanism. *Bone* 2015;76:58–66.
- [104] Huang C, Ogawa R. Mechanotransduction in bone repair and regeneration. *FASEB J* 2010;24:3625–32.
- [105] Lau E, Al-Dujaili S, Guenther A, Liu D, Wang L, You L. Effect of low-magnitude, high-frequency vibration on osteocytes in the regulation of osteoclasts. *Bone* 2010;46:1508–15.
- [106] Sawakami K, Robling AG, Ai M, Pitner ND, Liu D, Warden SJ, et al. The Wnt co-receptor LRP5 is essential for skeletal mechanotransduction but not for the anabolic bone response to parathyroid hormone treatment. *J Biol Chem* 2006;281:23698–711.
- [107] Ogasawara A, Arakawa T, Kaneda T, Takuma T, Sato T, Kaneko H, et al. Fluid shear stress-induced cyclooxygenase-2 expression is mediated by C/EBP $\gamma$ , cAMP-response element-binding protein, and AP-1 in osteoblastic MC3T3-E1 cells. *J Biol Chem* 2000;276:7048–54.
- [108] Pilbeam CC, Raisz LG, Voznesensky O, Alander CB, Delman BN, Kawaguchi H. Autoregulation of inducible prostaglandin G/H synthase in osteoblastic cells by prostaglandins. *J Bone Miner Res* 1995;10:406–14.

- [109] Weinreb M, Machwate M, Shir N, Abramovitz M, Rodan GA, Harada S. Expression of the prostaglandin E(2) (PGE(2)) receptor subtype EP(4) and its regulation by PGE(2) in osteoblastic cell lines and adult rat bone tissue. *Bone* 2001;28:275–81.
- [110] Raisz LG. Prostaglandins and bone: physiology and pathophysiology. *Osteoarthritis Cartilage* 1999;7:419–21.
- [111] Akhter MP, Cullen DM, Gong G, Recker RR. Bone biomechanical properties in prostaglandin EP1 and EP2 knockout mice. *Bone* 2001;29:121–5.
- [112] Akhter MP, Cullen DM, Pan LC. Bone biomechanical properties in EP4 knockout mice. *Calcif Tissue Int* 2006;78:357–62.
- [113] Jee WS, Ma YF. The in vivo anabolic actions of prostaglandins in bone. *Bone* 1997;21:297–304.
- [114] Jee W, Zhu KH, Jian LX. Long-term anabolic effects of prostaglandin-E , on tibial diaphyseal bone in male rats. *Bone Miner* 1991;15:33–55.
- [115] Yao W, Jee WS, Zhou H, Lu J, Cui L, Setterberg R, et al. Anabolic effect of prostaglandin E2 on cortical bone of aged male rats comes mainly from modeling-dependent bone gain. *Bone* 1999;25:697–702.
- [116] Ke HZ, Li XJ, Jee WS. Partial loss of anabolic effect of prostaglandin E2 on bone after its withdrawal in rats. *Bone* 1991;12:173–83.
- [117] Saponitzki I, Weinreb M. Differential anabolic effects of PGE2 in long bones and calvariae of young rats. *J Endocrinol* 1998;156:51–7.
- [118] Keila S, Kelner A, Weinreb M. Systemic prostaglandin E2 increases cancellous bone formation and mass in aging rats and stimulates their bone marrow osteogenic capacity in vivo and in vitro. *J Endocrinol* 2001;168:131–9.
- [119] Ramirez-yanez GO, Symons AL. Prostaglandin E2 affects osteoblast biology in a dose-dependent manner: An in vitro study. *Arch Oral Biol* 2012;57:1274–81.
- [120] Ramirez-Yañez GO, Seymour GJ, Walsh LJ, Forwood MR, Symons AL. Prostaglandin E2 enhances alveolar bone formation in the rat mandible. *Bone* 2004;35:1361–8.
- [121] Quinn JM, Sabokbar A, Denne M, de Vernejoul MC, McGee JO, Athanasou NA. Inhibitory and stimulatory effects of prostaglandins on osteoclast differentiation. *Calcif Tissue Int* 1997;60:63–70.
- [122] Fujita D, Yamashita N, Iita S, Amano H, Yamada S, Sakamoto K. Prostaglandin E2 induced the differentiation of osteoclasts in mouse osteoblast-depleted bone marrow cells. *Prostaglandins Leukot Essent Fatty Acids* 2003;68:351–8.
- [123] Tian XY, Zhang Q, Zhao R, Setterberg RB, Zeng QQ, Iturria SJ, et al. Continuous PGE2 leads to net bone loss while intermittent PGE2 leads to net bone gain in lumbar vertebral bodies of adult female rats. *Bone* 2008;42:914–20.
- [124] Gao Q, Xu M, Alander CB, Choudhary S, Pilbeam CC, Raisz LG. Effects of prostaglandin E2 on bone in mice in vivo. *Prostaglandins Other Lipid Mediat* 2009;89:20–5.
- [125] Golde B. New clues into the etiology of osteoporosis: The effects of prostaglandins (E2 and F2a) on bone. *Med Hypotheses* 1991;38:125–31.

- [126] Weinreb M, Rutledge SJ, Rodan GA. Systemic administration of an anabolic dose of prostaglandin E2 induces early-response genes in rat bones. *Bone* 1997;20:347–53.
- [127] Weinreb M, Suponitzky I, Keila S. Systemic administration of an anabolic dose of PGE2 in young rats increases the osteogenic capacity of bone marrow. *Bone* 1997;20:521–6.
- [128] Suda M, Tanaka K, Sakuma Y, Yasoda a, Ozasa a, Fukata J, et al. Prostaglandin E(2) (PGE(2)) induces the c-fos and c-jun expressions via the EP(1) subtype of PGE receptor in mouse osteoblastic MC3T3-E1 cells. *Calcif Tissue Int* 2000;66:217–23.
- [129] Liu X-H, Kirschenbaum A, Yao S, Levine AC. Cross-talk between the interleukin-6 and prostaglandin E(2) signaling systems results in enhancement of osteoclastogenesis through effects on the osteoprotegerin/receptor activator of nuclear factor-kappaB (RANK) ligand/RANK system. *Endocrinology* 2005;146:1991–8.
- [130] Okuda a, Taylor LM, Heersche JN. Prostaglandin E2 initially inhibits and then stimulates bone resorption in isolated rabbit osteoclast cultures. *Bone Miner* 1989;7:255–66.
- [131] Han SY, Lee NK, Kim KH, Jang IW, Yim M, Kim JH, et al. Transcriptional induction of cyclooxygenase-2 in osteoclast precursors is involved in RANKL-induced osteoclastogenesis. *Blood* 2005;106:1240–5.
- [132] Luong C, Miller A, Barnett J, Chow J, Ramesha C, Browner MF. Flexibility of the NSAID binding site in the structure of human cyclooxygenase-2. *Nat Struct Biol* 1996;3:927–33.
- [133] Gierse JK, Hauser SD, Creely DP, Koboldt C, Rangwala SH, Isakson PC, et al. Expression and selective inhibition of the constitutive and inducible forms of human cyclo-oxygenase. *Biochem J* 1995;305 ( Pt 2:479–84.
- [134] Gierse JK, Koboldt CM, Walker MC, Seibert K, Isakson PC. Kinetic basis for selective inhibition of cyclo-oxygenases. *Biochem J* 1999;339:607–14.
- [135] Walker MC, Kurumbail RG, Kiefer JR, Moreland KT, Koboldt CM, Isakson PC, et al. A three-step kinetic mechanism for selective inhibition of cyclo-oxygenase-2 by diarylheterocyclic inhibitors. *Biochem J* 2001;357:709–18.
- [136] Kalgutkar AS, Daniels JS. Carboxylic acids and their bioisosteres. In: Smith DA, editor. *Metab. Pharmacokinet. Toxic. Funct. Groups*, Cambridge: RSC Publishing; 2010, p. 103–6.
- [137] Ouellet M, Percival MD. Effect of inhibitor time-dependency on selectivity towards cyclooxygenase isoforms. *Biochem J* 1995;306 ( Pt 1:247–51.
- [138] Mengle-Gaw LJ, Schwartz BD. Cyclooxygenase-2 inhibitors: promise or peril? *Mediators Inflamm* 2002;11:275–86.
- [139] Brideau C, Kargman S, Liu S, Dallob AL, Ehrich EW, Rodger IW, et al. A human whole blood assay for clinical evaluation of biochemical efficacy of cyclooxygenase inhibitors. *Inflamm Res* 1996;45:68–74.

- [140] Masferrer JL, Zweifel BS, Manning PT, Hauser SD, Leahy KM, Smith WG, et al. Selective inhibition of inducible cyclooxygenase 2 in vivo is antiinflammatory and nonulcerogenic. *Proc Natl Acad Sci U S A* 1994;91:3228–32.
- [141] Schwartz B. COX-2 inhibitors: a safer class of drugs for inflammatory pain. Novel targets in the treatment of pain. *Int. Bus. Commun. Compend.*, Southborough, Massachusetts: 1997.
- [142] Feldman M, McMahon AT. Do cyclooxygenase-2 inhibitors provide benefits similar to those of traditional nonsteroidal anti-inflammatory drugs, with less gastrointestinal toxicity? *Ann Intern Med* 2000;132:134–43.
- [143] Masferrer JL, Zweifel BS, Seibert K, Needleman P. Selective regulation of cellular cyclooxygenase by dexamethasone and endotoxin in mice. *J Clin Invest* 1990;86:1375–9.
- [144] Chang J-K, Wang G-J, Tsai S-T, Ho M-L. Nonsteroidal anti-inflammatory drug effects on osteoblastic cell cycle, cytotoxicity, and cell death. *Connect Tissue Res* 2005;46:200–10.
- [145] Chang J-K, Li C-J, Wu S-C, Yeh C-H, Chen C-H, Fu Y-C, et al. Effects of anti-inflammatory drugs on proliferation, cytotoxicity and osteogenesis in bone marrow mesenchymal stem cells. *Biochem Pharmacol* 2007;74:1371–82.
- [146] Ho ML, Chang JK, Chuang LY, Hsu HK, Wang GJ. Effects of nonsteroidal anti-inflammatory drugs and prostaglandins on osteoblastic functions. *Biochem Pharmacol* 1999;58:983–90.
- [147] Chang JK, Li CJ, Liao HJ, Wang CK, Wang GJ, Ho ML. Anti-inflammatory drugs suppress proliferation and induce apoptosis through altering expressions of cell cycle regulators and pro-apoptotic factors in cultured human osteoblasts. *Toxicology* 2009;258:148–56.
- [148] Evans CE, Butcher C. The influence on human osteoblasts in vitro of non-steroidal anti-inflammatory drugs which act on different cyclooxygenase enzymes. *J Bone Joint Surg Br* 2004;86:444–9.
- [149] Kellinsalmi M, Parikka V, Risteli J, Hentunen T, Leskelä H-V, Lehtonen S, et al. Inhibition of cyclooxygenase-2 down-regulates osteoclast and osteoblast differentiation and favours adipocyte formation in vitro. *Eur J Pharmacol* 2007;572:102–10.
- [150] Pountos I, Giannoudis P V, Jones E, English A, Churchman S, Field S, et al. NSAIDs inhibit in vitro MSC chondrogenesis but not osteogenesis: implications for mechanism of bone formation inhibition in man. *J Cell Mol Med* 2011;15:525–34.
- [151] Fujimori A, Tsutsumi M, Fukase M, Fujita T. Cyclooxygenase inhibitors enhance cell growth in an osteoblastic cell line, MC3T3-E1. *J Bone Miner Res* 1989;4:697–704.
- [152] Lerner U. Indomethacin inhibits bone resorption in vitro without affecting bone collagen synthesis. *Agents Actions* 1982;12:466–70.
- [153] Kawashima M, Fujikawa Y, Itonaga I, Takita C, Tsumura H. The effect of selective cyclooxygenase-2 inhibitor on human osteoclast precursors to influence osteoclastogenesis in vitro. *Mod Rheumatol* 2009;19:192–8.

- [154] Igarashi K, Woo J-T, Stern PH. Effects of a selective cyclooxygenase-2 inhibitor, celecoxib, on bone resorption and osteoclastogenesis in vitro. *Biochem Pharmacol* 2002;63:523–32.
- [155] Liu Y, Cui Y, Chen Y, Gao X, Su Y, Cui L. Effects of dexamethasone, celecoxib, and methotrexate on the histology and metabolism of bone tissue in healthy Sprague Dawley rats. *Clin Interv Aging* 2015;10:1245–53.
- [156] Tsuji S, Tomita T, Nakase T, Hamada M, Kawai H, Yoshikawa H. Celecoxib, a selective cyclooxygenase-2 inhibitor, reduces level of a bone resorption marker in postmenopausal women with rheumatoid arthritis. *Int J Rheum Dis* 2014;17:44–9.
- [157] Kasukawa Y, Miyakoshi N, Srivastava AK, Nozaka K, Maekawa S, Baylink DJ, et al. The selective cyclooxygenase-2 inhibitor celecoxib reduces bone resorption, but not bone formation, in ovariectomized mice in vivo. *Tohoku J Exp Med* 2007;211:275–83.
- [158] Yoon DS, Yoo JH, Kim YH, Paik S, Han CD, Lee JW. The effects of COX-2 inhibitor during osteogenic differentiation of bone marrow-derived human mesenchymal stem cells. *Stem Cells Dev* 2010;19:1523–33.
- [159] Bauer DC, Orwoll ES, Fox KM, Vogt TM, Lane NE, Hochberg MC, et al. Aspirin and NSAID use in older women: effect on bone mineral density and fracture risk. Study of Osteoporotic Fractures Research Group. *J Bone Miner Res* 1996;11:29–35.
- [160] Carbone LD, Tylavsky FA, Cauley JA, Harris TB, Lang TF, Bauer DC, et al. Association between bone mineral density and the use of nonsteroidal anti-inflammatory drugs and aspirin: impact of cyclooxygenase selectivity. *J Bone Miner Res* 2003;18:1795–802.
- [161] Richards JB, Joseph L, Schwartzman K, Kreiger N, Tenenhouse a, Goltzman D. The effect of cyclooxygenase-2 inhibitors on bone mineral density: results from the Canadian Multicentre Osteoporosis Study. *Osteoporos Int* 2006;17:1410–9.
- [162] Cauley JA, Fullman RL, Stone KL, Zmuda JM, Bauer DC, Barrett-Connor E, et al. Factors associated with the lumbar spine and proximal femur bone mineral density in older men. *Osteoporos Int* 2005;16:1525–37.
- [163] Morton DJ, Barrett-Connor EL, Schneider DL. Nonsteroidal anti-inflammatory drugs and bone mineral density in older women: the Rancho Bernardo study. *J Bone Miner Res* 1998;13:1924–31.
- [164] Vestergaard P, Rejnmark L, Mosekilde L. Fracture risk associated with use of nonsteroidal anti-inflammatory drugs, acetylsalicylic acid, and acetaminophen and the effects of rheumatoid arthritis and osteoarthritis. *Calcif Tissue Int* 2006;79:84–94.
- [165] Brunner RL, Gass M, Aragaki A, Hays J, Granek I, Woods N, et al. Effects of conjugated equine estrogen on health-related quality of life in postmenopausal women with hysterectomy: results from the Women’s Health Initiative Randomized Clinical Trial. *Arch Intern Med* 2005;165:1976–86.

- [166] Cauley JA, Blackwell T, Zmuda JM, Fullman RL, Ensrud KE, Stone KL, et al. Correlates of trabecular and cortical volumetric bone mineral density at the femoral neck and lumbar spine: the osteoporotic fractures in men study (MrOS). *J Bone Miner Res* 2010;25:1958–71.
- [167] van Staa TP, Leufkens HG, Cooper C. Use of nonsteroidal anti-inflammatory drugs and risk of fractures. *Bone* 2000;27:563–8.
- [168] Vestergaard P, Hermann P, Jensen J-EB, Eiken P, Mosekilde L. Effects of paracetamol, non-steroidal anti-inflammatory drugs, acetylsalicylic acid, and opioids on bone mineral density and risk of fracture: results of the Danish Osteoporosis Prevention Study (DOPS). *Osteoporos Int* 2012;23:1255–65.
- [169] Bakker a. D, Klein-Nulend J, Burger EH. Mechanotransduction in bone cells proceeds via activation of COX-2, but not COX-1. *Biochem Biophys Res Commun* 2003;305:677–83.
- [170] Cunningham D. Ibuprofen administered pre- or post- simulated resistance exercise training does not diminish gains in bone formation or bone mass. Texas A&M University, 2011.
- [171] Duff W, Kontulainen S, Rooke J, Taylor-Gievre R, Nair B, Szafron M, et al. Effect of ibuprofen and exercise training on bone, body composition, and strength in older women. *Am. Coll. Sport. Med. San Diego, CA*, 2015.
- [172] Li J, Norvell S, Ponik S, Pavalko F, Burr D, Turner C. Relationship between prostaglandins and cyclooxygenase- 2 in response to mechanical stimuli and their role in load- induced bone formation. *J Bone Miner Res* 2001;16:S482.
- [173] Brighton CT, Fisher JR, Levine SE, Corsetti JR, Reilly T, Landsman a S, et al. The biochemical pathway mediating the proliferative response of bone cells to a mechanical stimulus. *J Bone Joint Surg Am* 1996;78:1337–47.
- [174] Somjen D, Binderman I, Berger E, Harell A. Bone remodelling induced by physical stress is prostaglandin E2 mediated. *Biochim Biophys Acta* 1980;627:91–100.
- [175] Jiang JX, Cheng B. Mechanical stimulation of gap junctions in bone osteocytes is mediated by prostaglandin E2. *Cell Commun Adhes* 2001;8:283–8.
- [176] Lane N, Coble T, Kimmel DB. Effect of naproxen on cancellous bone in ovariectomized rats. *J Bone Miner Res* 1990;5:1029–35.
- [177] Turkozan N, Ulusoy A, Balcioglu H, Bal F, Ozel S. The effects of ovariectomy and naproxen treatment on the strength of femoral midshaft and molar alveolar region in rats. *Int J Morphol* 2009;27:659–66.
- [178] Gregory LS, Kelly WL, Reid RC, Fairlie DP, Forwood MR. Inhibitors of cyclooxygenase-2 and secretory phospholipase A2 preserve bone architecture following ovariectomy in adult rats. *Bone* 2006;39:134–42.
- [179] Jiang Y, Zhao J, Genant HK, Dequeker J, Geusens P. Bone mineral density and biomechanical properties of spine and femur of ovariectomized rats treated with naproxen. *Bone* 1998;22:509–14.
- [180] Kimmel DB, Coble T, Lane N. Long-term effect of naproxen on cancellous bone in ovariectomized rats. *Bone* 1992;13:167–72.

- [181] Saino H, Matsuyama T, Takada J, Kaku T, Ishii S. Long-term treatment of indomethacin reduces vertebral bone mass and strength in ovariectomized rats. *J Bone Miner Res* 1997;12:1844–50.
- [182] Sibonga JD, Bell NH, Turner RT. Evidence that ibuprofen antagonizes selective actions of estrogen and tamoxifen on rat bone. *J Bone Miner Res* 1998;13:863–70.
- [183] Shen C-L, Yeh JK, Rasty J, Li Y, Watkins B a. Protective effect of dietary long-chain n-3 polyunsaturated fatty acids on bone loss in gonad-intact middle-aged male rats. *Br J Nutr* 2006;95:462.
- [184] Boiskin I, Epstein S, Ismail F, Fallon MD, Levy W. Long term administration of prostaglandin inhibitors in vivo fail to influence cartilage and bone mineral metabolism in the rat. *Bone Miner* 1988;4:27–36.
- [185] Martin EA, Ritman EL, Turner RT. Time course of epiphyseal growth plate fusion in rat tibiae. *Bone* 2003;32:261–7.
- [186] Uthgenannt B a, Silva MJ. Use of the rat forelimb compression model to create discrete levels of bone damage in vivo. *J Biomech* 2007;40:317–24.
- [187] Satterwhite JH, Boudinot FD. Effects of age and dose on the pharmacokinetics of ibuprofen in the rat. *Drug Metab Dispos* 1991;19:61–7.
- [188] Paulson SK, Zhang JY, Breau AP, Hribar JD, Liu NW, Jessen SM, et al. Pharmacokinetics, tissue distribution, metabolism, and excretion of celecoxib in rats. *Drug Metab Dispos* 2000;28:514–21.
- [189] Wiseman E, Y N. Limitations of laboratory models in predicting gastrointestinal toleration of oxicams and other anti-inflammtory drugs. In: Rainsford K, Velo G, editors. *Side-Effects Anti-inflamm. Drugs Part Two - Stud. Major Organ Syst.*, England: MTP Press Limited; 1985, p. 41–54.
- [190] Davies NM, McLachlan AJ, Day RO, Williams KM. Clinical pharmacokinetics and pharmacodynamics of celecoxib: a selective cyclo-oxygenase-2 inhibitor. *Clin Pharmacokinet* 2000;38:225–42.
- [191] Waxman DJ, Dannan GA, Guengerich FP. Regulation of rat hepatic cytochrome P-450: age-dependent expression, hormonal imprinting, and xenobiotic inducibility of sex-specific isoenzymes. *Biochemistry* 1985;24:4409–17.
- [192] Kaiser DG, Glenn EM. Plasma ibuprofen levels with biological activity. *J Pharm Sci* 1974;63:784–6.
- [193] Nurfazreen A, Julianto B, Khuriah A. Determination of a poorly soluble drug, ibuprofen in rat plasma by a simple HPLC analysis and its application in pharmacokinetic study. *Int J Pharm Sci Res* 2015;6:96–102.
- [194] Vilenchik R, Berkovitch M, Jossifoff A, Ben-Zvi Z, Kozer E. Oral versus rectal ibuprofen in healthy volunteers. *J Popul Ther Clin Pharmacol* 2012;19:179–86.
- [195] Davies NM. Clinical pharmacokinetics of ibuprofen. The first 30 years. *Clin Pharmacokinet* 1998;34:101–54.
- [196] Bushra R, Aslam N. An overview of clinical pharmacology of Ibuprofen. *Oman Med J* 2010;25:155–1661.
- [197] Bo J, Sudmann E, Marton PF. Effect of indomethacin on fracture healing in rats. *Acta Orthop Scand* 1976;47:588–99.

- [198] Yoshida T, Gomita Y, Oishi R. Effect of cigarette smoke on pharmacokinetics of oral, intrarectal, or intravenous indomethacin in rats. *Naunyn Schmiedebergs Arch Pharmacol* 1991;344:500–4.
- [199] Hucker H, Zacchei A, Cox S, Brodie D, Cantwell N. Studies on the absorption, distribution and excretion of indomethacin in various species. *J Pharmacol Exp Ther* 1966;153:237–49.
- [200] Helleberg L. Clinical pharmacokinetics of indomethacin. *Clin Pharmacokinet* 1981;6:245–58.
- [201] Lucas S. The pharmacology of indomethacin. *Headache* 2016;56:436–46.
- [202] Alván G, Orme M, Bertilsson L, Ekstrand R, Palmér L. Pharmacokinetics of indomethacin. *Clin Pharmacol Ther* 1975;18:364–73.
- [203] Euchenhofer C, Maihöfner C, Brune K, Tegeder I, Geisslinger G. Differential effect of selective cyclooxygenase-2 (COX-2) inhibitor NS 398 and diclofenac on formalin-induced nociception in the rat. *Neurosci Lett* 1998;248:25–8.
- [204] Gilroy DW, Tomlinson A, Willoughby DA. Differential effects of inhibitors of cyclooxygenase (cyclooxygenase 1 and cyclooxygenase 2) in acute inflammation. *Eur J Pharmacol* 1998;355:211–7.
- [205] Elder CL, Dahners LE, Weinhold PS. A cyclooxygenase-2 inhibitor impairs ligament healing in the rat. *Am J Sports Med* 2001;29:801–5.
- [206] Mullis BH, Copland ST, Weinhold PS, Miclau T, Lester GE, Bos GD. Effect of COX-2 inhibitors and non-steroidal anti-inflammatory drugs on a mouse fracture model. *Injury* 2006;37:827–37.
- [207] Rapuano BE, Boursiquot R, Tomin E, MacDonald DE, Maddula S, Raghavan D, et al. The effects of COX-1 and COX-2 inhibitors on prostaglandin synthesis and the formation of heterotopic bone in a rat model. *Arch Orthop Trauma Surg* 2008;128:333–44.
- [208] Hawkey C. COX-2 inhibitors. *Lancet* 1999;353:307–14.
- [209] Huo MH, Troiano NW, Pelker RR, Gundberg CM, Friedlaender GE. The influence of ibuprofen on fracture repair: biomechanical, biochemical, histologic, and histomorphometric parameters in rats. *J Orthop Res* 1991;9:383–90.
- [210] Altman R, Latta L, Keer R, Renfree K, Homicek F, Banovac K. Effect of nonsteroidal antiinflammatory drugs on fracture healing: a laboratory study in rats. *J Orthop Trauma* 1995;9:392–400.
- [211] Kidd LJ, Cowling NR, Wu AC, Kelly WL, Forwood MR. Selective and non-selective cyclooxygenase inhibitors delay stress fracture healing in the rat ulna. *J Orthop Res* 2013;31:235–42.
- [212] Barr SI, McKay HA. Nutrition, exercise, and bone status in youth. *Int J Sport Nutr* 1998;8:124–42.
- [213] van Gaalen SM, Kruyt MC, Geuze RE, de Bruijn JD, Alblas J, Dhert WJA. Use of fluorochrome labels in in vivo bone tissue engineering research. *Tissue Eng Part B Rev* 2010;16:209–17.
- [214] Karakolis T. Mechanical induction of bone formation: comparison between rat and mouse forelimb models. McMaster University, 2009.

- [215] Alam I, Warden SJ, Robling AG, Turner CH. Mechanotransduction in bone does not require a functional cyclooxygenase-2 (COX-2) gene. *J Bone Miner Res* 2004;20:438–46.
- [216] Rissing JP, Buxton TB. Effect of ibuprofen on gross pathology, bacterial count, and levels of prostaglandin E2 in experimental staphylococcal osteomyelitis. *J Infect Dis* 1986;154:627–30.
- [217] Nakayama K, Kodama Y, Fukumoto H, Fuse H, Takahashi H, Kawaguchi H, et al. Mechanical loading induces rapid and transient increase in C-fos expression in tail suspended rat periosteum. *J Bone Miner Res* 1996;11:S150.
- [218] Forwood MR, Kelly WL, Worth NF. Localisation of prostaglandin endoperoxide H synthase (PGHS)-1 and PGHS-2 in bone following mechanical loading in vivo. *Anat Rec* 1998;252:580–6.
- [219] Salvemini D, Seibert K, Masferrer JL, Settle SL, Misko TP, Currie MG, et al. Nitric oxide and the cyclooxygenase pathway. *Adv Prostaglandin Thromboxane Leukot Res* 1995;23:491–3.
- [220] Riviere J. Basic principles and techniques of pharmacokinetic modelling. *J Zoo Wildl Med* 1997;28:3–19.
- [221] Mahmood I, Balian JD. Interspecies scaling: predicting clearance of drugs in humans. Three different approaches. *Xenobiotica* 1996;26:887–95.
- [222] Kirkwood JK. Influence of body size in animals on health and disease. *Vet Rec* 1983;113:287–90.
- [223] Morris TH. Antibiotic therapeutics in laboratory animals. *Lab Anim* 1995;29:16–36.
- [224] Meakin LB, Udeh C, Galea GL, Lanyon LE, Price JS. Exercise does not enhance aged bone's impaired response to artificial loading in C57Bl/6 mice. *Bone* 2015;81:47–52.
- [225] Miyagi M, Morishita M, Iwamoto Y. Effects of sex hormones on production of prostaglandin E2 by human peripheral monocytes. *J Periodontol* 1993;64:1075–8.
- [226] Chillingworth NL, Morham SG, Donaldson LF. Sex differences in inflammation and inflammatory pain in cyclooxygenase-deficient mice. *Am J Physiol Regul Integr Comp Physiol* 2006;291:R327-34.
- [227] Walker JS, Nguyen T V, Day RO. Clinical response to non-steroidal anti-inflammatory drugs in urate-crystal induced inflammation: a simultaneous study of intersubject and intrasubject variability. *Br J Clin Pharmacol* 1994;38:341–7.
- [228] Kawaguchi H, Pilbeam CC, Vargas SJ, Morse EE, Lorenzo JA, Raisz LG. Ovariectomy enhances and estrogen replacement inhibits the activity of bone marrow factors that stimulate prostaglandin production in cultured mouse calvariae. *J Clin Invest* 1995;96:539–48.
- [229] Myers SI. Effect of estrogen on rabbit gallbladder prostaglandin biosynthesis. *J Surg Res* 1985;38:630–4.
- [230] Shoda T, Hatanaka K, Saito M, Majima M, Ogino M, Harada Y, et al. Induction of cyclooxygenase type-2 (COX-2) in rat endometrium at the peak of serum estradiol during the estrus cycle. *Jpn J Pharmacol* 1995;69:289–91.

- [231] Allen MR, Burr DB. Techniques in Histomorphometry. In: Allen MR, Burr DB, editors. *Basic Appl. Bone Biol.*, London: Elsevier; 2014, p. 139.
- [232] Norman SC, Wagner DW, Beaupre GS, Castillo AB. Comparison of three methods of calculating strain in the mouse ulna in exogenous loading studies. *J Biomech* 2015;48:53–8.
- [233] Srinivasan S, Ausk BJ, Poliachik SL, Warner SE, Richardson TS, Gross TS. Rest-inserted loading rapidly amplifies the response of bone to small increases in strain and load cycles. *J Appl Physiol* 2007;102:1945–52.
- [234] Hsieh Y, Turner CH. Effects of Loading Frequency on Mechanically Induced Bone Formation. *J Bone Miner Res* 2001;16:918–24.
- [235] Rubin CT, Lanyon LE. Regulation of bone mass by mechanical strain magnitude. *Calcif Tissue Int* 1985;37:411–7.
- [236] Turner CH, Forwood MR, Rho JY, Yoshikawa T. Mechanical loading thresholds for lamellar and woven bone formation. *J Bone Miner Res* 1994;9:87–97.
- [237] McKenzie JA, Bixby EC, Silva MJ. Differential gene expression from microarray analysis distinguishes woven and lamellar bone formation in the rat ulna following mechanical loading. *PLoS One* 2011;6:e29328.
- [238] Meakin LB, Price JS, Lanyon LE. The contribution of experimental in vivo models to understanding the mechanisms of adaptation to mechanical loading in bone. *Front Endocrinol (Lausanne)* 2014;5:154.
- [239] Robling AG, Burr DB, Turner CH. Skeletal loading in animals. *J Musculoskeletal Neuronal Interact* 2001;1:249–62.
- [240] Albouaini K, Egred M, Alahmar A, Wright DJ. Cardiopulmonary exercise testing and its application. *Postgrad Med J* 2007;83:675–82.
- [241] Cianferotti L, Brandi ML. Muscle-bone interactions: basic and clinical aspects. *Endocrine* 2014;45:165–77.
- [242] Brotto M, Johnson ML. Endocrine crosstalk between muscle and bone. *Curr Osteoporos Rep* 2014;12:135–41.
- [243] Pedersen BK. Special feature for the Olympics: effects of exercise on the immune system: exercise and cytokines. *Immunol Cell Biol* 2000;78:532–5.
- [244] Manolagas SC. Role of cytokines in bone resorption. *Bone* 1995;17:63S–67S.
- [245] Festing MFW, Altman DG. Guidelines for the design and statistical analysis of experiments using laboratory animals. *ILAR J* 2002;43:244–58.
- [246] Faul F, Erdfelder E, Lang A, Buchner A. G\*Power 3: A flexible statistical power analysis program for the social, behavioral, and biomedical sciences. *Behav Res Methods* 2007;39:175–91.
- [247] Wallace BA, Cumming RG. Systematic review of randomized trials of the effect of exercise on bone mass in pre- and postmenopausal women. *Calcif Tissue Int* 2000;67:10–8.
- [248] Charan J, Kantharia ND. How to calculate sample size in animal studies? *J Pharmacol Pharmacother* 2013;4:303–6.
- [249] Mukaka MM. Statistics corner: A guide to appropriate use of correlation coefficient in medical research. *Malawi Med J* 2012;24:69–71.

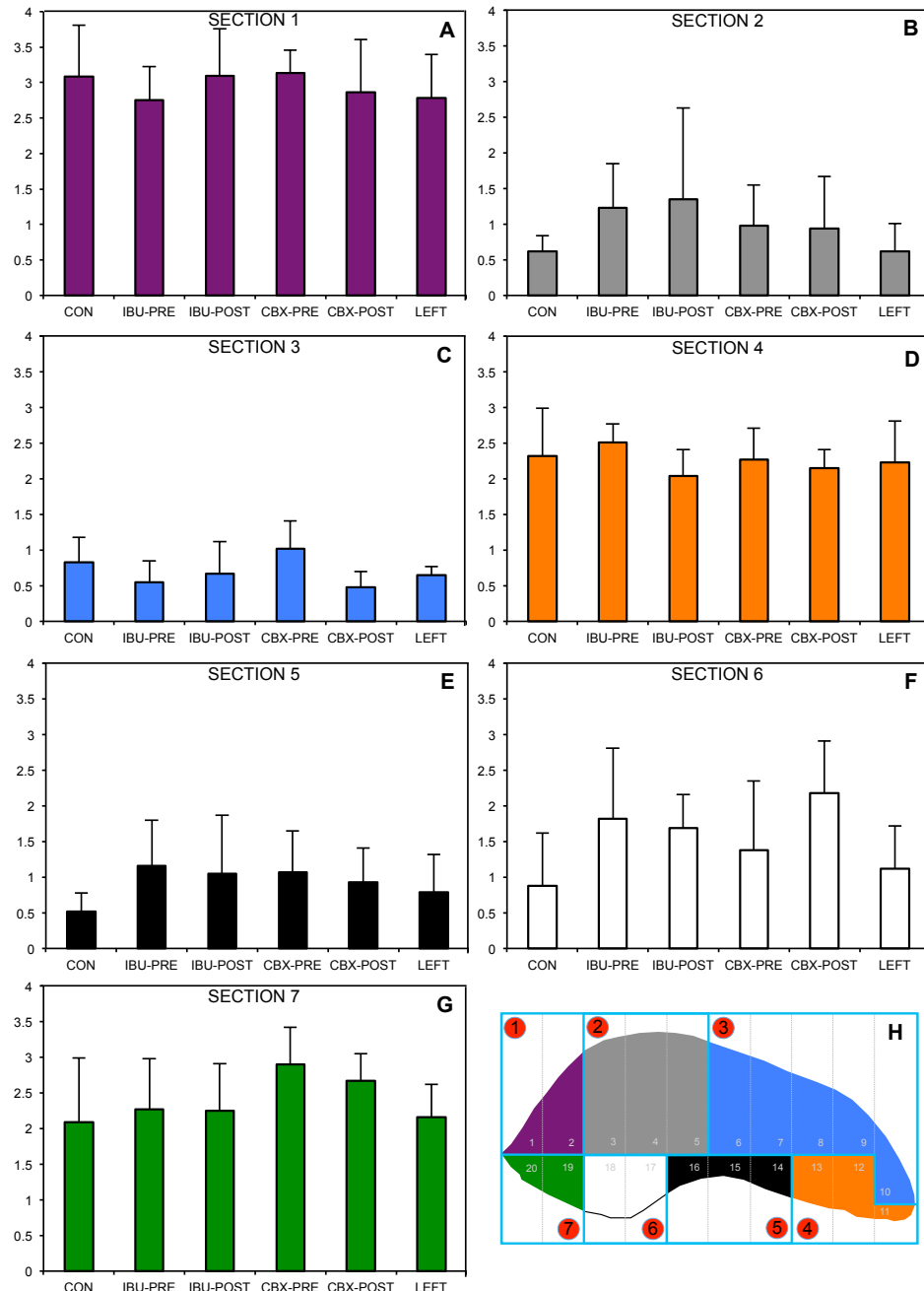
- [250] Bonewald L. Establishment and characterization of an osteocyte-like cell line, MLO-Y4. *J Bone Miner Res* 1999;17:61–5.
- [251] Cheng B, Kato Y, Zhao S, Luo J, Sprague E, Bonewald LF, et al. PGE(2) is essential for gap junction-mediated intercellular communication between osteocyte-like MLO-Y4 cells in response to mechanical strain. *Endocrinology* 2001;142:3464–73.
- [252] Cherian PP, Cheng B, Gu S, Sprague E, Bonewald LF, Jiang JX. Effects of mechanical strain on the function of Gap junctions in osteocytes are mediated through the prostaglandin EP2 receptor. *J Biol Chem* 2003;278:43146–56.
- [253] Genetos DC, Kephart CJ, Zhang Y, Yellowley CE, Donahue HJ. Oscillating fluid flow activation of gap junction hemichannels induces ATP release from MLO-Y4 osteocytes. *J Cell Physiol* 2007;212:207–14.
- [254] Ponik SM, Triplett JW, Pavalko FM. Osteoblasts and osteocytes respond differently to oscillatory and unidirectional fluid flow profiles. *J Cell Biochem* 2007;100:794–807.
- [255] Kato Y, Windle JJ, Koop BA, Mundy GR, Bonewald LF. Establishment of an osteocyte-like cell line, MLO-Y4. *J Bone Miner Res* 1997;12:2014–23.
- [256] Mikuni-Takagaki Y, Kakai Y, Satoyoshi M, Kawano E, Suzuki Y, Kawase T, et al. Matrix mineralization and the differentiation of osteocyte-like cells in culture. *J Bone Miner Res* 1995;10:231–42.
- [257] Robling AG, Niziolek PJ, Baldrige LA, Condon KW, Allen MR, Alam I, et al. Mechanical stimulation of bone in vivo reduces osteocyte expression of Sost/sclerostin. *J Biol Chem* 2008;283:5866–75.
- [258] McCarthy TL, Casinghino S, Centrella M, Canalis E. Complex pattern of insulin-like growth factor binding protein expression in primary rat osteoblast enriched cultures: regulation by prostaglandin E2, growth hormone, and the insulin-like growth factors. *J Cell Physiol* 1994;160:163–75.
- [259] Hung CT, Pollack SR, Reilly TM, Brighton CT. Real-time calcium response of cultured bone cells to fluid flow. *Clin Orthop Relat Res* 1995:256–69.
- [260] Young SRL, Hum JM, Rodenberg E, Turner CH, Pavalko FM. Non-overlapping functions for Pyk2 and FAK in osteoblasts during fluid shear stress-induced mechanotransduction. *PLoS One* 2011;6:e16026.
- [261] Berson RE, Purcell MR, Sharp MK. Computationally determined shear on cells grown in orbiting culture dishes. *Adv Exp Med Biol* 2008;614:189–98.
- [262] Thomas JMD, Chakraborty A, Sharp MK, Berson RE. Spatial and temporal resolution of shear in an orbiting petri dish. *Biotechnol Prog* 2011;27:460–5.
- [263] Kido S, Kuriwaka-Kido R, Imamura T, Ito Y, Inoue D, Matsumoto T. Mechanical stress induces Interleukin-11 expression to stimulate osteoblast differentiation. *Bone* 2009;45:1125–32.
- [264] Worton LE, Kwon RY, Gardiner EM, Gross TS, Srinivasan S. Enhancement of flow-induced AP-1 gene expression by cyclosporin A requires NFAT-independent signaling in bone cells. *Cell Mol Bioeng* 2014;7:254–65.

- [265] Ley K, Lundgren E, Berger E, Arfors KE. Shear-dependent inhibition of granulocyte adhesion to cultured endothelium by dextran sulfate. *Blood* 1989;73:1324–30.
- [266] Cayman Chemical. Prostaglandin E2 ELISA Kit - Monoclonal - Kit Booklet 2016.
- [267] Joldersma M, Burger EH, Semeins CM, Klein-Nulend J. Mechanical stress induces COX-2 mRNA expression in bone cells from elderly women. *J Biomech* 2000;33:53–61.
- [268] Kamel M a, Picconi JL, Lara-Castillo N, Johnson ML. Activation of  $\beta$ -catenin signaling in MLO-Y4 osteocytic cells versus 2T3 osteoblastic cells by fluid flow shear stress and PGE2: Implications for the study of mechanosensation in bone. *Bone* 2010;47:872–81.
- [269] Govey PM, Jacobs JM, Tilton SC, Loisel AE, Zhang Y, Freeman WM, et al. Integrative transcriptomic and proteomic analysis of osteocytic cells exposed to fluid flow reveals novel mechano-sensitive signaling pathways. *J Biomech* 2014;47:1838–45.
- [270] Klein-Nulend J, Bakker AD, Bacabac RG, Vatsa A, Weinbaum S. Mechanosensation and transduction in osteocytes. *Bone* 2013;54:182–90.
- [271] Bacabac RG, Mizuno D, Schmidt CF, MacKintosh FC, Van Loon JJWA, Klein-Nulend J, et al. Round versus flat: bone cell morphology, elasticity, and mechanosensing. *J Biomech* 2008;41:1590–8.
- [272] Emori HW, Paulus H, Bluestone R, Champion GD, Pearson C. Indomethacin serum concentrations in man. Effects of dosage, food, and antacid. *Ann Rheum Dis* 1976;35:333–8.
- [273] Caillé G, Du Souich P, Gervais P, Besner JG. Single dose pharmacokinetics of ketoprofen, indomethacin, and naproxen taken alone or with sucralfate. *Biopharm Drug Dispos n.d.*;8:173–83.
- [274] Gu G, Nars M, Hentunen TA, Metsikkö K, Väänänen HK. Isolated primary osteocytes express functional gap junctions in vitro. *Cell Tissue Res* 2006;323:263–71.
- [275] Zhao S, Zhang YKY, Harris S, Ahuja SS, Bonewald LF. MLO-Y4 osteocyte-like cells support osteoclast formation and activation. *J Bone Miner Res* 2002;17:2068–79.
- [276] Bakker AD, Zandieh-Doulabi B, Klein-Nulend J. Strontium Ranelate affects signaling from mechanically-stimulated osteocytes towards osteoclasts and osteoblasts. *Bone* 2013;53:112–9.
- [277] Salek MM, Sattari P, Martinuzzi RJ. Analysis of fluid flow and wall shear stress patterns inside partially filled agitated culture well plates. *Ann Biomed Eng* 2012;40:707–28.
- [278] Dardik A, Chen L, Frattini J, Asada H, Aziz F, Kudo FA, et al. Differential effects of orbital and laminar shear stress on endothelial cells. *J Vasc Surg* 2005;41:869–80.
- [279] Anderson EJ, Falls TD, Sorkin AM, Knothe Tate ML. The imperative for controlled mechanical stresses in unraveling cellular mechanisms of mechanotransduction. *Biomed Eng Online* 2006;5:27.

- [280] Mantila Roosa SM, Turner CH, Liu Y. Regulatory mechanisms in bone following mechanical loading. *Gene Regul Syst Bio* 2012;6:43–53.
- [281] Lean JM, Mackay AG, Chow JW, Chambers TJ. Osteocytic expression of mRNA for c-fos and IGF-I: an immediate early gene response to an osteogenic stimulus. *Am J Physiol* 1996;270:E937-45.

**APPENDIX I**

**MAR ( $\mu\text{m}/\text{day}$ ) of the male ulnas that underwent the 2-week loading protocol in the IBU/CBX experiment. A-G) MAR of Sections 1-7, respectively. H) Colour coded 7-Section grid of ulna cross-section. Values are mean  $\pm$  standard deviation (STD). No differences ( $p>0.05$ ) were detected between the LEFT group and the CON group in any of the Sections.  $n=5/\text{CON}$ , IBU-PRE, IBU-POST, CBX-PRE;  $n=4/\text{CBX-POST}$ ;  $n=6/\text{LEFT}$ .**



**APPENDIX II**

**MAR ( $\mu\text{m}/\text{day}$ ) of the male ulnas that underwent the 2-week loading protocol in the IBU/CBX experiment.** Values are mean  $\pm$  STD. No differences ( $p>0.05$ ) were detected between the LEFT group and the CON group in any of the Sections. n=5/CON, IBU-PRE, IBU-POST, CBX-PRE; n=4/CBX-POST; n=6/LEFT.

	Section 1	Section 2	Section 3	Section 4	Section 5	Section 6	Section 7
<b>CON</b>	3.10 $\pm$ 0.72	0.62 $\pm$ 0.22	0.83 $\pm$ 0.35	2.32 $\pm$ 0.67	0.52 $\pm$ 0.26	0.87 $\pm$ 0.75	2.08 $\pm$ 0.90
<b>IBU-PRE</b>	2.76 $\pm$ 0.47	1.23 $\pm$ 0.62	0.55 $\pm$ 0.30	2.51 $\pm$ 0.26	1.16 $\pm$ 0.64	1.82 $\pm$ 0.99	2.27 $\pm$ 0.72
<b>IBU-POST</b>	3.09 $\pm$ 0.67	1.35 $\pm$ 1.29	0.66 $\pm$ 0.46	2.03 $\pm$ 0.37	1.04 $\pm$ 0.83	1.69 $\pm$ 0.47	2.25 $\pm$ 0.66
<b>CBX-PRE</b>	3.13 $\pm$ 0.32	0.97 $\pm$ 0.57	1.01 $\pm$ 0.40	2.26 $\pm$ 0.44	1.06 $\pm$ 0.59	1.38 $\pm$ 0.97	2.90 $\pm$ 0.52
<b>CBX-POST</b>	2.87 $\pm$ 0.74	0.93 $\pm$ 0.74	0.48 $\pm$ 0.22	2.14 $\pm$ 0.27	0.93 $\pm$ 0.48	2.18 $\pm$ 0.73	2.67 $\pm$ 0.38
<b>LEFT</b>	2.78 $\pm$ 0.62	0.62 $\pm$ 0.40	0.64 $\pm$ 0.12	2.23 $\pm$ 0.58	0.78 $\pm$ 0.54	1.11 $\pm$ 0.61	2.16 $\pm$ 0.46

## APPENDIX III

The *p*-values determined by post-hoc analyses for each Section of the male IBU/CBX experiment. A-G) *p*-values of Sections 1-7, respectively. ■  $p < 0.05$  ■  $p < 0.10$

<b>A</b>	<b>SECTION 1</b>	<b>IBU-PRE</b>	<b>IBU-POST</b>	<b>CBX-PRE</b>	<b>CBX-POST</b>	<b>LEFT</b>
	CON	0.954	1.00	1.00	0.992	0.962
	IBU-PRE		0.950	0.939	1.00	1.00
	IBU-POST			1.00	0.991	0.958
	CBX-PRE				0.986	0.948
	CBX-POST					1.00

<b>B</b>	<b>SECTION 2</b>	<b>IBU-PRE</b>	<b>IBU-POST</b>	<b>CBX-PRE</b>	<b>CBX-POST</b>	<b>LEFT</b>
	CON	0.750	0.601	0.975	0.980	1.00
	IBU-PRE		1.00	0.994	0.985	0.714
	IBU-POST			0.969	0.94	0.555
	CBX-PRE				1.00	0.970
	CBX-POST					0.976

<b>C</b>	<b>SECTION 3</b>	<b>IBU-PRE</b>	<b>IBU-POST</b>	<b>CBX-PRE</b>	<b>CBX-POST</b>	<b>LEFT</b>
	CON	0.752	0.964	0.947	0.531	0.932
	IBU-PRE		0.993	0.292	0.999	0.997
	IBU-POST			0.583	0.937	1.00
	CBX-PRE				0.162	0.486
	CBX-POST					0.952

<b>D</b>	<b>SECTION 4</b>	<b>IBU-PRE</b>	<b>IBU-POST</b>	<b>CBX-PRE</b>	<b>CBX-POST</b>	<b>LEFT</b>
	CON	0.986	0.918	1.00	0.989	0.999
	IBU-PRE		0.588	0.966	0.806	0.912
	IBU-POST			0.975	0.999	0.980
	CBX-PRE				0.999	1.00
	CBX-POST					1.00

<b>E</b>	<b>SECTION 5</b>	<b>IBU-PRE</b>	<b>IBU-POST</b>	<b>CBX-PRE</b>	<b>CBX-POST</b>	<b>LEFT</b>
	CON	0.507	0.702	0.720	0.864	0.971
	IBU-PRE		0.999	1.00	0.987	0.885
	IBU-POST			1.00	1.00	0.774
	CBX-PRE				0.999	0.973
	CBX-POST					0.998

<b>F</b>	<b>SECTION 6</b>	<b>IBU-PRE</b>	<b>IBU-POST</b>	<b>CBX-PRE</b>	<b>CBX-POST</b>	<b>LEFT</b>
	CON	0.386	0.547	0.914	0.110	0.995
	IBU-PRE		1.00	0.952	0.975	0.645
	IBU-POST			0.990	0.909	0.808
	CBX-PRE				0.633	0.993
	CBX-POST					0.229

<b>G</b>	<b>SECTION 7</b>	<b>IBU-PRE</b>	<b>IBU-POST</b>	<b>CBX-PRE</b>	<b>CBX-POST</b>	<b>LEFT</b>
	CON	0.997	0.998	0.405	0.682	1.00
	IBU-PRE		1.00	0.667	0.909	1.00
	IBU-POST			0.639	0.892	1.00
	CBX-PRE				0.994	0.468
	CBX-POST					0.759

**APPENDIX IV**

**Dehydrating, infiltration and embedding procedure and schedule.** This procedure prepares the bone samples for histology.

<b>Day</b>	<b>Procedure</b>	<b>Solution</b>	<b>Time</b>	<b># of Changes</b>	<b>Storage</b>
1	dehydration	70% ethanol	1 hour	2	3°C
		95% ethanol	1 hour	2	3°C
		95% ethanol	overnight		3°C
2	dehydration	100% ethanol	1 hour	3	3°C
		xylenes	1 hour	2	3°C
		xylenes	overnight	N/A	3°C
3, 4	infiltration 1	85 ml methyl methacrylate 15 ml dibutyl phthalate	24 hours	daily	3°C
5, 6	infiltration 2	85 ml methyl methacrylate 15 ml dibutyl phthalate 1 gram benzoyl peroxide	24 hours	daily	3°C
7, 8	infiltration 3	85 ml methyl methacrylate 15 ml dibutyl phthalate 2 grams benzoyl peroxide	24 hours	daily	3°C
9	embedding	85 ml methyl methacrylate 15 ml dibutyl phthalate 2 grams benzoyl peroxide	leave for 2-3 days	N/A	37°C (water bath)

**APPENDIX V**

**MAR ( $\mu\text{m}/\text{day}$ ) of the male ulnas that underwent the 1-month loading protocol in the indomethacin experiment.** Values are mean  $\pm$  STD. \*Different from LEFT.

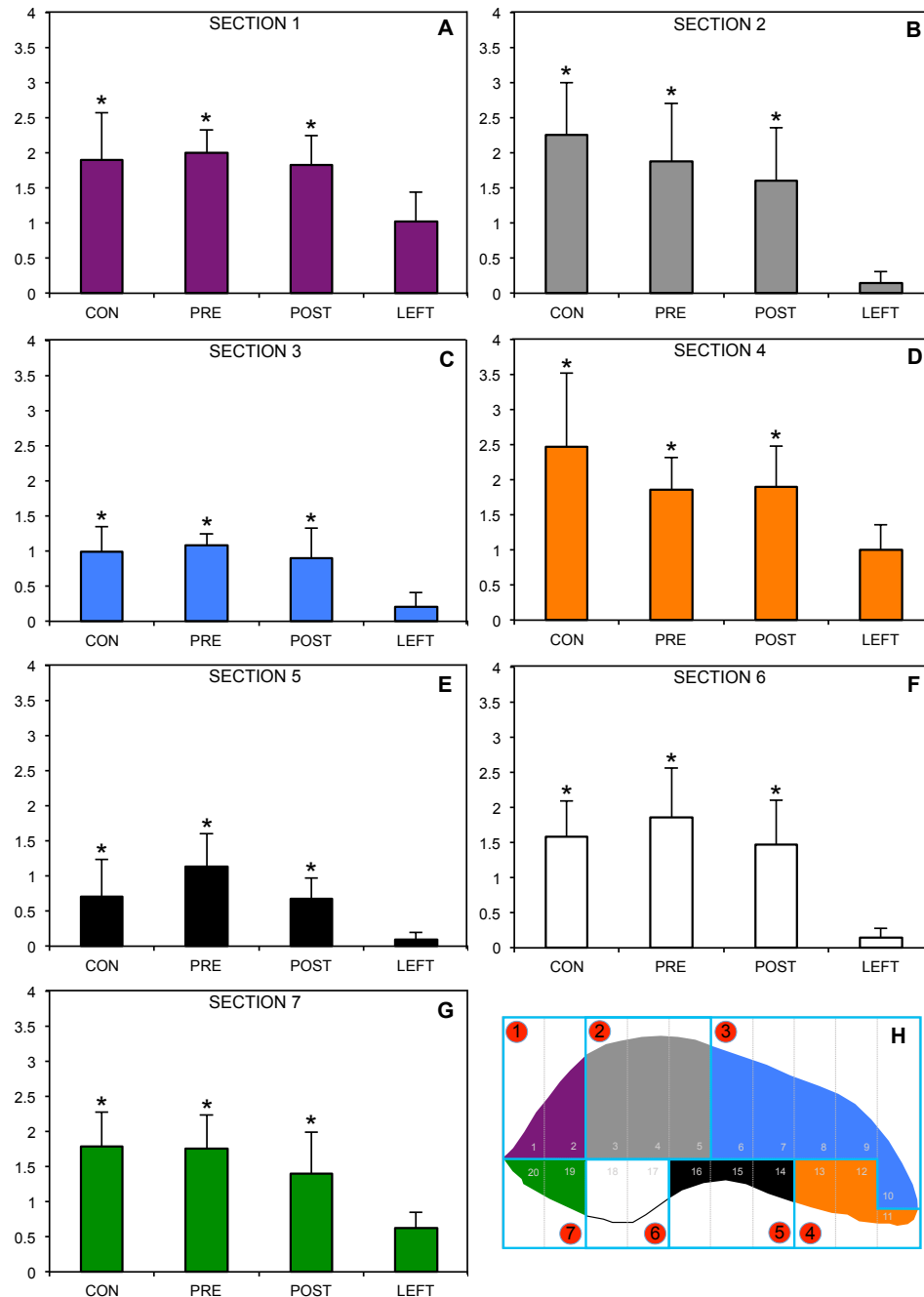
CON=no indomethacin dosing (n=4). L-PRE=low dose before (n=3); L-POST=low dose after (n=3); H-PRE=high dose before (n=4); H-POST=high dose after (n=3).

LEFT=non-loaded ulnas (n=18). low dose=0.2mg/kg; high dose=2mg/kg.

	Section 1	Section 2	Section 3	Section 4	Section 5	Section 6	Section 7
<b>CON</b>	2.33 $\pm$ 0.64*	3.02 $\pm$ 0.91*	1.13 $\pm$ 0.50*	1.83 $\pm$ 0.51	1.45 $\pm$ 0.27*	2.46 $\pm$ 0.41*	2.57 $\pm$ 0.87*
<b>L-PRE</b>	1.51 $\pm$ 0.26	3.13 $\pm$ 1.02*	1.30 $\pm$ 0.69*	1.86 $\pm$ 0.67	1.71 $\pm$ 0.88*	2.64 $\pm$ 0.38*	1.89 $\pm$ 0.50*
<b>L-POST</b>	2.35 $\pm$ 0.65*	2.98 $\pm$ 0.46*	1.47 $\pm$ 0.13*	1.82 $\pm$ 0.21	1.80 $\pm$ 0.33*	2.94 $\pm$ 0.27*	2.37 $\pm$ 0.56*
<b>H-PRE</b>	2.38 $\pm$ 0.27*	2.48 $\pm$ 0.52*	0.83 $\pm$ 0.16*	2.09 $\pm$ 0.53	1.09 $\pm$ 0.73*	1.88 $\pm$ 0.66*	1.76 $\pm$ 0.45*
<b>H-POST</b>	2.07 $\pm$ 0.54*	3.14 $\pm$ 1.04*	1.20 $\pm$ 0.22*	2.29 $\pm$ 0.53	1.71 $\pm$ 0.65*	2.56 $\pm$ 0.55*	2.25 $\pm$ 0.44*
<b>LEFT</b>	1.20 $\pm$ 0.49	0.21 $\pm$ 0.24	0.27 $\pm$ 0.17	1.30 $\pm$ 0.77	0.11 $\pm$ 0.15	0.15 $\pm$ 0.17	0.87 $\pm$ 0.37

**APPENDIX VI**

**MAR ( $\mu\text{m}/\text{day}$ ) of the male ulnas that underwent the 1-month loading protocol in the NS-398 experiment. A-G) MAR of Sections 1-7, respectively. H) Colour coded 7-Section grid of ulna cross-section. Values are mean  $\pm$  STD. \*Different from LEFT. CON=no NS-398 dosing (n=8); PRE=dose before (n=9); POST=dose after (n=9); LEFT=non-loaded ulnas (n=15).**



**APPENDIX VII**

**MAR ( $\mu\text{m}/\text{day}$ ) of the male ulnas that underwent the 1-month loading protocol in the NS-398 experiment.** Values are mean  $\pm$  STD. \*Different from LEFT. CON=no NS-398 dosing (n=8); PRE=dose before (n=9); POST=dose after (n=9); LEFT=non-loaded ulnas (n=15).

	Section 1	Section 2	Section 3	Section 4	Section 5	Section 6	Section 7
<b>CON</b>	1.90 $\pm$ 0.68*	2.26 $\pm$ 0.74*	1.00 $\pm$ 0.35*	2.47 $\pm$ 1.05*	0.71 $\pm$ 0.53*	1.58 $\pm$ 0.52*	1.79 $\pm$ 0.49*
<b>PRE</b>	2.00 $\pm$ 0.33*	1.87 $\pm$ 0.83*	1.08 $\pm$ 0.16*	1.86 $\pm$ 0.46*	1.13 $\pm$ 0.47*	1.86 $\pm$ 0.70*	1.76 $\pm$ 0.48*
<b>POST</b>	1.83 $\pm$ 0.42*	1.60 $\pm$ 0.76*	0.91 $\pm$ 0.43*	1.90 $\pm$ 0.58*	0.67 $\pm$ 0.29*	1.47 $\pm$ 0.63*	1.40 $\pm$ 0.59*
<b>LEFT</b>	1.02 $\pm$ 0.42	0.15 $\pm$ 0.17	0.21 $\pm$ 0.20	1.00 $\pm$ 0.35	0.10 $\pm$ 0.10	0.14 $\pm$ 0.14	0.62 $\pm$ 0.22

**APPENDIX VIII**

The *p*-values determined by post-hoc analyses for each Section of the male NS-398 experiment. A-G) *p*-values of Sections 1-7, respectively.

**A**

SECTION 1	PRE	POST	LEFT
CON	0.969	0.988	0.001
PRE		0.854	<0.0005
POST			0.001

**B**

SECTION 2	PRE	POST	LEFT
CON	0.592	0.153	<0.0005
PRE		0.790	<0.0005
POST			<0.0005

**C**

SECTION 3	PRE	POST	LEFT
CON	0.930	0.919	<0.0005
PRE		0.579	<0.0005
POST			<0.0005

**D**

SECTION 4	PRE	POST	LEFT
CON	0.194	0.242	<0.0005
PRE		0.999	0.01
POST			0.007

  $p < 0.05$

  $p < 0.10$

**E**

SECTION 5	PRE	POST	LEFT
CON	0.086	0.996	0.002
PRE		0.044	<0.0005
POST			0.002

**F**

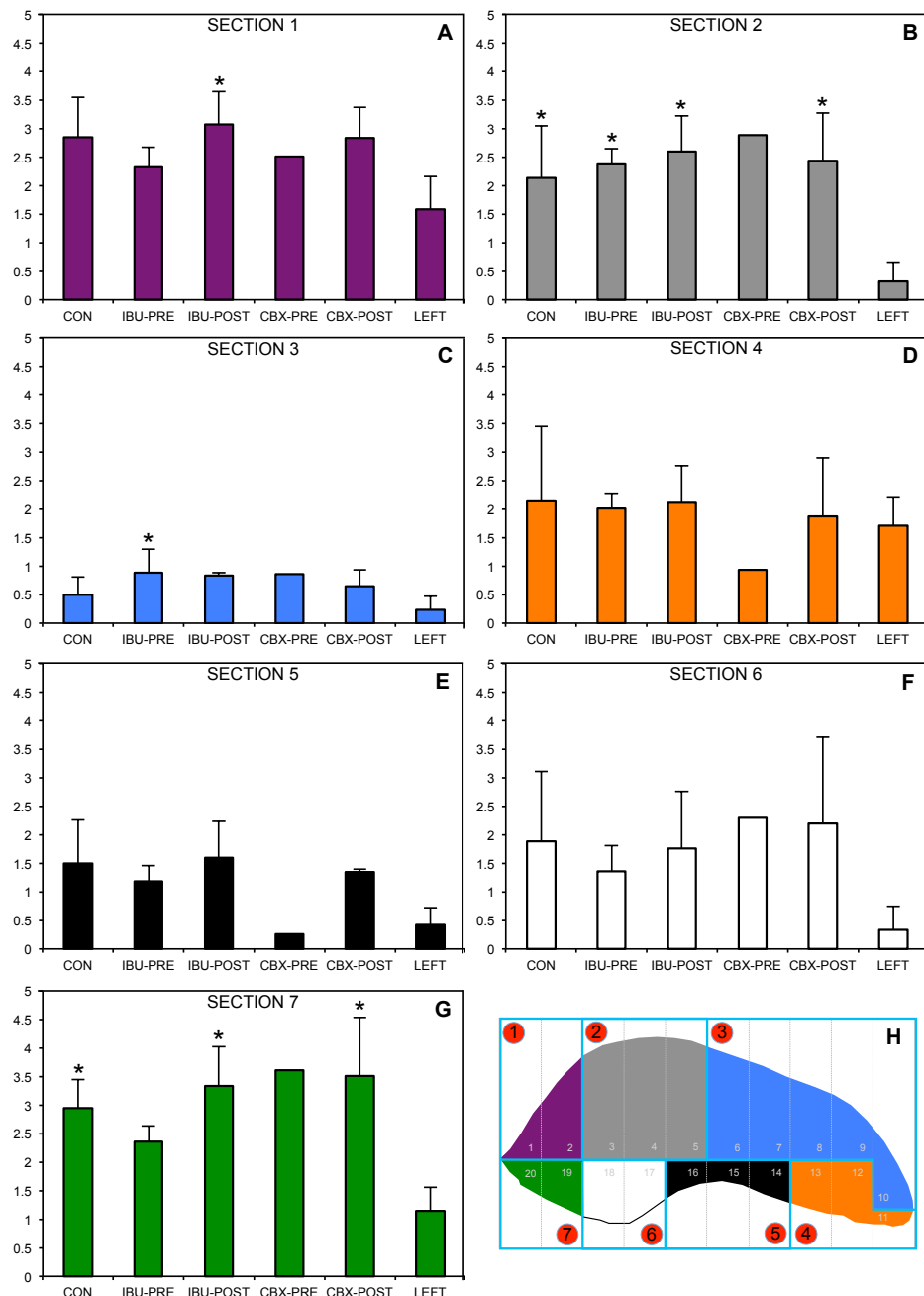
SECTION 6	PRE	POST	LEFT
CON	0.666	0.968	<0.0005
PRE		0.365	<0.0005
POST			<0.0005

**G**

SECTION 7	PRE	POST	LEFT
CON	0.999	0.281	<0.0005
PRE		0.32	<0.0005
POST			0.001

**APPENDIX IX**

**MAR ( $\mu\text{m}/\text{day}$ ) of the female ulnas that underwent the 2-week loading protocol in the IBU/CBX experiment. A-G) MAR of Sections 1-7, respectively. H) Colour coded 7-Section grid of ulna cross-section. Values are mean  $\pm$  STD. \*Different from LEFT. CON=no NSAID dosing (n=3); IBU-PRE=ibuprofen dosing before (n=4); IBU-POST=ibuprofen dosing after (n=3); CBX-PRE=Celebrex dosing before (n=1); CBX-POST= Celebrex dosing after (n=2); LEFT=non-loaded ulnas (n=5).**



**APPENDIX X**

**MAR ( $\mu\text{m}/\text{day}$ ) of the female ulnas that underwent the 2-week loading protocol in the IBU/CBX experiment.** Values are mean  $\pm$  STD. \*Different from LEFT.

CON=no NSAID dosing (n=3); IBU-PRE=ibuprofen dosing before (n=4);

IBU-POST=ibuprofen dosing after (n=3); CBX-PRE=Celebrex dosing before (n=1);

CBX-POST= Celebrex dosing after (n=2); LEFT=non-loaded ulnas (n=5).

	Section 1	Section 2	Section 3	Section 4	Section 5	Section 6	Section 7
<b>CON</b>	2.84 $\pm$ 0.71	2.14 $\pm$ 0.91*	0.50 $\pm$ 0.31	2.14 $\pm$ 1.31	1.49 $\pm$ 0.77	1.88 $\pm$ 1.23	2.95 $\pm$ 0.49*
<b>IBU-PRE</b>	2.33 $\pm$ 0.35	2.37 $\pm$ 0.27*	0.89 $\pm$ 0.41*	2.01 $\pm$ 0.25	1.18 $\pm$ 0.28	1.36 $\pm$ 0.45	2.36 $\pm$ 0.28
<b>IBU-POST</b>	3.07 $\pm$ 0.58*	2.60 $\pm$ 0.62*	0.84 $\pm$ 0.05	2.12 $\pm$ 0.64	1.60 $\pm$ 0.64	1.76 $\pm$ 1.00	3.34 $\pm$ 0.69*
<b>CBX-PRE</b>	2.51	2.89	0.86	0.94	0.27	2.30	3.61
<b>CBX-POST</b>	2.83 $\pm$ 0.55	2.44 $\pm$ 0.83*	0.65 $\pm$ 0.29	1.87 $\pm$ 1.03	1.35 $\pm$ 0.05	2.20 $\pm$ 1.51	3.51 $\pm$ 1.02*
<b>LEFT</b>	1.59 $\pm$ 0.58	0.32 $\pm$ 0.34	0.24 $\pm$ 0.24	1.72 $\pm$ 0.49	0.42 $\pm$ 0.30	0.33 $\pm$ 0.42	1.15 $\pm$ 0.41

APPENDIX XI

The *p*-values determined by post-hoc analyses for each Section of the female IBU/CBX experiment. A-G) *p*-values of Sections 1-7, respectively.

**A**

SECTION 1	IBU-PRE	IBU-POST	CBX-POST	LEFT
CON	0.737	0.986	1.00	0.053
IBU-PRE		0.432	0.755	0.322
IBU-POST			0.982	0.020
CBX-POST				0.057

**B**

SECTION 2	IBU-PRE	IBU-POST	CBX-POST	LEFT
CON	0.983	0.863	0.967	0.007
IBU-PRE		0.984	1.00	0.001
IBU-POST			0.997	0.001
CBX-POST				0.002

**C**

SECTION 3	IBU-PRE	IBU-POST	CBX-POST	LEFT
CON	0.444	0.635	0.968	0.725
IBU-PRE		0.999	0.818	0.035
IBU-POST			0.932	0.088
CBX-POST				0.340

**D**

SECTION 4	IBU-PRE	IBU-POST	CBX-POST	LEFT
CON	0.999	1.00	0.992	0.936
IBU-PRE		1.00	0.999	0.978
IBU-POST			0.994	0.948
CBX-POST				0.998

 *p* < 0.05

 *p* < 0.10

**E**

SECTION 5	IBU-PRE	IBU-POST	CBX-POST	LEFT
CON	0.890	0.998	0.994	0.039
IBU-PRE		0.748	0.988	0.139
IBU-POST			0.957	0.022
CBX-POST				0.086

**F**

SECTION 6	IBU-PRE	IBU-POST	CBX-POST	LEFT
CON	0.941	1.00	0.992	0.200
IBU-PRE		0.976	0.749	0.483
IBU-POST			0.975	0.261
CBX-POST				0.092

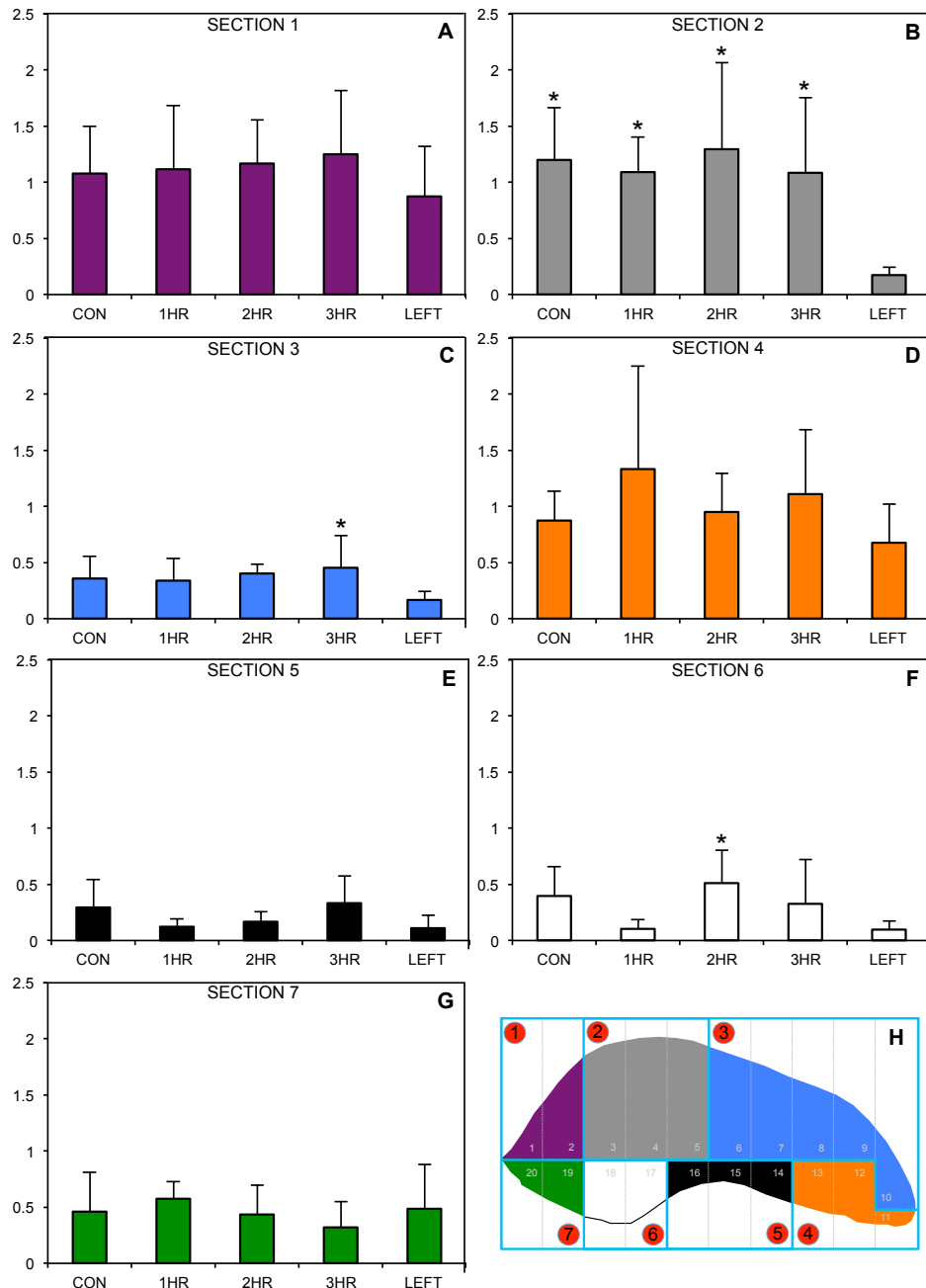
**G**

SECTION 7	IBU-PRE	IBU-POST	CBX-POST	LEFT
CON	0.676	0.925	0.769	0.007
IBU-PRE		0.241	0.131	0.055
IBU-POST			0.996	0.001
CBX-POST				0.001

**APPENDIX XII**

**MAR of ( $\mu\text{m}/\text{day}$ ) of the female ulnas that underwent the 1-month loading protocol in the ibuprofen timing experiment. A-G) MAR of Sections 1-7, respectively.**

**H) Colour coded 7-Section grid of ulna cross-section. Values are mean  $\pm$  STD. \*Different from LEFT. CON=no ibuprofen dosing (n=5); 1HR=ibuprofen dosing 1hr before (n=4); 2HR=ibuprofen dosing 2hrs before (n=6); 3HR=ibuprofen dosing 3hrs before (n=5); LEFT=non-loaded ulnas (n=8).**



**APPENDIX XIII**

**MAR of ( $\mu\text{m}/\text{day}$ ) of the female ulnas that underwent the 1-month loading protocol in the ibuprofen timing experiment.** Values are mean  $\pm$  STD. \*Different from LEFT. CON=no ibuprofen dosing (n=5); 1HR=ibuprofen dosing 1hr before (n=4); 2HR=ibuprofen dosing 2hrs before (n=6); 3HR=ibuprofen dosing 3hrs before (n=5); LEFT=non-loaded ulnas (n=8).

	Section 1	Section 2	Section 3	Section 4	Section 5	Section 6	Section 7
<b>CON</b>	1.08 $\pm$ 0.43	1.20 $\pm$ 0.46*	0.36 $\pm$ 0.20	0.87 $\pm$ 0.27	0.30 $\pm$ 0.25	0.39 $\pm$ 0.27	0.46 $\pm$ 0.36
<b>1HR</b>	1.12 $\pm$ 0.57	1.09 $\pm$ 0.32*	0.34 $\pm$ 0.19	1.33 $\pm$ 0.92	0.13 $\pm$ 0.07	0.10 $\pm$ 0.08	0.57 $\pm$ 0.15
<b>2HR</b>	1.17 $\pm$ 0.39	1.29 $\pm$ 0.77*	0.40 $\pm$ 0.09	0.95 $\pm$ 0.35	0.17 $\pm$ 0.09	0.51 $\pm$ 0.29*	0.43 $\pm$ 0.26
<b>3HR</b>	1.25 $\pm$ 0.57	1.09 $\pm$ 0.67*	0.46 $\pm$ 0.28*	1.11 $\pm$ 0.58	0.33 $\pm$ 0.24	0.33 $\pm$ 0.39	0.32 $\pm$ 0.23
<b>LEFT</b>	0.87 $\pm$ 0.45	0.17 $\pm$ 0.07	0.17 $\pm$ 0.08	0.68 $\pm$ 0.34	0.11 $\pm$ 0.11	0.10 $\pm$ 0.08	0.49 $\pm$ 0.40

**APPENDIX XIV**

The *p*-values determined by post-hoc analyses for each Section of the female IBU timing experiment. A-G) *p*-values of Sections 1-7, respectively.

**A**

SECTION 1	1HR	2HR	3HR	LEFT
CON	1.00	0.998	0.975	0.941
1HR		1.00	0.993	0.912
2HR			0.998	0.779
3HR				0.628

**B**

SECTION 2	1HR	2HR	3HR	LEFT
CON	0.997	0.998	0.996	0.013
1HR		0.971	1.00	0.049
2HR			0.961	0.004
3HR				0.033

**C**

SECTION 3	1HR	2HR	3HR	LEFT
CON	1.00	0.992	0.878	0.320
1HR		0.983	0.850	0.462
2HR			0.981	0.116
3HR				0.046

**D**

SECTION 4	1HR	2HR	3HR	LEFT
CON	0.634	0.999	0.940	0.956
1HR		0.750	0.958	0.222
2HR			0.984	0.836
3HR				0.551

  $p < 0.05$

  $p < 0.10$

**E**

SECTION 5	1HR	2HR	3HR	LEFT
CON	0.537	0.684	0.997	0.311
1HR		0.995	0.353	1.00
2HR			0.467	0.997
3HR				0.165

**F**

SECTION 6	1HR	2HR	3HR	LEFT
CON	0.413	0.938	0.992	0.251
1HR		0.112	0.657	1.00
2HR			0.740	0.038
3HR				0.498

**G**

SECTION 7	1HR	2HR	3HR	LEFT
CON	0.980	1.00	0.957	1.00
1HR		0.953	0.749	0.990
2HR			0.977	0.997
3HR				0.885

## APPENDIX XV

**Body mass of the rats used in the *in vivo* mechanical loading experiments. A)** Body mass of the male rats in the indomethacin experiment. **B)** Body mass of the male rats in the male IBU/CBX experiment. **C)** Body mass of the male rats in the NS-398 experiment. **D)** Body mass of the female rats in the IBU/CBX experiment. **E)** Body mass of the female rats in the ibuprofen timing experiment.

**A**

Group	Body Mass (g)
CON	612.5 ± 46.9
L-PRE	630.8 ± 43.6
L-POST	581.5 ± 4.8
H-PRE	622.0 ± 42.9
H-POST	641.3 ± 47.9

**B**

Group	Body Mass (g)
CON	552.7 ± 67.1
PRE	569.0 ± 45.1
POST	533.5 ± 36.7

**C**

Group	Body Mass (g)
CON	686.6 ± 40.6
IBU-PRE	650.6 ± 37.6
IBU-POST	622.4 ± 57.2
CBX-PRE	661.2 ± 32.5
CBX-POST	647.0 ± 29.7

**D**

Group	Body Mass (g)
CON	326.2 ± 11.1
IBU-PRE	302.8 ± 29.1
IBU-POST	321.3 ± 31.0
CBX-PRE	328.4 ± 20.7
CBX-POST	333.2 ± 24.1

**E**

Group	Body Mass (g)
CON	271.6 ± 8.2
1HR	271.2 ± 9.15
2HR	259.7 ± 17.7
3HR	275.2 ± 19.5